



Baker, Laurie Louise (2019) *Outfoxing rabies: robust vaccination designs for disease elimination*. PhD thesis.

<https://theses.gla.ac.uk/41011/>

Copyright and moral rights for this work are retained by the author

A copy can be downloaded for personal non-commercial research or study, without prior permission or charge

This work cannot be reproduced or quoted extensively from without first obtaining permission in writing from the author

The content must not be changed in any way or sold commercially in any format or medium without the formal permission of the author

When referring to this work, full bibliographic details including the author, title, awarding institution and date of the thesis must be given

Enlighten: Theses

<https://theses.gla.ac.uk/>
research-enlighten@glasgow.ac.uk

Outfoxing Rabies: Robust Vaccination Designs For Disease Elimination

by

Laurie Louise Baker



A thesis submitted for the degree of
Doctor of Philosophy (Ph.D.)

Institute of Biodiversity, Animal Health and Comparative Medicine
College of Medical, Veterinary and Life Sciences
University of Glasgow

February 12, 2019

Abstract

Prediction of pathogen dynamics and the design of effective interventions to control and eliminate disease are key goals in epidemiology. While progress has been made towards the elimination of many infectious diseases, only two, smallpox and rinderpest, have been globally eradicated. Mass vaccination can greatly reduce the burden of vaccine-preventable diseases. However, there is relatively little scientific guidance on the optimal duration, frequency and placement of control interventions for achieving elimination. Such insights could greatly inform policy and practice.

Rabies is a deadly and terrifying disease that exacts a heavy toll on human lives and national economies, with over 50,000 human deaths each year and many millions more requiring expensive life-saving post-exposure vaccines. Elimination of rabies is feasible through vaccination, and oral rabies vaccination (ORV) campaigns have eliminated fox rabies from Western Europe. However, scientific guidance could improve elimination efforts elsewhere, and is still needed for contingency planning to maintain rabies freedom and for emergency response to incursions.

My thesis focuses on two pivotal questions in infectious disease ecology: what are the underlying determinants of disease persistence, and how can vaccination strategies be optimized to eliminate infection? To answer these questions, I analysed a rich and highly resolved spatial dataset of fox rabies cases and ORV efforts over three decades in Germany and neighbouring countries. The long-term, large-scale nature of these data provides a unique opportunity to improve our understanding of wildlife rabies dynamics in response to vaccination using novel spatial modeling techniques.

In chapter 2, I explore the extent to which metapopulation persistence depends on local transmission (within regions) or spatial coupling (between regions) using a hierarchical Bayesian state-space model. In chapter 3, I extend the model developed in chapter 2 to determine the best vaccination strategy, in terms of scale and duration of ORV efforts for three common epidemiological scenarios: **endemic** circulation of rabies; **high-risk** situations when rabies-free but neighbor endemic areas; and an **endgame** scenario when only a single endemic foci remains. In chapter 4, I develop a space-time model of fox rabies dynamics and explore

the effect of scale on estimates of transmission terms by aggregating rabies case data at different spatial resolutions. I then relate these estimates to the scaling of individual interactions to regional dynamics through population mixing.

Collectively, the findings from this thesis contribute to our understanding of how infectious diseases persist and can be controlled through vaccination. The methods generated can be used to explore tradeoffs in the scale and duration of ORV efforts, and generate recommendations on the time horizon and investment required to achieve and maintain freedom from disease. The model developed in chapter 4 also presents the first steps to developing a highly resolved spatial model of local rabies dynamics. These findings have immediate application to the design of cordon sanitaires in Europe, and to strategies aiming to rapidly eliminate re-emergence in high-risk countries such as Greece and Turkey. The analytical and statistical framework developed in this thesis is also applicable to answering analogous questions for the elimination of dog-mediated rabies and for other vaccine preventable diseases.

Contents

List of Figures	vii
List of Tables	xii
Chapter 1: Introduction	1
1.1 Concepts in disease dynamics	2
1.1.1 Definition of persistence	2
1.1.2 Threshold Populations and Critical Community Size	3
1.1.3 Modelling transmission	5
1.2 Processes influencing persistence	6
1.2.1 Population connectivity	6
1.2.2 Host demography	6
1.2.3 Behaviour and internal dynamics	7
1.3 Vaccination	8
1.4 Wildlife disease	8
1.5 Rabies	9
1.6 The elimination of fox rabies in Western Europe	10
1.7 Thesis overview	13
1.8 Thesis organisation	13
Chapter 2: Capturing local rabies transmission and metapopulation persistence in European foxes	15
2.1 Abstract	16
2.2 Introduction	17
2.3 Methods	19
2.3.1 Data Collection	19
2.3.2 Bayesian State-Space Model	20
2.3.3 Model evaluation	25
2.4 Model Fitting	26
2.5 Results	31
2.6 Discussion	41
Chapter 3: Optimising spatial and seasonal deployment of vaccination cam-	

paigns to eliminate wildlife rabies	44
3.1 Abstract	45
3.2 Introduction	46
3.3 Methods	47
3.3.1 Hierarchical Bayesian state-space model	49
3.3.2 Rabies Scenario Simulation	49
3.4 Results	51
3.4.1 Vaccination placement	51
3.4.2 Time to control vs. time to elimination	54
3.5 Discussion	58
3.5.1 Vaccination Placement	58
3.5.2 Time to control vs. time to elimination	59
3.5.3 Incursions	59
3.5.4 Future directions	60
3.5.5 Conclusion	61
Chapter 4: Resolving the spatial scale of rabies transmission	62
4.1 Abstract	63
4.2 Introduction	63
4.3 Methods	66
4.3.1 Data Collection	66
4.3.2 Space-time SPDE Fox Rabies Model	66
4.3.3 Creating the infected density surface	66
4.3.4 Creating the susceptible density surface	68
4.3.5 Constructing a GLM from the infected and susceptible density surfaces.	69
4.3.6 Exploring the spatial autocorrelation using kernel density smoothing .	70
4.4 Results	71
4.5 Discussion	82
Chapter 5: Discussion	85
5.1 How do infectious diseases persist?	86
5.2 How can control strategies be optimized to eliminate infection?	87
5.3 What advances have been made in the modelling of wildlife diseases?	89
5.3.1 Dealing with incomplete and missing data	90
5.3.2 Dealing with aggregated data	91
5.3.3 Modelling the spatiotemporal dynamics of disease	91
5.4 Future Work	93
5.5 Conclusion	94
Appendix A: Chapter 2: Carrying Capacity Derivation and Trace, Posterior, and Autocorrelation Plots	95
A.1 Carrying Capacity Derivation	96

A.2 Posteriors, Trace Plots, and Correlation of fitted parameters	97
Appendix B: Introduction to the intrinsically stationary iterated heat equation in Chapter 4	101
Bibliography	105

List of Figures

1.1	Stages of rabies infection in the red fox. ©Friedrich Loeffler Institut	9
1.2	The decadal spread of rabies from the 1940s to 1990s. ©Friedrich Loeffler Institut	10
1.3	Fixed wing aircraft were used to distribute vaccine-loaded chicken heads in the early days of vaccine distribution. ©Friedrich Loeffler Institut	11
1.4	Map of Western Europe showing detected rabies cases (red dots) and areas vaccinated (blue polygons). Over 30 years, 2.36 million km ² (2 times the size of Europe) were vaccinated leading to the elimination of rabies from 9 countries in Western Europe.	12
2.1	The posterior distribution and priors for the parameters estimated in the hierarchical Bayesian state-space model. The posterior distribution is shaded in blue, the black line represents the prior distribution. In order from top to bottom and left to right are the parameters representing fluctuations in fecundity due to environmental noise τ , migration of rabid foxes between regions c i.e. ρ_{max} in the equation, rabies transmission h , and the annual probability of observing rabies cases θ . The posterior and prior for the transmission parameter h is shown again in the bottom left panel of the plot to better show the prior chosen.	27
2.2	State-space model results for 5 federal states in Eastern Germany: Brandenburg, Mecklenburg-Vorpommern, Sachsen-Anhalt, Sachsen, and Thüringen. The left y-axis is the number of observed cases, the right y-axis is the percentage of the population vaccinated. The x-axis indicates the time (months). The gray line represents estimated percentage of the population vaccinated. The dark blue line is the monthly reported rabies cases for each region. The light blue shaded region is the 95% credible intervals.	34
2.3	Observational and environmental noise estimates over time (months). The blue line is the upper 95% CI and the red line is the lower 95% CI. The environmental noise parameter fluctuates between -10 and $+15\%$. The observational noise term peaks at around 18%	35

2.4	The total number of simulated rabies cases at monthly time steps across all 5 regions from the model using the linear transmission form $I/(hA + I)$. Several values for h were explored: 1.6-1.8 (blue to red orange) at 0.025 intervals. The linear form of the transmission equation seems to be very sensitive to the value of h chosen. The resulting time series show unrealistically large epidemics early on when values between 1.6-1.7 are chosen (around 20-40,000 cases across all regions) or an early drop in the number of cases to also unrealistic levels. I hypothesize that these two characteristics may explain why the jags model was unable to fit the model with the linear transmission form.	36
2.5	Probability Integral Transform for the model fit. The top panel shows the model fit to the observed rabies cases over time in Region 1. The dark blue line represents the observed rabies cases and the light and dark shaded blue region represents the 95% and 50% Credible Intervals (CI) estimated from the MCMC samples, respectively. The bottom panel shows the probability integral transform over time (where the observed case falls in the cumulative distribution function). The colours in the probability integral transform plot indicate whether the observed cases falls inside (red) the 95% CI, outside (turquoise) the 95% CI but within the 100% CI	37
2.6	Probability Integral Transform: Prediction with first data point. The top panel shows the model fit to the observed rabies cases over time in Region 1. The dark blue line represents the observed rabies cases and the light and dark shaded blue region represents the 95% and 50% Credible Intervals (CI) estimated from the MCMC samples, respectively. The bottom panel shows the probability integral transform over time (where the observed case falls in the cumulative distribution function). The colours in the probability integral transform plot indicate whether the observed cases falls inside (red) the 95% CI, outside (turquoise) the 95% CI but within the 100% CI, or outlier (green) when the case falls outside the CI entirely.	38
2.7	Probability Integral Transform: Prediction with first 20 points. The top panel shows the model fit to the observed rabies cases over time in Region 1. The dark blue line represents the observed rabies cases and the light and dark shaded blue region represents the 95% and 50% Credible Intervals (CI) estimated from the MCMC samples, respectively. The bottom panel shows the probability integral transform over time (where the observed case falls in the cumulative distribution function). The colours in the probability integral transform plot indicate whether the observed cases falls inside (red) the 95% CI, outside (turquoise) the 95% CI but within the 100% CI, or outlier (green) when the case falls outside the CI entirely.	39
2.8	Histograms of the Probability Integral Transform. The panels from top to bottom show the probability integral transform for the model fit, the model projection with 1 data point, and for the model projection with 20 data points.	40

3.1	Map showing epidemiological scenarios investigated in Eastern Germany where red = Rabies, white = Rabies free. A. Endemic: All regions have rabies, B. High-risk: Rabies is partly eliminated but remains in more than half of the regions. C. Endgame: Rabies has been eliminated in all regions but one. D. Illustration of the algorithm used to decide the order of campaign placement. Campaigns are sequentially placed based on the position (month and region) that resulted in the greatest increase in the probability of eliminating rabies across all 5 regions. The numbers 1-3 in the grid cells represent when (month) and where (region) the first 3 campaigns were placed. The grey boxes represent possible campaign slots where campaigns can be allocated for the 4, 5, ... 25 campaigns.	48
3.2	The posterior distribution and priors for the parameters estimated in the hierarchical Bayesian state-space model. The posterior distribution is shaded in blue, the black line represents the prior distribution. In the simulation I took random draws from the posterior distribution of parameters estimated for rabies transmission h , migration of rabid foxes between regions ρ_{max} , fluctuations in fecundity due to environmental noise τ , and the annual probability of observing rabies cases θ . The posterior and prior for the transmission parameter h is shown again in the bottom left panel of the plot to better show the prior chosen. Random draws were taken from the posterior distribution of parameters estimated and used to simulate the different rabies scenarios. . . .	51
3.3	Proportion of runs where rabies was eliminated from all 5 regions in response to incremental vaccination (mean and shaded 95% CI). In the endemic scenario, 22 campaigns were required to eliminate rabies from all regions. Labels mark the proportion of runs eliminated in response to no vaccination and 5, 10, 15 and 20 campaigns. Map showing the endemic scenario where all regions have rabies. Order of vaccination in the endemic scenario was determined based on the campaign placement that increased the proportion of runs eliminated. . .	52
3.4	Ratio of the proportion of infected individuals in the population with vaccination and without vaccination (blue) and the proportion of the population vaccinated (grey). Vertical lines indicate the month where the ratio of infected individuals dropped to 10% and elimination ($> 99.9\%$ of runs eliminated). . .	53

3.5 Proportion of runs where rabies was eliminated from all 5 regions over time in response to incremental vaccination (mean and shaded 95% CI). The high-risk scenario required 20 campaigns to eliminate rabies from all regions. Labels mark the proportion of runs eliminated in response to no vaccination and 5, 10, 15, and 20 campaigns. Map showing the high-risk scenario where some regions are free (white) but neighbour infected regions (red). Heatmap shows the order of vaccination in the high-risk scenario determined based on the campaign placement that increased the proportion of runs eliminated. Vaccination of the endemic regions was prioritised first, with vaccination after the birth pulse in month 56 and 68 having the greatest reductions in the proportion of runs eliminated. A minimum of 3-4 campaigns was required in neighbouring, previously rabies free regions. 54

3.6 Proportion of runs where rabies was eliminated from all 5 regions over time in response to incremental vaccination (mean and shaded 95% CI). In the endgame scenario, 9 campaigns were required to eliminate rabies from all regions. Labels mark the proportion of runs eliminated in response to no vaccination and 5 and 9 campaigns. Heatmap shows the order of vaccination in the endgame scenario, determined based on the campaign placement that increased the proportion of runs eliminated. Vaccination of the last remaining endemic region was prioritised first. Three campaigns were required in region 2, which is the largest neighbouring region in terms of both size and shared border. One campaign was required in the two other neighbouring regions (region 3 and 4). 55

3.7 Proportion of runs where rabies was eliminated from all 5 endemic regions over time under different logistical scenarios (mean and shaded 95% CI). Facets show the impact of missing 1 set of vaccination campaigns, missing 2 consecutive campaigns, and missing 2 non-consecutive campaigns and the response of adding one or two additional campaigns. Lines are coloured according to which set of campaigns were missed as shown in the legend. Sets are labeled in order of vaccination date: 1st set (month 51), 2nd set (month 58), 3rd set (month 63), 4th set (month 70), 5th set (month 75) and combinations thereof. 56

3.8 Time to elimination in response to missed campaign sets with and without additional campaign sets. Panels 1-3 show the time to elimination with no additional campaign sets, 1 additional campaign set, and 2 additional campaign sets respectively. 57

4.1 Scales explored when estimating the transmission parameters using a generalized linear model. Grid sizes range from 50x50 km² to 2x2 km². 71

4.2	Kernel density estimation of observed rabies cases in Thuringen at months 3, 20 and 50. The top panel shows the resulting smoothed kernel density surfaces for different bandwidths ($h = 1, 3, 5,$ and 10 km) where red = no rabies cases, yellow = rabies cases. The bottom panel shows the variogram and correlation estimated in cases with distance. Colours represent the different bandwidths used: $h = 1, 3, 5, 10$ (black, red, green, blue).	73
4.3	Model fit of the true infected individuals over space and time shown at 3 month intervals from 1987-1989. Colours reflect cases per sq km. Red represents high rabies incidence, gray represents low incidence, and blue represents little to no rabies incidence. In this plot you can see the different rabies foci, varying intensity in rabies cases, and the movement of rabies through time.	75
4.4	Estimated observed rabies cases from the non-separable space-time SPDE model fit to every 3rd month for each federal state level in East Germany. The red line is the mean fit to rabies case data, the shaded red region represents the 95% confidence intervals, and the black x's represent the observed cases.	76
4.5	Marginal spatial autocorrelation estimate from the non-separable space-time random process $d(s, t)$ in Equation 4.3 with mean (blue line) and 95% credible intervals (shaded).	77
4.6	Estimates of c , the heterogeneity parameter, and ρ , the transmission parameter. The multiple black circles are the parameter estimates for the different grid sizes for different realisations of the Susceptible population simulation. The red dotted line is the line of best fit used to predict ρ when c is 1. The blue dotted line shows the uncertainty (95% credible intervals) around the prediction for ρ	78
4.7	Estimates of c , the heterogeneous mixing parameter (top panel), and ρ , the transmission rate (bottom panel) plotted against the log of the aggregated grid cell size (range: log of 2 km^2 to 50 km^2).	79
4.8	GLM model fit of infected cases at time t for the smallest 6 grid sizes ($2 \times 2 \text{ km}^2$ - $10 \times 10 \text{ km}^2$) as a function of past infected cases at time $t-1$	80
4.9	GLM model fit of infected cases at time t for the larger 6 grid sizes ($13 \times 13 \text{ km}^2$ - $50 \times 50 \text{ km}^2$) as a function of past infected cases at time $t-1$	81

List of Tables

2.1	Fixed parameters used in the Bayesian hierarchical model	29
2.2	Priors used for the stochastic parameters in the Bayesian hierarchical model .	30

To my Grandpa Snuff for introducing me to Biology and my Granny Gill for reminding me of the important things in life.

Acknowledgements

On finishing my masters on grey seal movement in marine biology at Dalhousie University, I contacted Jason Matthiopoulos about projects he might have for PhD students. There were potential projects on roe deer, harbour seals, and one that probably wouldn't interest me... a project on rabies in foxes.

Not knowing much about rabies or foxes, but possessing a childhood fascination with infectious disease and thinking that studying an animal on land surely would be more straightforward than in the sea, I signed up for this endeavour.

Three and a half years later, this thesis is the result of many long hours spent learning about disease and statistical modelling techniques, research visits to Germany, Norway, Saudi Arabia, and Brazil, and incredible support from my supervisors, colleagues, collaborators, family, and friends. Thanks to the Medical Research Council for funding my PhD, especially Alexis Merry for coordinating our research training programme.

I'd like to start by thanking my supervisors Jason Matthiopoulos and Katie Hampson for their help and support throughout this PhD. I've learned so much from both of you. This project would not be what it is today without your help and guidance. Jason, you continue to amaze me with your ability to breakdown diverse ecological models into their mathematical processes all the while holding true to the underlying biology. Thank you for teaching me how to approach and analyse ecological problems, for helping me with statistics and programming, for your feedback on drafts and equations, and for getting the models out of tight places when they've been stuck. Katie, if ever there were a force of nature in infectious disease biology, it would be you. I'm amazed by the energy and passion you bring to your research every day. Thank you for answering my naïve questions about rabies and other infectious disease, for helping me with modelling and programming, and for your feedback on the many drafts, applications, and science blogs I've written these last few years. Your ability to see the wood for the trees has helped to keep this project focused on the end goal, which is to learn about rabies dynamics, improve vaccination strategies, and ultimately eliminate rabies. Thank you also for giving me the freedom to direct my training and gain experience in areas outside my PhD.

I would like to thank my co-supervisors Thomas Müller and Conrad Freuling at the Friedrich Loeffler Institut. Your expertise on foxes, rabies, and the oral rabies

vaccination programme and your feedback and guidance has been invaluable in shaping and directing the project. Thank you also to Ronald Schröder and Patrick Wysocki for helping me access the myriad of data used in this study and for being my guides in Greifswald.

I am very grateful to Håvard Rue for hosting me in Norway, Saudi Arabia, and suggesting I go to Brazil. I've benefited so much from your statistical expertise. Thank you for your kindness and willingness to teach, for taking on the role of unofficial supervisor for my last chapter, and for being so patient, especially with my semi-illiteracy when it comes to writing mathematical equations. To Håvard's lab groups and visitors who I met in Norway and Saudi Arabia, for making these places second homes and thanks to whom I now know a few statistics jokes: Anna, Tullia, Hanan, Håkon, Cristian, Henrique, Weihao, and Gulzhan. And to friends outside the department: Shelly, Marit, Helge, Roxane, Mette, Rachael, and Ivar, in Norway and Moises, Fares, Marco, Amedeo, Nick and Marco, the ultimate frisbee team, and others in Saudi Arabia who I met through diving, climbing, ultimate frisbee, and Italian.

To Elias Krainski, for hosting me in Curitiba and helping me to apply the space-time model in R-INLA to fox rabies. I've learned so much from you and could not have completed this analysis without you. Thank you for explaining countless times space-time models and model fitting in R-INLA, and for writing bespoke code to run the fox rabies model from my last chapter. I'm grateful for your friendship and advice and look forward to continuing this work in the future. To everyone at LEG: Paulo, Silvia, Walmes, Wagner, Cesar, Fernando and others, thank you for the churrasco, lunches, coffee and cake, and for going out of your way to welcome me and make me feel at home in Curitiba. To my friends Aline, Andryas and family, Vanessa, Daniela, Murillo, Jessica, Mauricio, and Tofu, for teaching me Portuguese and showing me around Curitiba and Florianópolis.

I wouldn't have finished this PhD were it not for the support of everyone in the Institute of Biodiversity, Animal Health, and Comparative Medicine (IBAHCM). I have never met such a wonderful group of scientists or worked in a more supportive and collaborative environment. You bring out the best in people and the best science from our work and I am so fortunate to be part of this wonderful community. I can't thank you enough. Thanks to Dan Haydon, Lorna Kennedy, and Heather Ferguson for their help throughout this PhD. To Jennifer Boyle at the writing centre for going through many parts of this thesis with me. Special thanks to my officemates in Rm 308: Claire, Kirstyn, Will, Joey, Nardus, Divine, Hannah, and Sonia, for putting up with me as the messiest officemate and for your advice and help navigating the PhD process. In particular thanks to Nardus, for your friendship, and for always being there to explain a technique or to help work through JAGs errors. Thank you also to Jason and Katie's lab groups, particu-

larly Mafalda and Jana, for advice on statistical modelling, interview preparation, and next steps. And also to Micaela De La Puente Leon, for discussions on fox rabies and help with the European data. And a big thank you to everyone who kept me sane by providing valuable breaks from research: Naturally Speaking, Millport, Tuesday football, Friday basketball, Cochno, ultimate frisbee, crafts, jewellery making, boardgames, Italian and Spanish, climbing and hiking. Thanks in particular to Luca, Rebby, Sara, and Davide for the many camping trips and to Jenn, Becca, and Lizzy for your friendship and emotional support. Thank you to my external examiner, Sebastian Funk, and my internal examiner, Louise Matthews, for their feedback and comments which greatly improved the content on this thesis.

Finally, I would not have made it this far without the unwavering support from my family. To my parents, Barney and Caroline, and sister Aylie who continue to inspire me, I'm so thankful for all your love and support. Thank you also to my aunts and uncles and cousins in Scotland and Ireland who have made St. Andrews and Glasgow home over the years: Looby and Johnny, Jerry and Sue, Tif and Collette, Danny, Ryan, Sarah, Katy, Lucy, Vanya and Turlough. To my Granny Gill, who despite being disappointed that I have not pursued a career in 'care for the elderly', has always been one of my biggest supporters. Thank you for reminding me of the important things in life and for teaching me to see the bright side in every situation. And to Davide, for filling each day with adventure and cheering me up when I need it most.

Declaration

This thesis, and the work contained within it, was conducted from January 2015 to June 2018 by myself, unless stated otherwise. No part of this thesis has been submitted for another degree. Elias Krainski developed the non-separable space-time model used in Chapter 4 and helped me to apply and implement this model to fox rabies using the R-INLA software.

Laurie Louise Baker

CHAPTER 1

Introduction

Introduction

Prediction of pathogen persistence and the design of effective interventions to reduce infectious disease prevalence and work towards disease elimination are key goals in epidemiology. While progress has been made towards elimination of endemic diseases, only two infectious diseases, smallpox and rinderpest in people and cattle respectively, have been successfully eradicated. There is relatively little scientific guidance as to how long control programmes must operate and how they should be best implemented to achieve elimination (Klepac *et al.*, 2013). Although it is well known that complex spatial, demographic and stochastic processes determine patterns in disease persistence, we lack full understanding of how these processes influence disease dynamics and how they can inform control programmes. Policy and practice should benefit from insights into what drives spatial and temporal patterns of persistence, how pathogens respond to control strategies, and most crucially, from statistical approaches that enable the exploration of control programmes to determine the most effective strategies.

I begin by introducing some general definitions and concepts relating to disease dynamics. I then summarise the processes influencing pathogen persistence and vaccination.

1.1 Concepts in disease dynamics

1.1.1 Definition of persistence

A range of definitions of persistence exist in the literature, with most authors using the term to suggest some degree of ‘permanence’ (Freuling *et al.*, 2013; Hay *et al.*, 2009; Lloyd-Smith *et al.*, 2005a; Onstad & Kornkven, 1992). However, how they apply the term differs and very few state the time or spatial scale over which persistence operates. Some authors reserve the term to describe when the ‘endemic state’ is reached (Onstad & Kornkven, 1992), others use persistence to also refer to the duration of an epidemic (Lloyd-Smith *et al.*, 2005a). For example, Onstad & Kornkven (1992) define endemicity as “the persistence or constant presence of a pathogen in an ecologically proper spatial unit over many generations.” In contrast, other studies often focus on the levels of infection (proportion of host population infected) in the endemic state (Hay *et al.*, 2009) and/or the presence of detected infection

(Freuling *et al.*, 2013).

In my thesis, I use persistence to refer to the continued circulation of a pathogen without extinction and I will specify a timeframe over which a pathogen persists. From a theoretical perspective persistence needs to be defined in probabilistic terms (every disease will go extinct eventually), but the debate about how to define persistence and elimination is a very practical one. Measurable criteria are needed for elimination programmes to work towards. Explicit time and spatial scales are critical when planning control strategies as these measures determine the spatial extent and duration of sustained effort required. Working definitions of persistence (or alternatively of elimination or control targets) will therefore change depending on the aims of control strategies and the geographic area and time periods that are defined. In the thesis I use the term elimination to refer to when the disease no longer circulates within a defined local extent, whereas the term eradication is reserved for when a disease is absent globally. In practice, the assessment of elimination generally relies on surveillance which is used to determine if the disease is no longer present.

1.1.2 Threshold Populations and Critical Community Size

A great deal of work in infectious disease epidemiology has focused on identifying thresholds at which a pathogen will persist or fade out. The basic reproductive number, R_0 , is defined as the number of secondary infections arising from a single case in a fully susceptible population (Anderson *et al.*, 1992). When R_0 is greater than 1, disease can spread and invade the population (Anderson *et al.*, 1992). The effective reproductive number, R_{eff} , is defined as the expected number of secondary cases caused by each infectious individual in a partially immune population (Lloyd-Smith *et al.*, 2005a). Therefore, many control measures aim to reduce the transmission such that R_{eff} is less than 1 (Barlow, 1991, 1996; Wobeser, 2002). Theoretical formulations of R_0 are typically derived for populations where homogeneous mixing (that is, individuals interacting randomly and uniformly with all others in the population) is assumed. Consequently, R_0 is never intended to apply once susceptibles are depleted. Alternative metrics and approaches have been proposed to address more complex situations (e.g. multiple classes of host (Diekmann *et al.*, 1990); spatial structure at the household and farm level (Ball *et al.*, 1997; Fulford *et al.*, 2002; Keeling, 1999; Prentice *et al.*, 2017); mechanistic movement between groups (e.g. (Cross *et al.*, 2005; Hess, 1996; Keeling & Rohani, 2002; Thrall *et al.*, 2000)). Although empirical estimates of R_0 take into account heterogeneous mixing, data is often lacking for many populations. Similarly, analytical solutions can be difficult to calculate in applied cases (Ball *et al.*, 2015; Cross *et al.*, 2007).

The concept of a threshold population has been a central one in epidemiology since the work of Bartlett on measles in the mid 1950s (Bartlett, 1956, 1957). Bartlett (1956, 1957) found that larger susceptible populations were able to better support pathogens than smaller populations

and introduced the concept of the critical community size (CCS) to define the population size for which the probability of persistence (ongoing non-extinction) after a major epidemic is 50 percent. Bartlett's seminal work has provided a basis for the use of population thresholds for disease persistence in the subsequent development of quantitative epidemiology (Lloyd-Smith *et al.*, 2005a). Lloyd-Smith *et al.* (2005a) defines critical community size (CCS) as "the host population size above which stochastic fadeout of a disease over a given period is less probable than not." Stochastic fadeout can occur either from the endemic or epidemic state. Endemic fadeout has been defined as the "extinction of the disease from a stable endemic state owing to random fluctuations in the number of infected individuals" (Lloyd-Smith *et al.*, 2005a). The main difference between endemic and epidemic fadeout is that epidemic fadeout can also occur when the pool of susceptible individuals is depleted following an epidemic, reducing the potential for ongoing transmission. Epidemic fadeout can arise from random fluctuations in the number of infected individuals or from a protracted period with $R_{eff} < 1$ (Lloyd-Smith *et al.*, 2005a).

Local elimination of infection can be achieved by driving incidence below the persistence threshold, which is defined as the point at which the disease is likely to go extinct during the troughs between epidemics (Bolker & Grenfell, 1996). However, because this does not preclude reinvasion by the disease which can be frequent (see Metcalf *et al.*, 2013), many theoretical estimates focus on the invasion threshold, the population density below which a pathogen is unable to invade the host population. Reinvasion, also termed 'rescue effects', may occur due to the migration of infected individuals (incursions) into a population following local extinction (Keeling & Grenfell, 1997; Metcalf *et al.*, 2013). Invasion thresholds relate to whether the remaining susceptible population during epidemic troughs can sustain ongoing circulation until susceptible replenishment can support a new epidemic. As a result, many control strategies aim to reduce the susceptible population below the invasion threshold through either culling or vaccination.

Vaccination decreases the probability of contact occurring between susceptible and infected individuals. Herd immunity is used in the literature to refer to the vaccination level at which there is an indirect form of protection from infectious disease that occurs when a large percentage of the population is vaccinated (Fine *et al.*, 2011). Considerable work has been spent defining threshold proportions of immune individuals to eliminate disease for diverse pathogens (Anderson, 1991; Fine *et al.*, 2011). Early theoretical work estimated the critical minimum proportion to be vaccinated as $V_c = (1 - 1/R_0)$ assuming homogeneous mixing of populations and vaccines inducing complete immunity against infection (Fine *et al.*, 2011). Other work has extended this basic model to include more realistic assumptions including imperfect immunity, heterogeneous populations, nonrandom vaccination, and freeloaders (Keeling & Rohani, 2008; Vynnycky & White, 2010).

Although some success has also been achieved in estimating the CCS in measles epidemics

(Bartlett, 1957), perhaps due to its short infectious period and high transmissibility, most diseases are unlikely to have an abrupt threshold effect, that is, a critical community size separating dynamical regimes of persistence and extinction (Lloyd-Smith *et al.*, 2005a). Instead, fadeout rates are determined by relationships between population size and the timescales of demography and transmission. The CCS is difficult to operationalize, especially for multi-host diseases, and fails to account for other relevant epidemiological characteristics such as sub-population connectivity (Mancy, 2015; Viana *et al.*, 2014). Quantifying the CCS for wildlife diseases is associated with several additional challenges, most notably a low level of study replication, lack of control effort, and little documentation on population size and failed invasion or persistence compared to datasets of infections in humans, making it difficult to assess the existence of a population threshold (Lloyd-Smith *et al.*, 2005a). Real world complexities including spatial and social structure (Hagenaars *et al.*, 2004; Keeling, 2000; Swinton *et al.*, 1998), demographic processes (Barlow, 1996; Sibly *et al.*, 2003), host pathogen coevolution (Woolhouse *et al.*, 2005), and environmental or behavioural variation (Bjørnstad *et al.*, 2002; Grenfell *et al.*, 2002) also violate the assumptions of a well-mixed host population living in a constant environment for directly transmitted pathogens (Lloyd-Smith *et al.*, 2005a). Still, threshold concepts provide a useful framework for characterising epidemics, designing control strategies, and providing targets for managers when population sizes are easily measured. Persistence increases gradually with population size (Keeling & Grenfell, 1997), therefore the size of the population can help to identify populations at greater risk. However, disease persistence also depends on demographic and transmission processes. Investigating the processes underlying thresholds including population connectivity (e.g. immigration), host demography (e.g. birth and death), and transmission can provide fundamental insights.

1.1.3 Modelling transmission

Transmission is fundamental to disease spread and persistence but is difficult to quantify. Transmission encompasses the contact rate between susceptible (S) and infectious (I) individuals, and the probability that transmission will occur during a contact (Anderson, 1991; Antolin, 2008; Begon *et al.*, 2002). In many cases these processes are captured by a single transmission term, β , and contact is assumed to be either frequency dependent ($\beta SI/N$ where N is the total host population) or density dependent (βSI). While these simplified transmission forms are mathematically convenient, they fail to capture nonlinearities and heterogeneities in transmission arising from population distribution and connectivity, local susceptible depletion, individual movement, and differences in individual behaviour. Another challenge is the scale at which transmission is approximated. Individuals tend to have more contacts with their neighbours, and the distribution of hosts and infected individuals will vary according to habitat suitability and landscape heterogeneities. However, incidence and host data is often aggregated at administrative units rather than biologically relevant units that capture local movement. Accounting for nonlinearities and heterogeneities in transmission

and extending epidemiological models to account for the spatial nature of these processes should lead to a better understanding of these processes and increase our ability to model disease dynamics.

1.2 Processes influencing persistence

1.2.1 Population connectivity

Population connectivity, also referred to as ‘spatial coupling’ (Bolker & Grenfell, 1996; Keeling & Rohani, 2002), affects both the time it takes to achieve elimination as well as how freedom from disease can be maintained once it is achieved. The distribution and density of susceptible hosts affects where disease spreads, the numbers that can be infected, and how long the disease circulates in a given location. Social systems often lead to natural fragmentation between social groups or age classes, broken only by introductions or contact with infected groups (McCallum & Dobson, 2002). Similarly, aggregation of resources will also increase contact rates (Becker *et al.*, 2015). Landscape heterogeneity and habitat quality influence both the distribution and abundance of hosts in an area as well as the reach of the pathogen. Regions with poor habitat quality and patchy resources are likely to support only weakly connected small groups of susceptible host species. Habitat fragmentation can result in decreased or limited movement of individuals between habitats and weakened connectivity between subpopulations. Fragmentation can have a positive effect of diminishing the impact of disease on a population by acting as an effective ‘quarantine’ on the infected patch. McCallum & Dobson (2002), found that where movement of the infected organism is severely limited, a ‘quarantine’ effect may occur, where the disease is confined to the isolated subpopulation. Understanding the connectivity of populations is particularly important therefore in the context of ‘rescue effects’. By seeding new epidemics and preventing localised extinctions, rescue effects prolong disease persistence (Brown & Kodric-Brown, 1977; Earn *et al.*, 2000, 1998; Hanski, 1998; Keeling, 2000).

1.2.2 Host demography

Demography refers to the processes of emigration, immigration, birth and death in a population. Host demography affects the rate of susceptible replenishment by determining the number of susceptible individuals that enter the population (birth, immigration) and the rate at which vaccinated individuals leave the population (death, emigration). Vaccination works to interrupt the transmission of infection as contacts with vaccinated individuals, which do not result in infections, occur more frequently. Indirect protection of non-vaccinated individuals from infectious disease can occur when a sufficient proportion of the population is

vaccinated to achieve ‘herd immunity’, often defined as the critical vaccination coverage, V_c , above which incidence will decline (Fine *et al.*, 2011). Herd immunity is spatially and temporal dynamic as a result of demographic processes, including the birth of new susceptible individuals and deaths of both vaccinated and non-vaccinated individuals. This is especially true for wildlife populations which are often characterized by faster population turnover compared to humans and where seasonal birth pulses are frequently observed (Peel *et al.*, 2014). Influxes of new susceptible animals may support ongoing transmission by reducing levels of herd immunity (Peel *et al.*, 2014). It is therefore important to consider how demographic processes may affect vaccination strategies for wildlife. The timing and causes of seasonality can substantially impact herd immunity and should be considered in determining how and when control measures should be applied. Optimal timing in relation to demographic processes should be explored. Birth pulses are common in many wildlife populations (Peel *et al.*, 2014). Birth pulses increase the overall size of the susceptible population and reduce the proportion of the population vaccinated and herd immunity. As such, vaccination strategies should be coordinated to coincide with the timing of important demographic events such that levels of herd immunity are maintained.

1.2.3 Behaviour and internal dynamics

Various other factors can affect persistence such as heterogeneities in transmission, including extended incubation periods, and animal behaviour (e.g. biting and running) (Hampson *et al.*, 2009). An individual’s infectiousness (i.e. the number of individuals infected) depends on host, environmental, and individual factors. Contact may occur at specific times of the year in response to seasonal drivers of food resources or at key points in the life cycle such as the mating period (Hosseini *et al.*, 2004). Another example is the seasonality in measles that is driven by mixing associated with school terms (Bolker & Grenfell, 1995). Together these factors can cause transmission to vary seasonally and act in combination with external factors with unknown impacts on disease dynamics (Bjørnstad *et al.*, 2002; Grenfell *et al.*, 2002; Koelle & Pascual, 2004). ‘Superspreading events’, in which certain individuals infect an exceptionally large number of secondary cases, are more common in disease spread than previously thought (Lloyd-Smith *et al.*, 2005b). Contact tracing has been used to investigate variation in transmission (Gani & Leach, 2004; Hampson *et al.*, 2009). Lloyd-Smith *et al.* (2005b) investigated the role of individual variation in outbreak dynamics using continuous distributions to describe the ‘individual reproductive number’, ν to represent the number of secondary cases caused by a particular infected individual. While the importance of these factors are increasingly recognized, data on individual movement patterns and individual variation in immune responses and/or incubation periods are limited. In many cases, transmission is still modeled as an average transmission rate across a population of individuals (Diekmann & Heesterbeek, 2000).

1.3 Vaccination

Vaccination reduces the probability of transmission by interrupting the chain of infection as contacts occur between infected and vaccinated individuals. However, coverage, that is the proportion of the population vaccinated, is temporally and spatially dynamic as a result of demographic processes. As herd immunity wanes due to population turnover, isolated infections can become reconnected with susceptible hosts, maintaining transmission. Once a disease has been eliminated from a given region, the movement of infected individuals between regions and the transmissibility of the pathogen determine the probability of re-emergence, or ‘rescue effects’ (Klepac *et al.*, 2013). In the absence of vaccination, the number of susceptible individuals in the population may increase, leaving the region vulnerable to potentially large outbreaks if infection is reintroduced. It is therefore important to understand the role of turnover and population connectivity on disease dynamics when determining the timing and placement of vaccination efforts (Beyer *et al.*, 2012; Bourhy *et al.*, 2016).

Traditional efforts to control wildlife disease typically aim to reduce the size of the susceptible host population below a threshold, such that the population of susceptible hosts is small and weakly connected (Grenfell & Dobson, 1995; Ramsey *et al.*, 2002). Target vaccination coverages are determined for individual pathogens depending on their transmissibility (R_0) and demographic turnover (Pulliam *et al.*, 2007). However, common metrics used to study disease persistence including R_0 , critical community size, and population thresholds, do not account for heterogeneity of populations and control efforts over space and across time which can mean that empirical observations differ from theoretical predictions (Bolker & Grenfell, 1996; Lloyd-Smith *et al.*, 2005a).

1.4 Wildlife disease

Many animal populations are characterised by fast demographic rates compared to humans, such that the herd immunity achieved through vaccination is relatively short-lived (Grenfell & Dobson, 1995). Likewise, movement of wildlife is often very different to human movement (e.g. social groups, territory boundaries, limited dispersal, habitats and geographical features that direct/impede spread (Altizer *et al.*, 2003)). Moreover, observing transmission directly is rarely possible. In most cases, the state variable (disease incidence) is only known through indirect measures, with the probability of observing the disease varying over time. Because surveillance only captures a small proportion of circulating infections, failed invasions or low level persistence may be missed entirely. In addition, surveillance data is often aggregated, making the study of local transmission processes challenging. Wildlife populations are often not monitored closely, therefore key aspects of their size and spatial distribution are unknown. Lastly control programmes targeting wildlife are often difficult to implement and monitor.

Capturing local transmission processes and understanding the spatiotemporal dynamics of wildlife disease spread from coarse and incomplete data is a major technical challenge that holds the key to many theoretical questions and practical decisions. A wildlife disease that can shed light on many of these challenges is rabies.

1.5 Rabies

Rabies is a deadly and terrifying disease that exacts a heavy toll on human lives and national economies. Rabies is a negative stranded RNA virus belonging to the lyssavirus genus and causes acute encephalitis in a wide range of mammals (Rupprecht *et al.*, 2008). Despite infecting and being transmitted by a range of mammalian hosts, reservoirs only include mammals within the Orders *Carnivora* (e.g. dogs, raccoons, skunks, foxes, jackals) and *Chiroptera* (bats) (Lembo *et al.*, 2010). In the absence of vaccination the disease is nearly 100% fatal. More than 59,000 humans die of rabies each year, with many thousands more requiring expensive life-saving post-exposure vaccines (Hampson *et al.*, 2015). The majority of deaths occur in Africa and Asia from dog-mediated rabies, and worldwide economic losses are estimated at 8.6 billion USD (Hampson *et al.*, 2015).

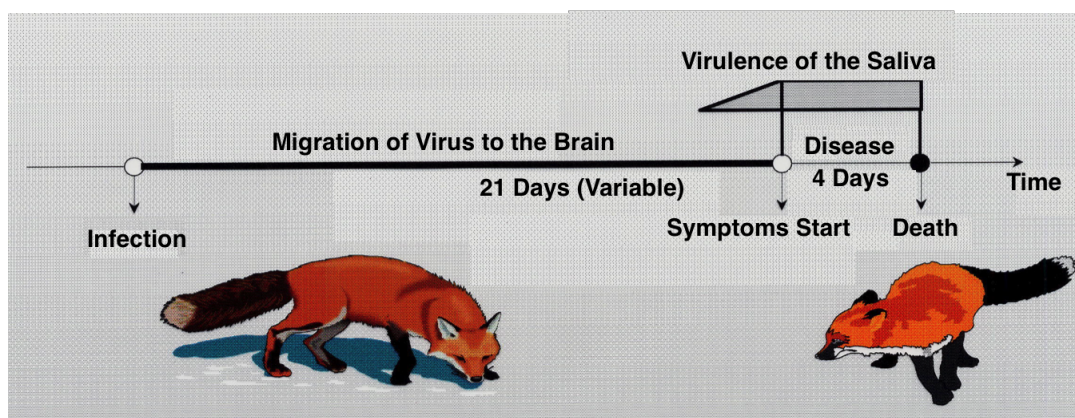


Figure 1.1: Stages of rabies infection in the red fox. ©Friedrich Loeffler Institut

In Europe, the main wildlife reservoir is the red fox (*Vulpes vulpes*). In foxes, disease progression follows several stages (Figure 1.1). Rabies virus is spread through the bite of an infected animal. After a fox is bitten, the animal passes into an ‘incubation period’, during which time the virus migrates from the site of the initial infection to the brain through the peripheral nervous system. During this period, that is on average 21 days (Toma & Andral, 1977), the fox shows no symptoms of the disease. At the end of this period, virus is shed in the fox’s saliva, and the animal shows signs of the disease. During the infectious period which lasts on average 5 days, the fox can pass on the infection (Anderson *et al.*, 1981).

The red fox is the most widespread terrestrial mammal (Schipper *et al.*, 2008). Foxes live in

both rural and urban areas and are found in habitats ranging from tundra to arid environments (Harris & Smith, 1987; Lindström, 1989; Pils & Martin, 1978; Saunders *et al.*, 2002). Foxes are territorial and divide the landscape into non-overlapping territories. They follow a distinct annual cycle: mating, reproduction, breeding, dispersal, resettlement, mating, etc. (Toma & Andral, 1977). They exhibit a marked birth pulse, with females giving birth to on average five young cubs with up to 14 cubs per litter (Ansorge, 1990; Lloyd *et al.*, 1976). In autumn (September-October), the young foxes leave the den and disperse.

1.6 The elimination of fox rabies in Western Europe

The origin of fox rabies in Europe is still a matter of debate. While some scientists believe that the epidemic of fox rabies started south of Kaliningrad during World War II as a result of a sustained spill-over from dogs, recent studies have revealed the existence of similar rabies virus lineages in the Asian part of Russia (Deviatkin *et al.*, 2017; Kuzmin *et al.*, 2004). Whatever the virus origins, the epidemic in foxes spread rapidly through Europe in coming decades (Figure 1.2).

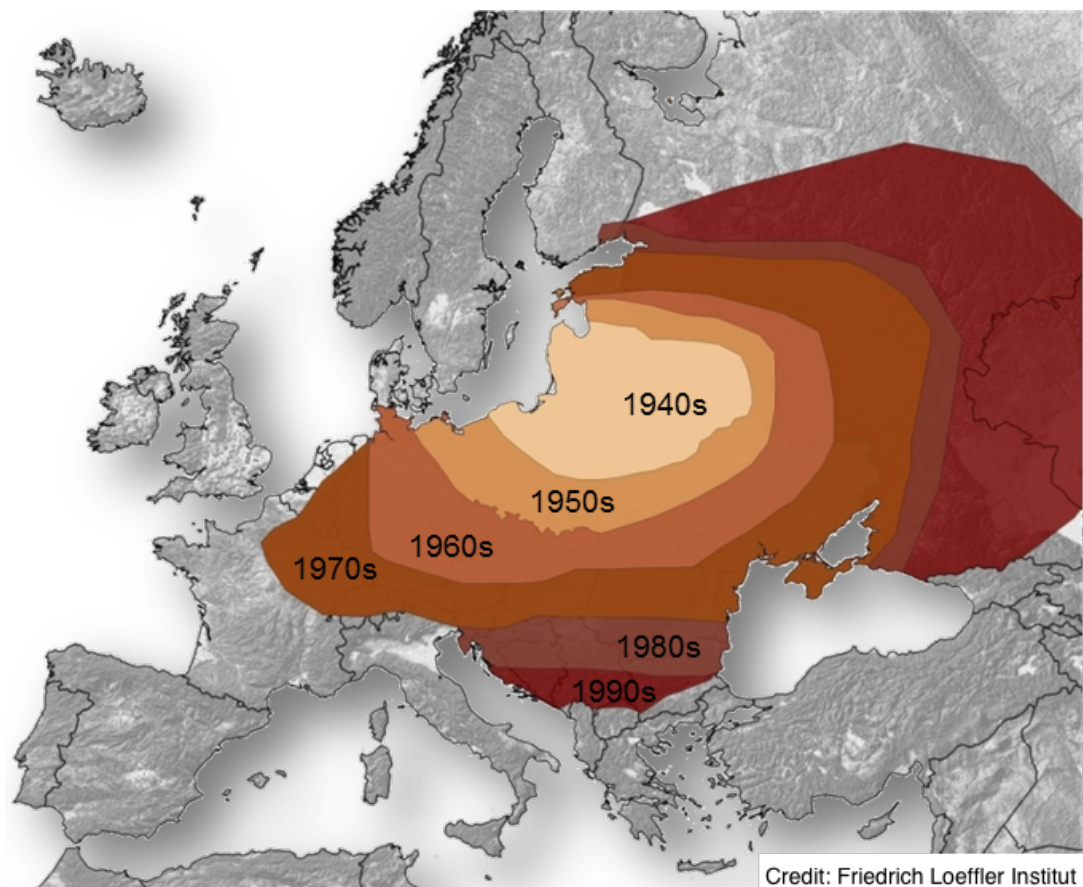


Figure 1.2: The decadal spread of rabies from the 1940s to 1990s. ©Friedrich Loeffler Institut

Rabies has since been eliminated from 9 countries in Western Europe using baits containing vaccine. Over 30 years, vaccine-loaded chicken heads (Pastoret *et al.*, 1988), later replaced by fish-meal baits (Brochier *et al.*, 1990), were distributed over 2.36 million square kilometres in one of the most successful, long-term, and large-scale attempts to control a wildlife disease (Figure 1.3).

This unique history is captured in the Rabies Bulletin Europe database which consists of national rabies surveillance data compiled by the World Health Organisation (WHO) Collaborating Centre for Rabies Surveillance and Research at the Friedrich Loeffler-Institut (FLI) in Germany. Spanning over 30 years and 15 countries, the fox rabies database consists of georeferenced rabies cases and vaccine control efforts (Figure 1.4).



Figure 1.3: Fixed wing aircraft were used to distribute vaccine-loaded chicken heads in the early days of vaccine distribution. ©Friedrich Loeffler Institut

The data is characterised by a wealth of natural experiments in the form of differences in the commencement, geographic extent, and timing of vaccination campaigns. The long-term and large-scale nature of the data provides the opportunity to explore the dynamics of spread and persistence in differing epidemiological situations. The high temporal and spatial resolution of the data also allow for the development and application of sophisticated spatial modelling techniques. Together these data have the potential to generate fundamental and applied insights into the elimination of infectious disease, specifically those relating to persistence and invasion dynamics.

The continued presence of rabies in Europe highlights the need for technical guidance and contingency planning to prevent outbreaks, maintain rabies freedom, and strategically implement control measures to rapidly eliminate emerging disease. Effective planning of vaccination programmes is central to achieving these objectives. However, we have only a limited quantitative understanding of how control measures should best be implemented under different scenarios. A key challenge faced by managers is determining realistic timelines for control and elimination. Ending control measures too early could lead to re-emergence (e.g. rinderpest), but costs of continued control can be difficult to justify especially when new cases are no longer being reported (Klepac *et al.*, 2013). Similarly, the impact of delayed or

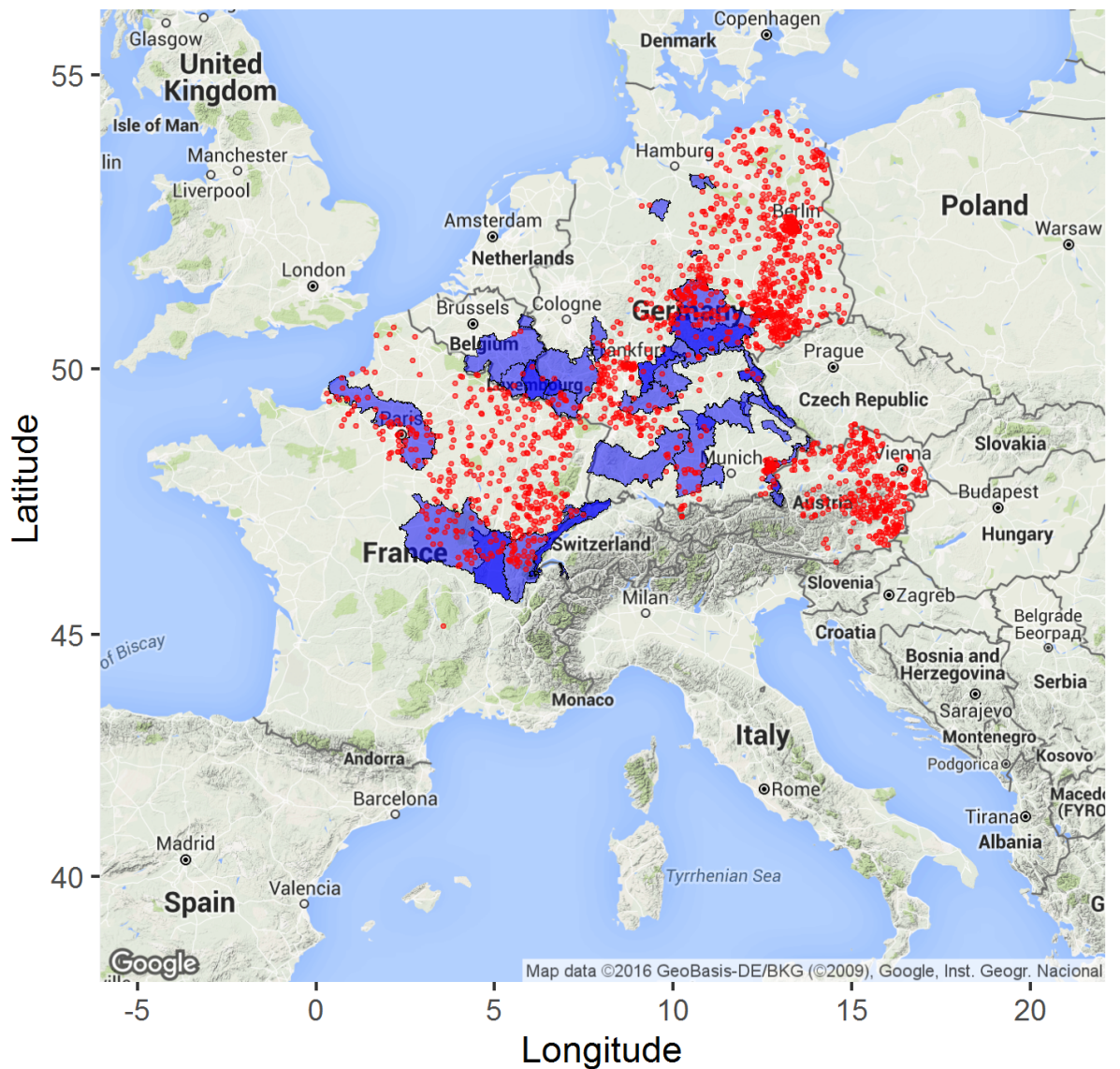


Figure 1.4: Map of Western Europe showing detected rabies cases (red dots) and areas vaccinated (blue polygons). Over 30 years, 2.36 million km² (2 times the size of Europe) were vaccinated leading to the elimination of rabies from 9 countries in Western Europe.

missed campaigns, due to budget or operational constraints, on time to elimination is not well understood. Until elimination is achieved in all regions, vaccination efforts, surveillance, and mobilized public health and veterinary staff are required in both affected and neighbouring areas. Realistic estimates of the time to eliminate a pathogen and greater understanding of the impact of logistical constraints on this timeline should help to guide policies and better manage expectations.

1.7 Thesis overview

My thesis focuses on two pivotal questions in infectious disease ecology: what are the underlying determinants of disease persistence and how can vaccination strategies be optimized to eliminate infection? To answer these questions, I analysed a rich and highly resolved spatial dataset of fox rabies cases in Germany. The long-term, large-scale nature of these data from the oral rabies vaccination (ORV) programme that eliminated rabies from over 9 countries, provides a unique opportunity to improve our understanding of wildlife rabies dynamics in response to vaccination using novel spatial modelling techniques.

Variability in epidemiological data arises from infectious disease dynamics, including stochastic spatial transmission processes, and observation errors in detecting cases. I used two Bayesian approaches to deal with these sources of uncertainty: state-space modelling and latent Gaussian models. Bayesian state-space models are able to accommodate uncertainty in epidemiological data through linked biological and observation process models. In the second approach, I fit the model using the computationally efficient integrated nested Laplace approximation (INLA) approach developed by Rue *et al.* (2009). INLA is designed to fit latent Gaussian models in a Bayesian context in which spatial and temporal autocorrelation in the latent field assume a shared spatial structure and are reflected by Gauss Markov random fields (GMRF) (Rue & Held, 2005). The flexibility and computational capacity of INLA has great potential to provide novel insights into epidemiological processes through the analysis of complex spatial data. Within the INLA framework, the stochastic partial differential equations (SPDE) approach constructs flexible fields that are able to handle datasets with complex spatial structure (Krainski, 2018; Lindgren *et al.*, 2011). Krainski (2018) has further extended these models to consider non-separable space-time models that are closely-linked to heat equations in physics and simultaneously capture spatial and temporal autocorrelation. The temporal extensions offered by this non-separable model mean that spatially-explicit dynamical problems can now be approached with numerical efficiency and provide the opportunity to generate new insights into these processes through fitting these models to data. This approach may be able to capture the spatiotemporal nature of disease transmission and therefore has considerable application for understanding epidemiological processes in disease ecology, particularly for wildlife diseases such as rabies that spread through direct contact.

1.8 Thesis organisation

My thesis is compiled as a collection of 3 chapters in paper format. As each chapter has its own introduction and discussion, I include only a brief introduction (chapter 1) and a general discussion (chapter 5).

Capturing regional connectivity and understanding the effectiveness of vaccination campaigns has immediate application to the rabies situation in Europe and elsewhere. In chapter 2, I create a model that incorporates local transmission (within regions) and spatial coupling (between regions) by fitting a Bayesian state-space model to three decades of observed fox rabies incidence and oral rabies vaccination campaigns from Eastern Germany.

Realistic estimates of the time required to eliminate a pathogen and greater understanding of the impact of missed campaigns should help to guide policies and better manage expectations. In chapter 3, I extend the model developed in chapter 2 to determine the best vaccination strategy, in terms of scale and duration of ORV efforts, for three common epidemiological scenarios: (1) endemic: rabies circulates endemically across all of space; (2) high-risk: several areas are rabies-free but neighbour endemic areas; (3) endgame: rabies has been largely eliminated but remains present in one region.

Targeted spatial vaccination planning has great potential to reduce costs and inform elimination strategies. However, developing models that can capture and explain the spatiotemporal infectious processes in wildlife populations remains a challenge. In chapter 4, I develop a space-time model capable of capturing the spatial and temporal dynamics of fox rabies dynamics over the last 3 decades in Eastern Germany. I then used the output from this model to estimate the spatial dependence between cases and explore the effect of scale on the estimates of transmission terms by aggregating incidence data at different spatial resolutions.

In chapter 5, I discuss how insights gained from my PhD work have helped shed light on fundamental questions of how infectious diseases persist and can be controlled. I then explain how these findings can be used to improved policies to guide elimination programmes. I also discuss the methodological contributions made in this thesis.

CHAPTER 2

Capturing rabies transmission and
metapopulation persistence in European
foxes

Capturing rabies transmission and metapopulation persistence in European foxes

2.1 Abstract

Disease dynamics play out across space, irrespective of borders. Yet, both data collection and control strategy implementation are often carried out at the level of administrative units rather than epidemiologically relevant ones. Capturing local transmission processes and spatial coupling between regions from coarse and incomplete data is therefore a major technical challenge that holds the key to both theoretical questions and practical decisions.

The European fox rabies epidemic has been brought largely under control by immunizing foxes using baits containing vaccine. Currently, the European Union (EU) co-finances oral vaccinations to eliminate rabies in EU member and border states and to maintain disease freedom via a cordon sanitaire. Developing a model to capture within region dynamics and spatial coupling has immediate application in Europe and to other parts of the world where oral vaccinations are planned.

By fitting a Bayesian state-space model to three decades of observed fox rabies incidence and oral rabies vaccination campaigns from Eastern Germany, I show that biological understanding can be gained from inference from partially observed data on wildlife disease. Specifically I find that (i) incorporating heterogeneous mixing into the functional form of the transmission can help capture rabies dynamics at the regional level; (ii) by allowing for incursions (migrating infected individuals) from other regions, re-emergence of the disease is possible even if eliminated locally from a region; (iii) herd immunity achieved through bi-annual vaccination campaigns is short-lived due to population turnover, highlighting the need for regular and sustained vaccination efforts. Together, these findings have important implications for ongoing vaccination efforts in large parts of Eastern and Southern Europe.

2.2 Introduction

Disease dynamics and their effective control are underpinned by the interplay between population connectivity and the localized nature of transmission (Bolker & Grenfell, 1995; Keeling *et al.*, 2001; Levin & Durrett, 1996; Rohani *et al.*, 1999). Many diseases circulate primarily through local interactions (Anderson *et al.*, 1992; Keeling & Rohani, 2008), but are managed at coarse administrative scales. We therefore typically only have aggregate population-level data on the occurrence of infections which makes it difficult to disentangle the extent to which metapopulation persistence depends on local transmission (within-region) or spatial coupling between subpopulations (between regions). Researchers therefore model the macroscopic characteristics of the disease (metapopulation dynamics) using approximations aiming to capture interactions between infected and susceptible individuals at the local level (local dynamics) (Glass *et al.*, 2003; Liu, 1987; Liu & Levin, 1989; Liu *et al.*, 1986; McCallum *et al.*, 2001, 2017).

Several studies have quantified the spatial components of transmission, including multiple classes of host (Diekmann *et al.*, 1990), spatial structure at the household and farm level (Ball *et al.*, 1997; Fulford *et al.*, 2002; Keeling, 1999; Prentice *et al.*, 2017) and mechanistic movement between groups (Cross *et al.*, 2005; Hess, 1996; Keeling & Rohani, 2002; Thrall *et al.*, 2000). However, these studies have largely focused on human and livestock populations where detailed information about movement, transmission, and host populations is available (e.g. Keeling *et al.* (2001); Matthews *et al.* (2003)). Few have studied the role of migrating infected individuals, incursions, in the persistence of disease in wildlife populations.

Many animal populations are characterised by fast demographic rates compared to humans, such that the herd immunity achieved through vaccination is relatively short-lived. Likewise, movement of wildlife is often very different to human movement (e.g. social groups, territory boundaries, limited dispersal, habitats and geographical features that direct/impede spread). Approaches to understand interactions between spatial and demographic processes are likely to reveal key insights into the persistence of disease in wildlife populations.

Epidemiological data are inherently complex due to variability arising from both the infectious disease dynamics, including stochastic spatial transmission processes, and the observation errors in detecting cases. The study of wildlife disease dynamics is particularly challenging for several reasons. First, observing transmission is rarely possible and surveillance only captures a proportion of circulating infections. Wildlife populations are often not monitored closely, and knowledge of their size and spatial distribution is typically limited and imprecise. Estimates of abundance are often based on hunting data rather than more costly density-based methods making it difficult to reliably estimate population density (Sonnenburg *et al.*, 2016). In many cases, the state variable (disease incidence) is only known through indirect measures (veterinary records, hunting reports), with large observation errors that may vary

over time. Low levels of disease detection mean that failed invasions or low level persistence may be missed entirely. Second, surveillance data is often necessarily aggregated in time and space based on administrative management units. This makes it challenging to capture and understand local dynamics of disease spread occurring at finer spatial scales. Finally, vaccination programmes targeting wildlife are often difficult to implement and monitor.

To capture the effect of individual interactions on disease dynamics at the population level, researchers have typically focused on population mixing. Traditional epidemiological models that assume homogenous mixing (that is, individuals interacting randomly and uniformly with all others in the population) have yielded important insights such as thresholds for disease invasion and control (Anderson *et al.*, 1992; Kermack & McKendrick, 1927; Smith *et al.*, 2005). But these models have not accounted for heterogeneous mixing as a result of local movement, which will be critical for directly transmitted diseases in wildlife populations. Individual-based models that include explicit interactions within discrete spatial or social neighbourhoods (Bolker & Grenfell, 1995; Pastor-Satorras & Vespignani, 2001) require detailed data that is rarely available for wildlife populations. Ecologists and epidemiologists have begun to use different approaches to account for heterogeneous mixing when the details of individual-level processes are unavailable. For example, heterogeneous mixing parameters to capture variation in contact patterns between susceptible and infected individuals (Glass *et al.*, 2003; Liu *et al.*, 1986; Roy & Pascual, 2006) as well as to prevent unrealistic epidemic sizes in predictions (Glass *et al.*, 2003). In practice, these parameters can be difficult to estimate because they are confounded with other transmission parameters in the model. These approaches have been effective for human diseases such as cholera (Koelle & Pascual, 2004) and measles (Bolker & Grenfell, 1995), but have not been applied to wildlife diseases such as rabies.

Rabies has been eliminated from fox populations throughout much of Europe by immunizing foxes using baits containing vaccine. In just over three decades, vaccine baits distributed across 2.36 million km², through Oral Rabies Vaccination (ORV) programmes, have resulted in the elimination of the disease from Western and Central Europe (Cliquet *et al.*, 2014; Freuling *et al.*, 2013; Müller & Freuling, 2012; Müller *et al.*, 2015). Since the late 1980s the European Union (EU) has co-financed ORV fox rabies elimination programmes in member and border states (Demetriou & Moynagh, 2011; Freuling *et al.*, 2013; Müller & Freuling, 2012). Understanding the role of regional connectivity and the effectiveness of vaccination campaigns therefore has immediate application to the rabies situation in Europe and elsewhere.

Metapopulation models explicitly model the spatial structure of processes by representing space as a network of multiple subpopulations or patches with different rates of movement (or coupling) between them (Bolker & Grenfell, 1996). Combined with state-space methods capable of accounting for the uncertainty inherent in epidemiological data, and a transmission process that approximates the scaling from individual interactions to metapopulation

dynamics, these models provide a framework to model local (within region) dynamics and to estimate the rate of incursions (migrating infected individuals).

Several studies have been central for guiding control of fox rabies in Europe. Anderson *et al.* (1981) incorporated red fox population biology into a simple deterministic, compartmental model to summarize the dynamics between host and pathogen interactions and to predict the effect of control methods such as culling and vaccination. Spatially explicit individual-based models (IBM) have been used since to evaluate vaccination strategies for elimination (Eisinger & Thulke, 2008; Thulke *et al.*, 1999) and emergency vaccination of rabies under limited resources (Eisinger *et al.*, 2005; Thulke *et al.*, 2008). My model adds to this considerable body of work by being the first to estimate the rate of incursions using a model fit to data.

Capturing local transmission and external incursions is key to modelling metapopulation persistence and has important implications for the planning of ongoing vaccination programmes in EU member and border states. Here, I examine fox rabies dynamics in response to vaccination using a hierarchical Bayesian state-space model fit to fox rabies incidence data from Eastern Germany from 1982-2013. I use a metapopulation approach to study rabies persistence and to quantify the rate of external incursions. Through simulation I demonstrate how incorporating heterogeneous mixing is important to capturing local (within region) rabies dynamics. Lastly, I evaluate the impact of ORV on rabies incidence. This study presents a first step towards capturing local transmission processes and connectivity between regions from coarse and incomplete data for wildlife rabies.

2.3 Methods

I investigated monthly time series of fox rabies cases for the period 1982-2013 from 5 federal states in Eastern Germany (Brandenburg, Mecklenburg-Vorpommern, Sachsen, Sachsen-Anhalt, and Thüringen) in relation to the timing of ORV campaigns in these areas. A hierarchical Bayesian state-space model was developed to explore within-region and between-region dynamics of rabies transmission and to evaluate the impact of ORV on monthly rabies incidence. I begin with an overview of the data used and then describe the structure of the state-space model and the fitting process.

2.3.1 Data Collection

Records of laboratory-confirmed rabies cases in foxes were compiled from regular reports by the national veterinary authorities and summarized for each federal state (hereafter referred to as region) on a monthly basis (Freuling *et al.*, 2013). Specimens of suspect rabid foxes were submitted by veterinarians, hunters, wildlife managers, and the general public (Freuling

et al., 2013). From 1993, cross-sectional sampling was also conducted, whereby a proportion of foxes hunted were tested for rabies providing a measure of rabies prevalence in the population. The timing of ORV campaigns in each region was also compiled (Müller & Freuling, 2012). The Rabies Bulletin Europe (RBE), is a database consisting of national rabies surveillance data collected and evaluated by the WHO Collaborating Centre for Rabies Surveillance and Research at the FLI in Germany (Freuling *et al.*, 2013). A monthly average number of confirmed rabies cases was calculated from the RBE quarterly reports for bordering regions in Poland and the Czech Republic.

2.3.2 Bayesian State-Space Model

A discrete time stochastic metapopulation model with three states: Susceptible (S), Infected (I), and Vaccinated (V), was developed to model the numbers of foxes and rabies cases in different regions through time. The Bayesian approach allowed me to complement the rabies case data with prior information on some of the model’s parameters from historical studies on fox rabies dynamics and fox demography and to compare explicit mechanistic processes. The model combined several latent demographic, vaccination, transmission, and observation processes.

A demographic process was used to model the numbers of susceptible and vaccinated foxes in each region at monthly time steps. The starting susceptible population and carrying capacity for each region were extracted from the literature and were based on the average density of foxes per km² and multiplying this by the region size (Ansorge, 1990; Iossa *et al.*, 2008; Lloyd *et al.*, 1976). Births occurred in April of each year, with newborn foxes entering the susceptible population in July coinciding with when they venture further from their den and are more likely to encounter a rabid fox. All susceptible and vaccinated foxes older than one year of age were considered reproductively active. This means that surviving newborns from the past year give birth the following April. I assume that infected individuals transmit rabies and die within the same month, such that infectious animals now (t), transmit infection to new animals that subsequently develop rabies the following month ($t+1$). No exposed class was considered because the latent period of rabies infection lasts an average of three weeks and thus all new infections at t become symptomatic by month $t+1$ (Toma & Andral, 1977). Data on the timing of vaccination campaigns in each region were incorporated explicitly. Here, I describe the model structure in terms of the three state variables: S, I, and V.

Susceptible individuals S in region r , in month t were modeled as a function of juvenile foxes entering the susceptible population three months after birth $j_{r,t}$ and surviving individuals $C_{r,t}$ and those removed due to vaccination $V_{r,t}$ or infection $I_{r,t}$:

$$S_{r,t+1} = j_{r,t} + C_{r,t} - V_{r,t} - I_{r,t} \quad (2.1)$$

Where the first term $j_{r,t}$ is a Binomial distributed variable representing juvenile foxes entering the susceptible population three months after birth and takes the form:

$$j_{r,t} \sim Bin(s, a_{r,t}) \quad (2.2)$$

where s is the survival probability and $a_{r,t}$ are the newborn foxes. Foxes have a maximum age of about 4 years (Iossa *et al.*, 2008). If we assume that only 1% of foxes are alive at age 4 years (48 months) we can use the following expression to determine the monthly survival probability: $s^{48} = 0.01$, $s = 0.01^{(1/48)} = 0.9085176$.

$$a_{r,t} \sim Poisson(\alpha_{r,t}(S_{r,t} + V_{r,t})e^{\epsilon_y}) \quad (2.3)$$

$$\text{where } \alpha_{r,t} = \begin{cases} \alpha_{r,t} & \text{if } t = t_0 + k12 \\ 0, & \text{otherwise} \end{cases}$$

$$\epsilon_y \sim N(0, \tau) \quad (2.4)$$

where α is the per capita annual birth rate in region r in month t applied to all susceptible S and vaccinated V individuals in the system. Fecundity is regulated by annual fluctuations in the environment, e^{ϵ_y} . Here, I use the exponential term e^{ϵ_y} and a normal prior centred around 0 for ϵ_y to capture the effect of environmental noise on the size of the birth pulse. Under the exponential, when ϵ is 0, then $e^0 = 1$, meaning there is no change in the size of the birth pulse. An ϵ smaller or greater than 0 will result in a smaller or larger birth pulse, respectively. The prior for the precision term, τ , is specified such that the birth pulse can vary by $\pm 10\%$ in line with fluctuations in the birth pulse observed in fox populations in the wild (Lindström, 1988).

The realised per capita annual birth rate with density dependence takes the form:

$$\alpha_{r,t} = \frac{b\lambda_r}{\lambda_r + S_{r,t} + V_{r,t}} \quad (2.5)$$

where b is the maximum annual per capita reproductive rate. Here, the inclusion of S and V leads to density dependence, whose strength is controlled by the parameter λ_r (derived in Appendix A) in the different regions r and takes the form:

$$\lambda_r = \frac{(s-1)K_r}{1-s-b/12} \quad (2.6)$$

where s is the survival probability and K_r is the carrying capacity in region r . Infecteds are ignored in expressions 2.5 (birth) and 2.15 (vaccination) because I believe that infected individuals health is significantly impaired by rabies such that they will not deplete baits or contribute to the population. There will be exceptions, and there is a question of timing (did the fox eat a bait before showing rabies symptoms?) but these are thought to be small enough that they can be ignored.

The second term in equation 2.1 comes from a Binomial distribution and represents the surviving susceptible individuals in region r and month t ,

$$C_{r,t} \sim Bin(s, S_{r,t}) \quad (2.7)$$

where s is the survival probability and is assumed to be fixed across time and regions.

Infected individuals are modelled as:

$$I_{r,t} = (1 - \rho_r)I_{r,t}^* + \sum_{i \neq r} \rho_i l_{i,r} I_{i,t}^* \quad (2.8)$$

where the $I_{r,t}^*$ is the number of infected individuals in region r prior to any movement. Infected individuals leave the region with probability ρ_r . The summation term represents incursions from other regions as a function of rabies incidence $I_{i,t}^*$ in region i , the proportion of infected animals leaving region i : ρ_i , and $l_{i,r}$ the proportion of those moving to region r . This can be modelled in different ways, but here I chose to equate it to the proportion of the border of region i that is shared with region r . I only considered the movement of infected animals as healthy animals are more likely to be faithful to their home range, with the exception of rare seasonal excursions. Where a healthy fox has moved outside its territory, I do not believe that there will be significant changes in the population in neighbouring regions that will affect the carrying capacity and density.

The probability of leaving ρ_i was calculated as:

$$\rho_i = \frac{\rho_{max} \sqrt{A_{min}}}{\sqrt{A_i}} \quad (2.9)$$

Where ρ_{max} is the maximum leaving rate. Under a diffusive assumption for movement the leaving rate is expected to decrease as the size of the region increases relative to its perimeter

and the probability that any given infected animal moves outside of its region declines. To capture this effect, I scaled the leaving rate by dividing it by the area of the region $\sqrt{A_i}$, which is proportional to how far individuals are from the perimeter of the region.

In the model, new infections are generated within region r from a Binomial distribution:

$$I_{r,t+1} \sim \text{Bin}(p_{r,t}, S_{r,t}) \quad (2.10)$$

where the new infected individuals $I_{r,t}$ at time $t + 1$ in region r are generated from the susceptible individuals S with a risk of transmission probability $p_{r,t}$ represented by:

$$p_{r,t} = \frac{I_{r,t}}{hA_r + I_{r,t}} \quad (2.11)$$

Here hA_r is the half-saturation point for $p_{r,t}$, that is the number of infected individuals that raise the transmission probability to 0.5. I assume that this number is only a function of the total area of the region, appropriately scaled by the constant h which is estimated from the data. Subsequently, the risk of infection $p_{r,t}$ depends on the density of infected individuals $\frac{I_{r,t}}{hA_r + I_{r,t}}$ in the region, with the transmission rate per infected individual decaying as the number of infecteds individuals grows.

The biological rationale behind this equation is that in larger areas, susceptible individuals are expected to be less accessible to infected individuals due to the greater travel distance required to reach them. The addition of infected individuals in the denominator allows us to account for saturation effects that occur at high incidence, when infected individuals might produce less infections because they have fewer susceptibles to infect due to disease-induced mortality or because local contacts might be made to already latent animals, corresponding to local correlations in infection. Local susceptible depletion then causes reductions in the transmission rate of each infected individual at high incidence, that is, each infected individual has a reduced probability of transmitting infection.

The functional form of the transmission is a special case of the general model in equation 35 from Liu *et al.* (1986): *Influence of nonlinear incidence rates upon the behavior of SIRS epidemiological models*,

$$S^q G(I) = S^q \frac{kI^{p-1}}{1 + mI^{p-1}} \quad (2.12)$$

Where S is the susceptible population, I is the number of infected individuals and k , p , q , and m are positive constants. If we assume that q is 1, $G(I)$ can be written as

$$G(I) = \frac{kI^{p-1}}{1 + mI^{p-1}} \quad (2.13)$$

If we consider the special case where $p = 2$, $m = (hA)^{-1}$, $k = hA$ and $q = 1$ then

$$G(I) = \frac{kI}{1 + mI} \quad (2.14)$$

$$G(I) = \frac{\frac{k}{m}I}{\frac{1}{m} + I} \quad (2.15)$$

which is equivalent to

$$G(I) = \frac{I}{hA + I} \quad (2.16)$$

The time evolution of the number of vaccinated individuals is modelled as:

$$V_{r,t+1} = v_{r,t} + X_{r,t} \quad (2.17)$$

where $v_{r,t}$ represents the newly vaccinated individuals drawn from a binomial distribution and $X_{r,t}$ represents surviving vaccinated individuals.

$$v_{r,t} \sim B\left(\nu \frac{S_{r,t}}{S_{r,t} + V_{r,t}}, S_{r,t}\right) \quad (2.18)$$

where ν is the rate of bait uptake by the population of susceptible and vaccinated individuals in region r at time t . To account for the depletion of baits by already vaccinated conspecifics, the rate of bait uptake by susceptible individuals is determined relative to their proportion in the population $\frac{S_{r,t}}{S_{r,t} + V_{r,t}}$. Vaccination is switched on and off by an indicator variable that is 0 in all months apart from those when a vaccination campaign occurred when it equals 1. The term X in eq. (10) represents the surviving vaccinated individuals from the previous time step drawn from a binomial distribution similar to eq. (6) where s is the survival probability.

$$X \sim Bin(s, S_{r,t}) \quad (2.19)$$

where s is the survival probability.

I assumed that the true number of infected individuals $I_{r,t}$ were observed imperfectly each year with annual probability θ_y :

$$\widehat{I}_{r,t} \sim \text{Bin}(\theta_y, I_{r,t}) \quad (2.20)$$

The observation probability θ varies stochastically on an annual basis.

In the cross-sectional sampling regime, hunted foxes $H_{r,t}$ had a probability of being observed to be infected equal to the risk of transmission $p_{r,t}$.

$$\widehat{H}pos_{r,t} \sim B(p_{r,t}, H_{r,t}) \quad (2.21)$$

where $\widehat{H}pos_{r,t}$ is the number of positive cases out of the total foxes hunted $H_{r,t}$.

2.3.3 Model evaluation

To assess the model fit I used a probability integral transform, testing whether the observed rabies cases can reasonably be assumed to be arising from the chosen model. This was done by comparing the observed number of rabies cases to the posterior distribution of the expected number of infected cases estimated from the MCMC samples, calculating the percentile where the data point fell within the cumulative distribution function (Czado *et al.*, 2009). Because the credible intervals are calculated from the posterior of the expected values and not the posterior of the prediction, which also includes an error term, the credible intervals are more conservative and reflect only the uncertainty around the regression and not the prediction. As a result, they are narrower than the credible intervals of the prediction because they do not include this error.

To assess the model fit through time I plotted the computed monthly probability integral transform values through time. To explore the full range of potential rabies epidemic scenarios within the parameter space I simulated from the model providing the same initial conditions including the size of the region, carrying capacity, initial number of starting susceptible and infected individuals, and rates of vaccination. I also assessed the model predictions when the model was provided with the first data point and when the model was provided with 20 data points.

2.4 Model Fitting

All models were fitted using the software JAGS (Plummer, 2002) which uses Gibbs sampling to generate posterior distributions of the parameters given the likelihood, prior distributions and the data itself. I ran the models for 3,000,000 iterations, with a burn-in of 30,000 and a thin interval of 300 giving 10,000 samples. I inspected the model for convergence and effective sample size. To account for the fact that rabies had been circulating in Germany since the late 1940s, I started the model 10 years (120 time steps) prior to when the time series began to allow the system to settle at an endemic equilibrium. Fitting of the model required considerable computational time and a compromise in what parameters were estimated in order for the model to converge. This was resolved pragmatically by fixing some parameters that were not central to the research questions or for which good quality information was available (Table 2.1). I was primarily interested in estimating four main parameters: the heterogeneity parameter for the transmission equation h , the probability of an infected fox leaving an area ρ_{max} , the observation rate θ , and the precision τ of the environmental noise (Table 2.2).

The heterogeneity parameter h for transmission was given a gamma prior with mean 4 and variance 9. The posterior for h was both within the broad support of the prior and much more precise than the prior, because of the data.

I experimented with the sensitivity of the model to the parameter θ , quantifying the detectability of cases. Allowing too much flexibility to this parameter caused the model to explain the majority of cases in terms of detectability, rather than incidence. However, these more flexible models tended to settle on posterior values for θ that were too large compared to expert opinion for rabies and the known limits of passive disease sampling in general. Specifically, I found that wider priors for θ (e.g. mean = 0.10, variance = 0.01), went to biologically implausible areas of parameter space (around 30-40% of cases observed). The more flexible model also resulted in larger unrealistic values of h and poor model convergence, that I believe is due to the biological processes not being captured effectively. I addressed this pragmatically by incorporating expert opinion into our prior for detectability (mean = 0.05, variance = 0.00025). I noticed that the posterior (while still remaining within plausible detectability values) tended to drift to the right of the prior with only a small increase in precision (Figure 2.1). The posterior was in the range of realistic values we would expect for θ . As this did not impact the model fit, this suggests that the functional form of transmission that I used captured the underlying epidemiological process and was able to reproduce patterns of incidence at the scale of administrative units.

I chose a prior for ρ_{max} (rate at which infected foxes leave their focal region) where the posterior, informed by data, would have to move away from 0, ‘no movement’, to support connectivity between regions. Because infected foxes have a limited dispersal range, I ex-

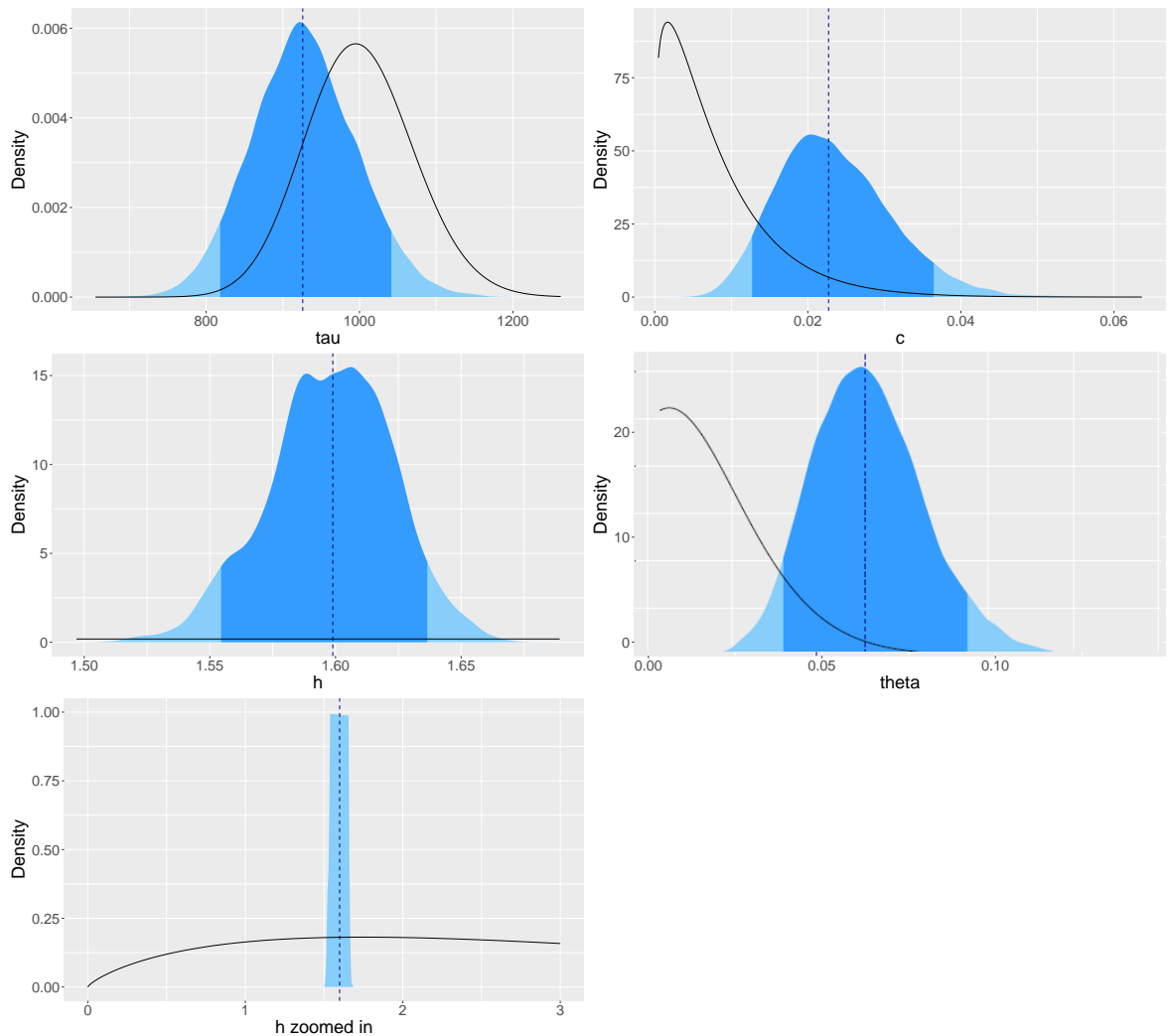


Figure 2.1: The posterior distribution and priors for the parameters estimated in the hierarchical Bayesian state-space model. The posterior distribution is shaded in blue, the black line represents the prior distribution. In order from top to bottom and left to right are the parameters representing fluctuations in fecundity due to environmental noise τ , migration of rabid foxes between regions c i.e. ρ_{max} in the equation, rabies transmission h , and the annual probability of observing rabies cases θ . The posterior and prior for the transmission parameter h is shown again in the bottom left panel of the plot to better show the prior chosen.

pected the value of ρ_{max} to be small. To limit the search to a biologically plausible range of values for the leaving rate, I used a Beta prior with mean 0.004 and variance 0.000005 that declined with distance from 0. The posterior supports this hypothesis by moving away from 0. The precision of the environmental noise term τ was given a gamma prior with mean 1000 and variance 5000, based on fluctuations in fox reproductive effort reported in the literature (Lindström, 1988). This allowed the litter size (or birth pulse) to vary between 0.9 and 1.1 of the mean litter size each year. The posterior distribution shifts to the left of the prior, which suggests that the population fluctuates slightly more than specified by the prior. Although this is larger than that reported for Lindström (1988), the posterior for

fluctuations rarely exceeded 10% with the largest values reaching 15%. This could be due to more extreme environmental changes during this period or in Germany in comparison to Sweden where Lindstrom's study was conducted.

I was not able to get the JAGs model to run with a linear functional form of transmission. I tested different initial values, as well as including a check to prevent the transmission rate, which has a binomial distribution from going above 1. However I was still not able to get the model to run in jags. From what I have observed in the simulation of the model with linear transmission, if the parameter h is slightly higher, this results in the epidemic fizzling out, whereas a lower value of the transmission parameter means that the epidemic is very large. My hypothesis is that the jags model struggles to fit the model because both scenarios are very far from the data observed. In contrast, the functional form of transmission that incorporates heterogeneous mixing, prevents this explosive behaviour by including the infected individuals in the denominator. This means that the transmission rate approaches an asymptote as the number of infected individuals increase. Because I have not been able to compare the models formally, I have explored this through simulation.

Variable	Description	Parameter	JAGS code	Value	References
Birth	per capita birth rate	b	b	4	Anderson <i>et al.</i> (1981); Iossa <i>et al.</i> (2008)
Survival	survival probability	s	s	0.908	Iossa <i>et al.</i> (2008); Thulke <i>et al.</i> (1999)
Area (km^2)	Size of region	A	A		
Shared border (km)	15 x 15 matrix	l	qb		
Carrying Capacity	region 1	K_1	$K[1]$	140000	
	region 2	K_2	$K[2]$	110000	
	region 3	K_3	$K[3]$	90000	
	region 4	K_4	$K[4]$	95000	
	region 5	K_5	$K[5]$	90000	
Area (km^2)	region 1	A_1	$A[1]$	29479	
	region 2	A_2	$A[2]$	23180	
	region 3	A_3	$A[3]$	18146	
	region 4	A_4	$A[4]$	20446	
	region 5	A_5	$A[5]$	16172	

Table 2.1: Fixed parameters used in the Bayesian hierarchical model

Variable	Parameter	JAGS code	Distribution	Prior	Mean and variance	Reference
Leaving probability	ρ	c	Beta	dbeta(1.26176, 156.45824)	(0.008, 5e-5)	
Heterogeneity parameter	h	h	Gamma	dgamma(1.7777, 0.4444)	(4, 9)	
Vaccination Rate	ν	v	Beta	dbeta(12.3, 28.7)	(0.3, 0.005)	Robardet <i>et al.</i> (2016)
Environmental Noise	τ	tau	Gamma	dgamma(200, 0.2)	(1000, 5000)	Lindström (1988)
Observation Probability	θ	obs1	Beta	dbeta(9.45, 179.55)	(0.05, 0.00001)	
Population Region 1		start_pop[1, 1]	Gamma	dgamma(50.06, 0.0007)	(70750, 100e6)	
Population Region 2		start_pop[2, 1]	Gamma	dgamma(30.95, 0.0006)	(55632, 100e6)	
Population Region 3		start_pop[3, 1]	Gamma	dgamma(18.97, 0.0004)	(43550, 100e6)	
Population Region 4		start_pop[4, 1]	Gamma	dgamma(24.08, 0.0005)	(49070, 100e6)	
Population Region 5		start_pop[5, 1]	Gamma	dgamma(15.06, 0.0004)	(38813, 100e6)	

Table 2.2: Priors used for the stochastic parameters in the Bayesian hierarchical model

2.5 Results

I fit a hierarchical Bayesian state-space model to fox rabies case data and ORV vaccination efforts from 5 federal states, hereafter referred to as regions, in Eastern Germany for the period 1982-2013 to explore local transmission (within-region) and spatial coupling (incursions) in metapopulation dynamics and to evaluate the impact of ORV on monthly records of rabies incidence. My model was able to accommodate uncertainty in the biological and observation processes, infer missing time series of infected, susceptible, and vaccinated individuals by latent process methods.

Across all regions the number of reported annual cases ranged from 959-2375 pre-vaccination. There was 2277 cases in 1990, the first year of vaccination, where vaccination occurred in either April or April and either September or October (depending on the year) in each region. This was followed by a swift decline in cases to 1643, 321, 28, 4 in the following years.

Fitting the model to the fox rabies case data generated key estimates of local rabies transmission and spatial coupling between regions that have important implications for rabies control. The model was able to capture key aspects of fox demography including the birth pulse, fluctuations in fecundity with environmental noise, and changes in monitoring, yielding a close fit to rabies case data from all 5 regions (Figure 2.2).

The multi-year peaks in the observed data are largely explained by the annual birth rate and variations in the annual observation rate and environmental noise which vary over time (Figure 2.3). The environmental noise term influences the size of the susceptible population by increasing or decreasing the size of the birth pulse. Under the current model this in turn results in more infected individuals. Similarly, a larger observation rate will mean that a greater number of cases were detected and a fewer number of cases overall.

I was not able to fit the model with the linear functional form of transmission in jags, therefore I cannot formally investigate the effect of individual-level interactions on local rabies transmission (heterogeneous mixing). However, I can comment on the behaviour observed when simulating from the model. My simulations of the model with the linear functional form of transmission show that when a linear transmission form is considered the dynamics are very fragile. Very small changes in the parameter h (values explored range from 1.6-1.8 (blue to red orange)) result in either an early fade out of disease or an explosive increase in the number of cases (Figure 2.4). These two characteristics, which disagree with the time series data provided, may explain why the jags model was unable to fit the model with the linear transmission form, despite the apparently minor difference in the two functional forms of transmission: $I/(hA+I)$ compared to $I/(hA)$. An important feature of the functional form of transmission that incorporates heterogeneous mixing is that it prevents this explosive behaviour by including the infected individuals in the denominator.

To investigate spatial coupling, I estimated the number of incursions (migrating rabid foxes) from neighbouring regions. Incursions accounted for on average 1% or less of monthly rabies cases in a region, with the mean number of incursions varying between 0 and 2 per month in each region and from 0-12 per year. Low numbers of estimated external incursions from 2000 onwards reflect coincident declines in rabies cases in all 5 regions resulting from coordinated vaccination efforts.

Herd immunity achieved through regular ORV campaigns, wanes rapidly due to the annual influx of susceptible individuals. Herd immunity peaked at between 60-75% of the population vaccinated in each region (Figure 2.2). Swift reductions in herd immunity occurred after entry of juvenile foxes into the population three months after the birth pulse (July), decreasing the percentage of vaccinated individuals in the population by more than half. Between annual entry of juvenile foxes, herd immunity is maintained as there is no difference between the survival of vaccinated or susceptible individuals. The rapid change in herd immunity following entry of juvenile foxes into the population highlights the need for regular and coordinated vaccination campaigns to maintain coverage. During the study period, the majority of vaccination campaigns were coordinated, with 65 campaigns (67%) occurring simultaneously in all 5 regions and only 12 campaigns (12.3%) conducted in isolation.

From the plot of the probability integral transform calculated from the MCMC samples of the model fit, we can see that model fails to capture the largest peaks in the observed cases (Figures 2.5 and 2.8). The model also misses some of the observed cases between the birth pulses, when the population is at its lowest. In the model mortality is constant across the population, however it has been shown in other studies that juvenile foxes experience a higher rate of mortality in the first months of life. Therefore, one might expect in nature that the population would swiftly drop after the birth pulse due to high juvenile mortality and be followed by more gradual changes in the population. The changes in the observed cases are more variable compared to that expected from the model. This is likely due to the fact that the model allows for annual changes in the probability of detection and environmental variability rather than monthly changes. This was a deliberate modelling choice, as I found that allowing for too much flexibility in the detection probability or environmental noise (i.e. allowing these variables to vary by month or have a wider prior) resulted in overfitting of the data and came at the expense of convergence of the other parameters, in particular the transmission parameter. Even though the fitted model expects a more gradual and smoothed number of cases than the observed data and the credible intervals are misleadingly narrow, the expectation is not far off from the actual number of cases observed and the model successfully captures the effect of vaccination.

To explore the characteristics and predictive capability of the model further, I simulated from the fitted model providing the same initial conditions including the size of the region, connectivity between regions, carrying capacity, starting susceptible and infected individuals,

and vaccination coverage. I explored the model predictions when provided with the first case in each region and the first 20 cases in each region using the probability integral transform to assess the prediction. In both predictions, the most dominant features were oscillations occurring due to entry of the juvenile foxes three months after the birth pulse (Figures 2.6, 2.7, and 2.8). In the first prediction, when the model is only provided with the first data point, all of the cases fall within the credible intervals and the majority of data points are within the middle 50% of the credible intervals. This suggests that the model overestimates uncertainty (Figures 2.6 and 2.8). The model predictions improves when provided with the first 20 starting data points and is good at projecting the long-term behaviour and decline of rabies, however it misses the tail end of the cases (Figures 2.7 and 2.8). Although the credible intervals around the model predictions reduced when more data was provided. However, the model was not able to capture multi-year oscillations in cases, which in the model fit were explained by annual fluctuations in environmental noise and variation in the annual observation rate.

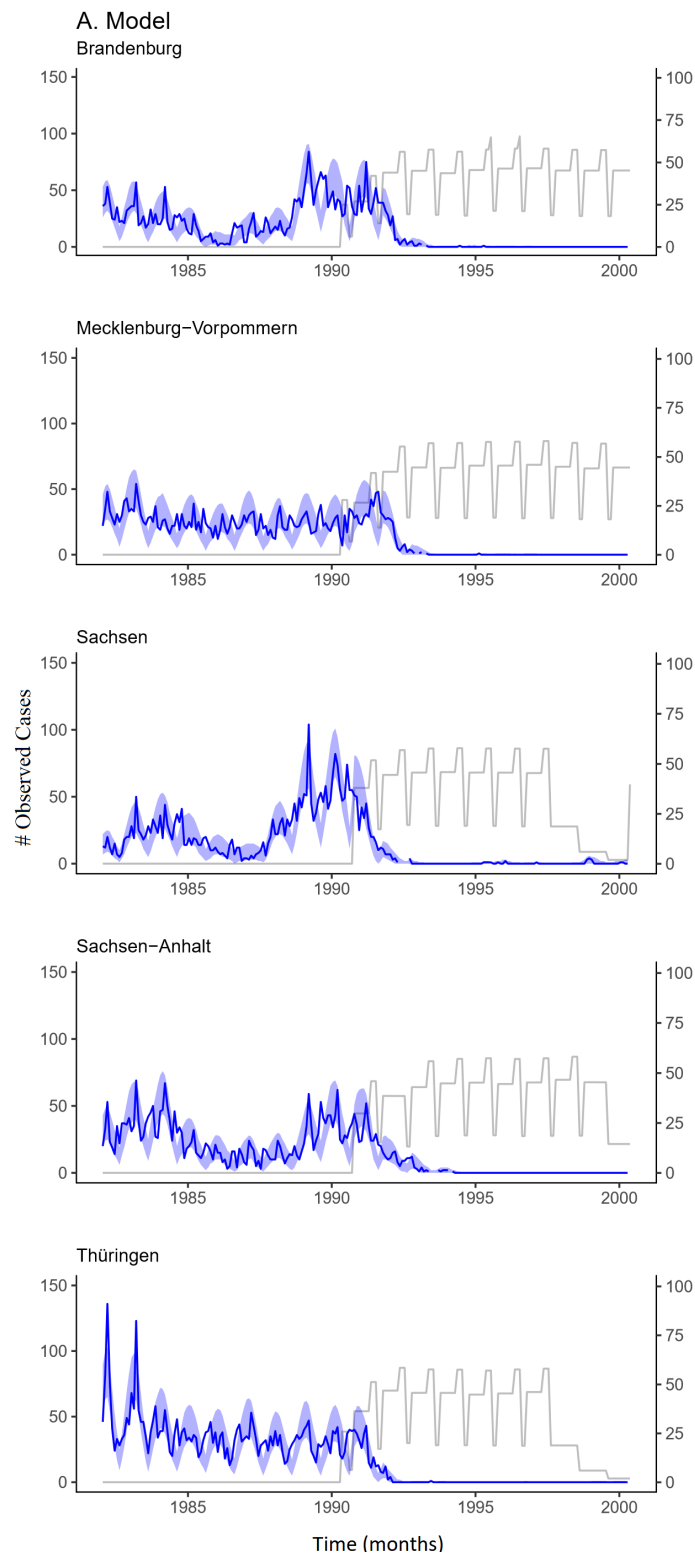


Figure 2.2: State-space model results for 5 federal states in Eastern Germany: Brandenburg, Mecklenburg-Vorpommern, Sachsen-Anhalt, Sachsen, and Thüringen. The left y-axis is the number of observed cases, the right y-axis is the percentage of the population vaccinated. The x-axis indicates the time (months). The gray line represents estimated percentage of the population vaccinated. The dark blue line is the monthly reported rabies cases for each region. The light blue shaded region is the 95% credible intervals.

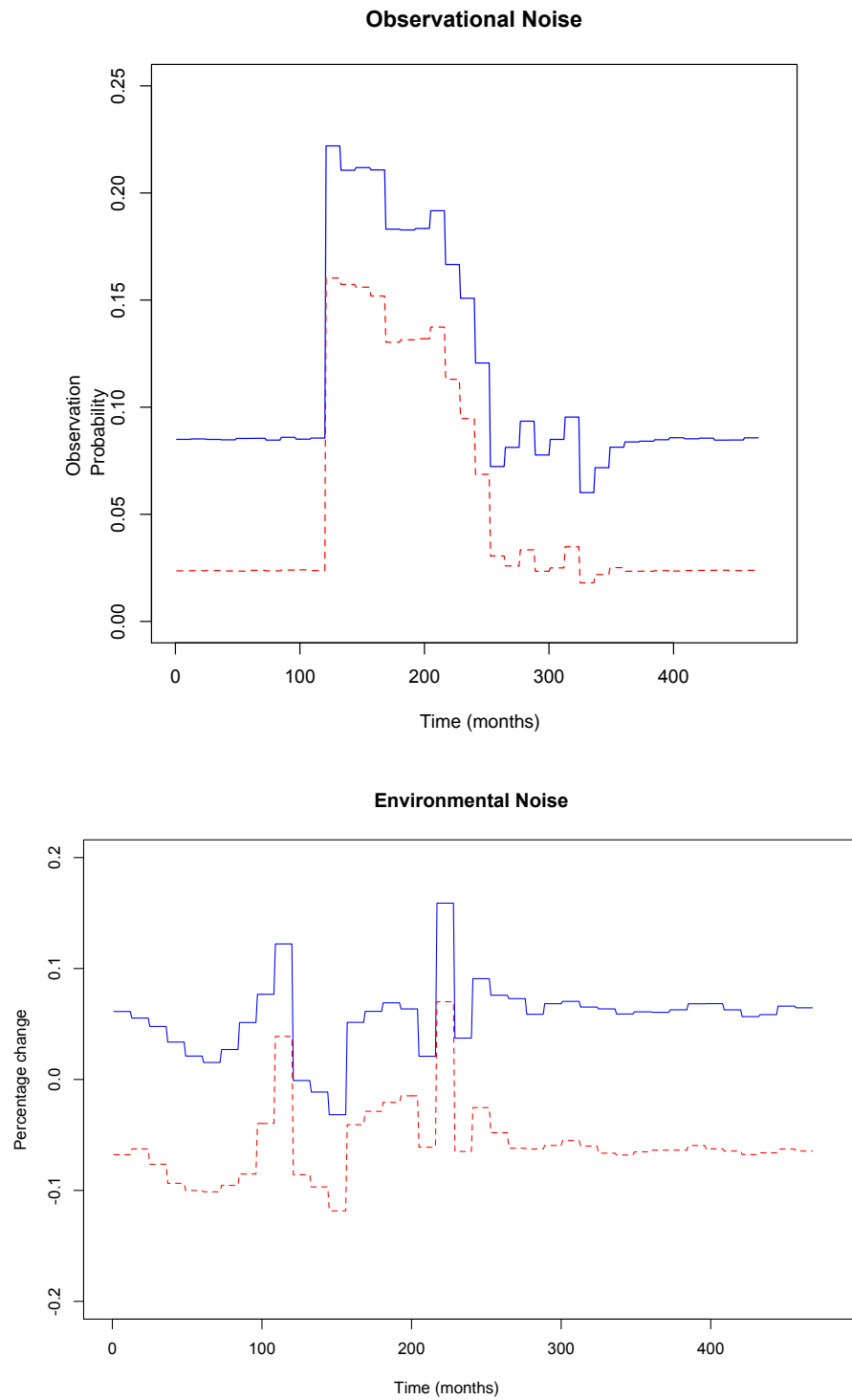


Figure 2.3: Observational and environmental noise estimates over time (months). The blue line is the upper 95% CI and the red line is the lower 95% CI. The environmental noise parameter fluctuates between -10 and $+15\%$. The observational noise term peaks at around 18%

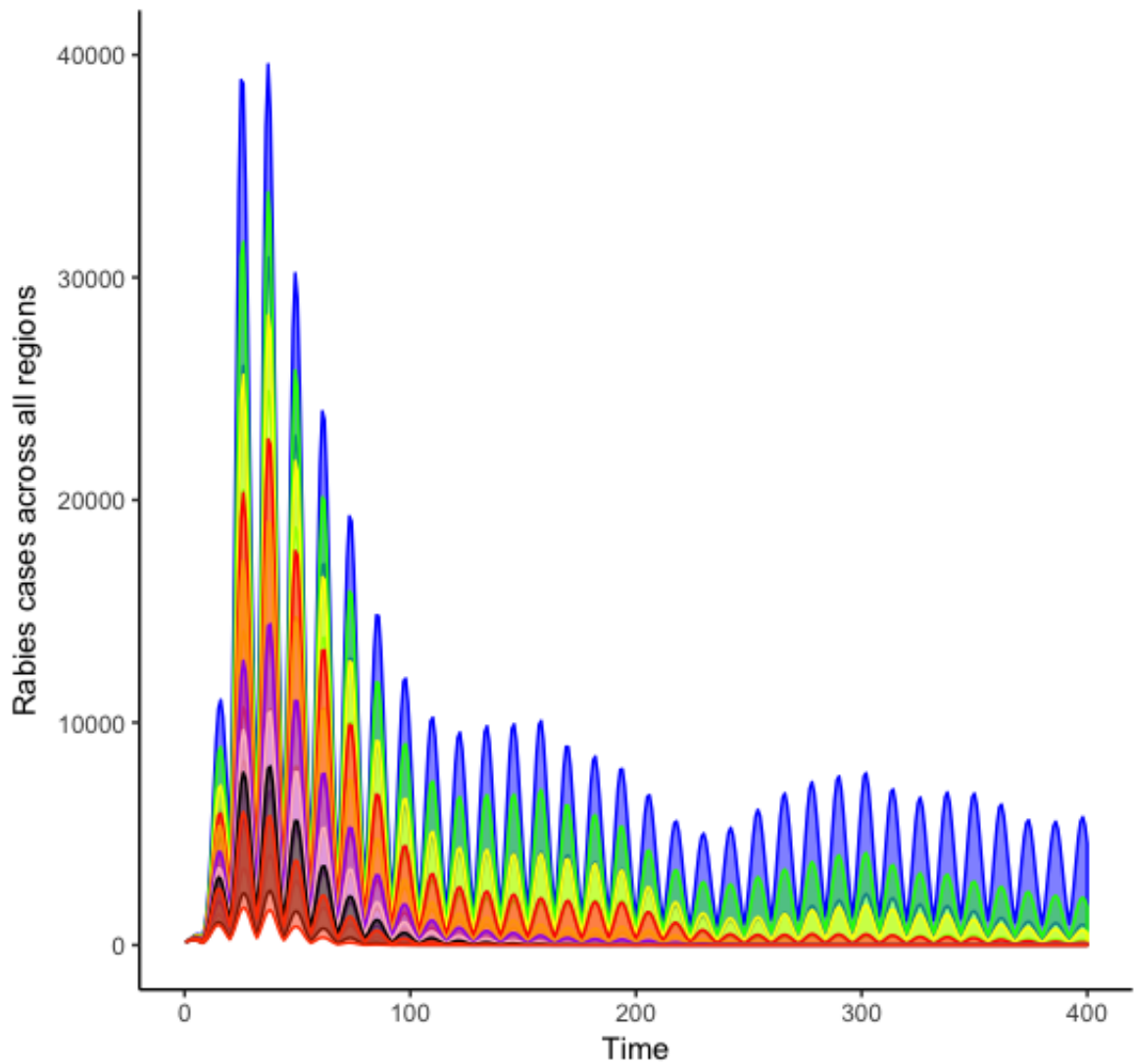


Figure 2.4: The total number of simulated rabies cases at monthly time steps across all 5 regions from the model using the linear transmission form $I/(hA + I)$. Several values for h were explored: 1.6-1.8 (blue to red orange) at 0.025 intervals. The linear form of the transmission equation seems to be very sensitive to the value of h chosen. The resulting time series show unrealistically large epidemics early on when values between 1.6-1.7 are chosen (around 20-40,000 cases across all regions) or an early drop in the number of cases to also unrealistic levels. I hypothesize that these two characteristics may explain why the jags model was unable to fit the model with the linear transmission form.

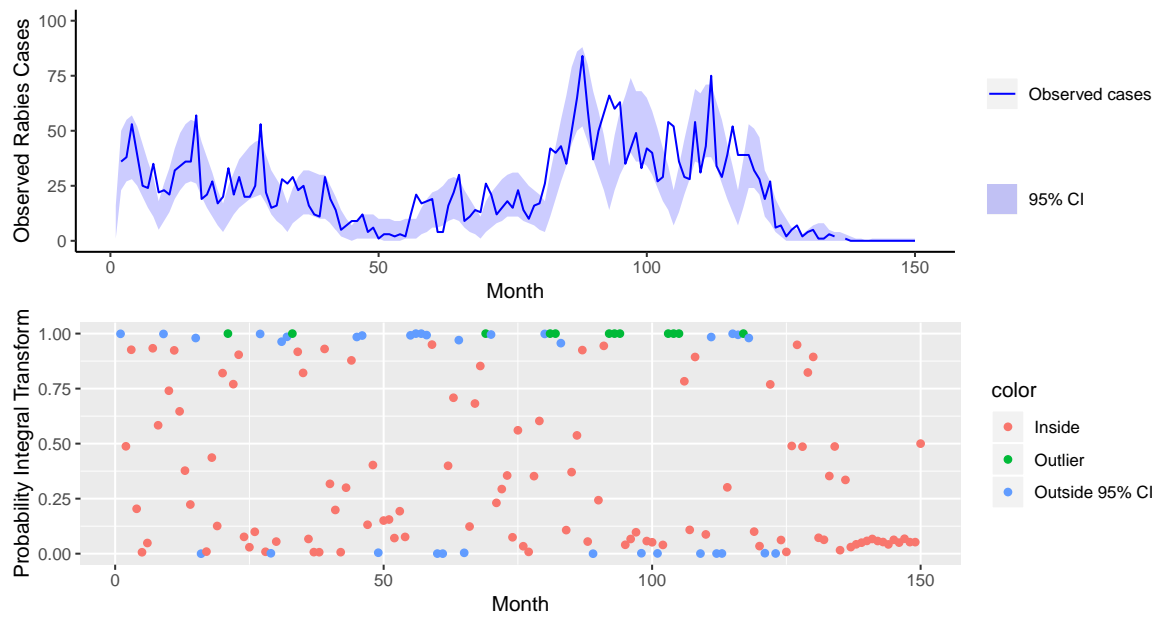


Figure 2.5: Probability Integral Transform for the model fit. The top panel shows the model fit to the observed rabies cases over time in Region 1. The dark blue line represents the observed rabies cases and the light and dark shaded blue region represents the 95% and 50% Credible Intervals (CI) estimated from the MCMC samples, respectively. The bottom panel shows the probability integral transform over time (where the observed case falls in the cumulative distribution function). The colours in the probability integral transform plot indicate whether the observed cases falls inside (red) the 95% CI, outside (turquoise) the 95% CI but within the 100% CI

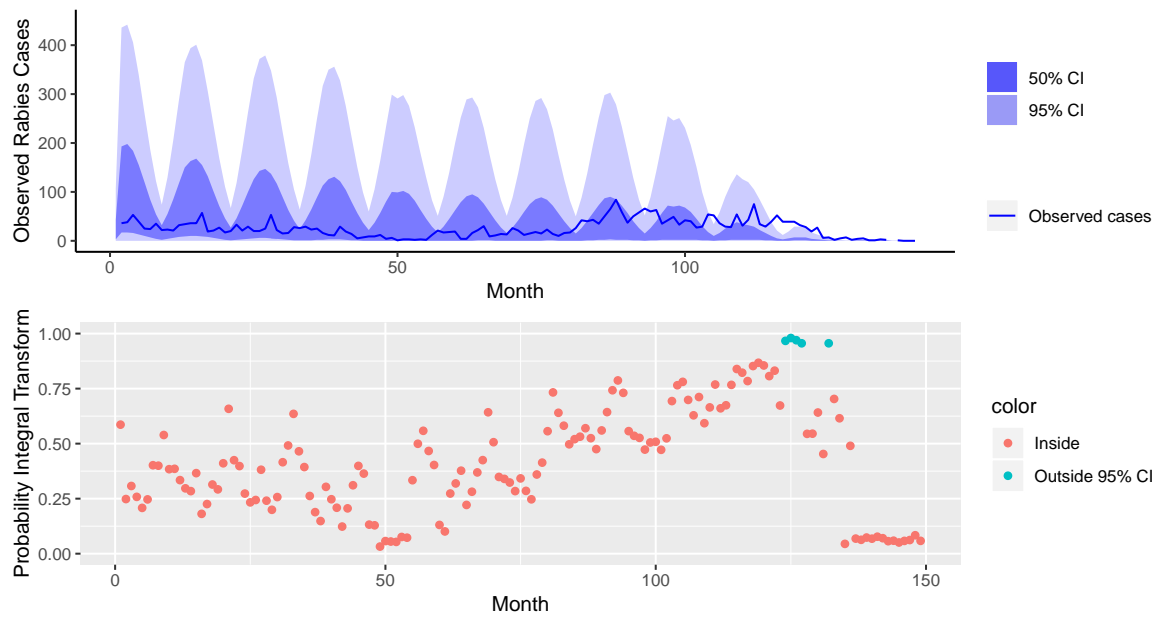


Figure 2.6: Probability Integral Transform: Prediction with first data point. The top panel shows the model fit to the observed rabies cases over time in Region 1. The dark blue line represents the observed rabies cases and the light and dark shaded blue region represents the 95% and 50% Credible Intervals (CI) estimated from the MCMC samples, respectively. The bottom panel shows the probability integral transform over time (where the observed case falls in the cumulative distribution function). The colours in the probability integral transform plot indicate whether the observed cases falls inside (red) the 95% CI, outside (turquoise) the 95% CI but within the 100% CI, or outlier (green) when the case falls outside the CI entirely.

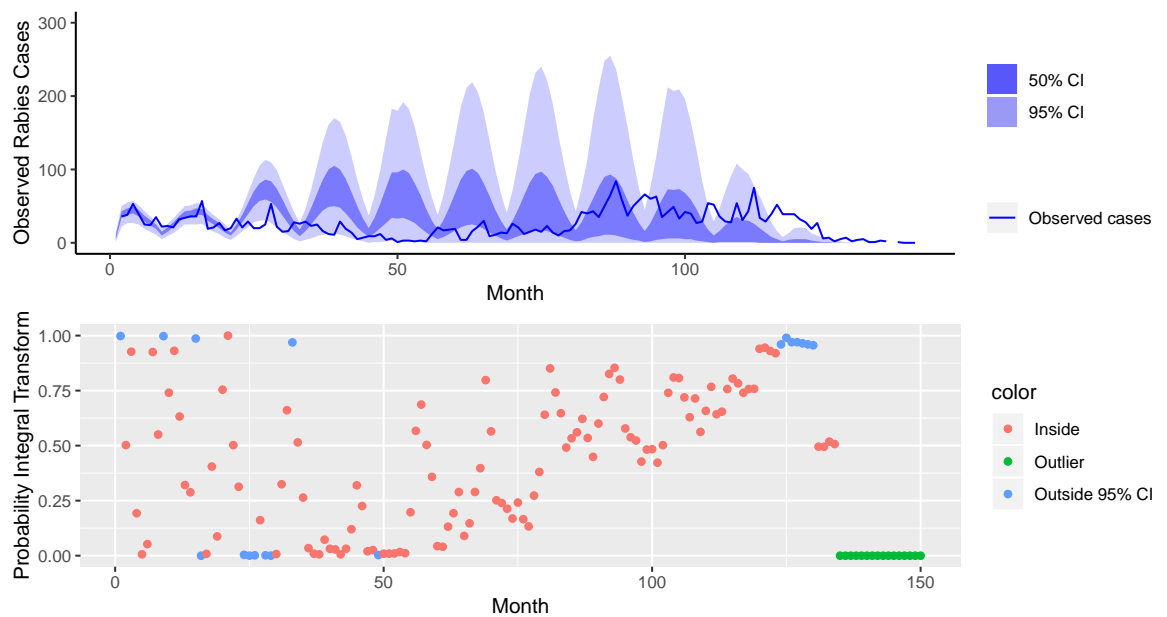


Figure 2.7: Probability Integral Transform: Prediction with first 20 points. The top panel shows the model fit to the observed rabies cases over time in Region 1. The dark blue line represents the observed rabies cases and the light and dark shaded blue region represents the 95% and 50% Credible Intervals (CI) estimated from the MCMC samples, respectively. The bottom panel shows the probability integral transform over time (where the observed case falls in the cumulative distribution function). The colours in the probability integral transform plot indicate whether the observed cases falls inside (red) the 95% CI, outside (turquoise) the 95% CI but within the 100% CI, or outlier (green) when the case falls outside the CI entirely.

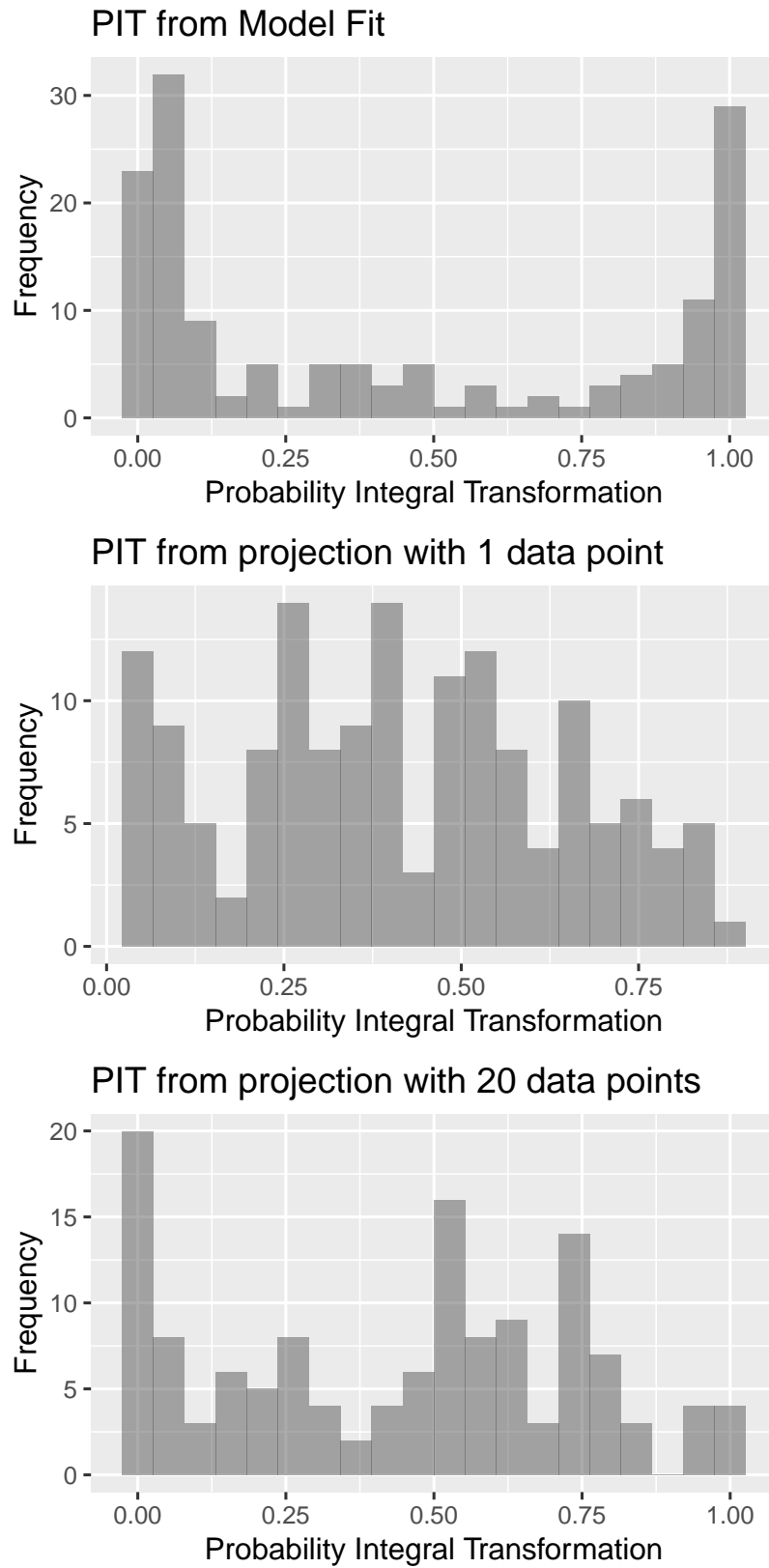


Figure 2.8: Histograms of the Probability Integral Transform. The panels from top to bottom show the probability integral transform for the model fit, the model projection with 1 data point, and for the model projection with 20 data points.

2.6 Discussion

Capturing local transmission and external incursions (migrating infectious individuals) is key to understanding disease transmission and is important to regional management of disease. Here, I present a method to capture local transmission processes and spatial coupling between regions. My work demonstrates that biological understanding and strategic guidance can be gained from inference from partially observed data on wildlife diseases.

Specifically I find that (i) incorporating heterogeneous mixing into the functional form of the transmission can help capture rabies dynamics at the regional level; (ii) by allowing for incursions (migrating infected individuals) from other regions, re-emergence of the disease is possible even if eliminated locally from a region; (iii) herd immunity achieved through bi-annual vaccination campaigns is short-lived due to population turnover, highlighting the need for regular and sustained vaccination efforts. Together these findings have important practical implications for designing control measures.

My results show that accounting for heterogeneous mixing is important to capturing fox rabies disease dynamics. In this model I used a decay function to approximate the scaling of local interactions (heterogeneous mixing) to the population-level. By allowing for a reduction in transmission as the number of infected individuals increased, the model was able to better capture rabies dynamics. Earlier studies have accounted for heterogeneous mixing in childhood diseases (Glass *et al.*, 2003; Roy & Pascual, 2006) and influenza (Liu *et al.*, 1986), however, this study is the first to use this approximation of heterogeneous mixing for wildlife rabies. This approach has potential application for other diseases that circulate through local interactions but for which surveillance data is aggregated.

External incursions can play a crucial role in sustaining transmission in the long-term, however many models don't consider between region transmission. The model estimated that external incursions comprise less than 1 % of overall cases, which may reflect the local nature of rabies transmission which is strongly linked to the movement of the infected fox as opposed to long-distance translocations. By allowing for resurgence of the disease as a result of incursions from neighbouring regions, my model presents an opportunity to test future vaccination scenarios (Chapter 3). Synchrony in the fade out of infections is considered advantageous, since the potential for ongoing transmission resulting from the movement of infected individuals between separate populations or 'rescue effects' is greatly reduced. This underscores the need for coordinated vaccination efforts between regions that act to isolate the dynamics (Grenfell & Harwood, 1997). Eastern Germany is a good example of the success of coordinated vaccination efforts. In contrast to the remaining areas in Germany they followed a common, coordinated vaccination strategy and were able to eliminate rabies more quickly (Müller *et al.*, 2012).

The strongest mechanistic feature driving fluctuations in rabies cases was the entry of juvenile foxes into the population after the birth pulse. This is evident from both model predictions (Figures 2.6, 2.7). Although the credible intervals around the model predictions reduced when more data was provided (20 data points compared to 1 data point), the model was not able to capture multi-year oscillations in cases. In the model fit multi-year fluctuations were explained by the environmental noise and observation noise parameters (Figure 2.3). However, it is difficult to pinpoint whether the environmental noise and observational noise parameters capture the true underlying process generating the peaks in the observed data. It is highly probable that changes in resource availability and variation in detection explains some of the variation in the process, however I did not have any data or information to inform these parameters aside from expert opinion. Furthermore, some of the nuances in the dynamics may also be obscured due to the aggregation of data. For instance, the behaviour of the observation process over time suggests either that there are marked differences in the detection of cases or that there are other things driving the rabies dynamics that the model is apportioning to the observation rate. Periodic dynamics have been observed in other diseases (e.g. measles and whooping cough, (Rohani *et al.*, 1999)). It is thought that at the local scale, regional persistence relies on both an adequate replenishment rate of susceptibles and for the movement of susceptible and infected hosts, i.e. spatial transmission, to be adequate (Keeling & Rohani, 2002). Because the data is aggregated at a coarser scale, the cases observed are in fact the result of multiple foci within a region (as is shown in Chapter 4), making it difficult to detect truly local dynamics from aggregated data. Although the fitted model expected a more gradual and smoothed number of cases than the observed data, the expectation is not far off from the actual number of cases observed and the model successfully captures the effect of vaccination. Therefore, although the model fit is too confident, overall it does a good job of capturing the overall disease dynamics.

Herd immunity is temporally and spatially dynamic as a result of demographic processes. The fox population undergoes rapid changes in size following entry of juvenile foxes into the population three months after the birth pulse. The influx of new susceptible individuals reduces herd immunity by more than half. This means that isolated infections can become rapidly reconnected with susceptible hosts and transmission maintained in the absence of adequate levels of herd immunity. My analyses of vaccination reveal that herd immunity is only maintained through regular ORV campaigns. This has important implications for other wildlife diseases with marked birth pulses (Peel *et al.*, 2014).

Using fox rabies as a case study, I demonstrate how different types of process error and observation error, unequal sample intervals, and missing values can be accounted for within the flexible framework of Bayesian state-space models. My model was able to accommodate uncertainty in the biological and observation processes and was able to recreate observed dynamics and infer missing time series by latent process methods. This has important practical implications for other wildlife diseases where only limited epidemiological and demographic

data are available.

The use of sophisticated state-space modelling techniques paired with long-term fox rabies data provide a unique opportunity to understand rabies dynamics and evaluate the impact of vaccination on rabies incidence. My study adds to the considerable body of work that has been central for guiding control of fox rabies in Europe (Anderson *et al.*, 1981; Eisinger *et al.*, 2005; Thulke *et al.*, 2008) by being the first to estimate the number of incursions in metapopulation persistence using a model fit to data. Together these findings have important implications for maintaining rabies freedom and ongoing vaccination of large parts of Eastern and Southern Europe (e.g. Russia and Greece). Lastly, this work makes an important methodological contribution to the study of spatial disease dynamics in other wildlife diseases where only limited epidemiological and demographic data are available.

CHAPTER 3

Optimising spatial and seasonal
deployment of vaccination campaigns to
eliminate wildlife rabies

Optimising spatial and seasonal deployment of vaccination campaigns to eliminate wildlife rabies

3.1 Abstract

The continued presence of fox rabies in Europe highlights the need for technical guidance and contingency planning to eliminate disease and prevent outbreaks. Effective planning of vaccination programmes is central to achieving these objectives. However, there is little scientific guidance on how long control programmes must operate or should be strategically implemented to eliminate disease in areas with varying degrees of endemicity.

Using detailed records documenting the long-term oral rabies vaccination (ORV) programme in Eastern Germany and fox rabies, I developed an epidemiological model that captures the main features of rabies spread and the impacts of vaccination. Here, I extend the model to determine the best vaccination strategy, in terms of placement and duration of ORV efforts, for three epidemiological scenarios characterised by varying degrees of endemicity representative of current situations found in Europe. I sought to determine where vaccination campaigns should be strategically placed to increase the probability of elimination in each scenario and explored the impact of logistical constraints on time to elimination.

My findings indicate that (i) consecutive campaign sets and coordinated vaccination across all regions are required to rapidly control and eliminate rabies, (ii) Autumn vaccination campaigns, which follow entry of juvenile foxes into the population three months after the birth pulse, have the greatest impact on increasing the probability of elimination and reducing time to elimination, (iii) incomplete vaccination (missing campaign sets) compromised time to elimination with the same or more vaccination effort required to meet similar timelines (iv) ensuring that sufficient resources are in place to eliminate rabies which requires considerable time and monetary investment beyond that required for control. To successfully eliminate rabies from a seasonal wildlife population, managers should implement coordinated vaccination campaigns, plan for twice the number of campaigns required to control the disease, and avoid missing campaign sets following the birth pulse.

3.2 Introduction

Despite a considerable body of theory underpinning the principles for infectious disease control through mass vaccination (Anderson *et al.*, 1981), there is little scientific guidance as to how long control programmes need to operate or are best implemented strategically to eliminate persistent foci of infection (Klepac *et al.*, 2013). A key challenge faced by disease control programme managers is estimating timelines for control and elimination and their resulting programmatic and budget implications. Scaling back control measures too early could lead to disease re-emergence (e.g. rinderpest), but costs of continued control can be difficult to justify especially when new cases are no longer being reported (Del Rio Vilas *et al.*, 2017; Klepac *et al.*, 2013). Until elimination is achieved, vaccination efforts, surveillance, and mobilized public health and veterinary staff are required in both affected and neighbouring unaffected areas. Theoretical estimates of the time required to eliminate a pathogen are typically shorter than what is observed in practice (Wearing *et al.*, 2005). Infectious diseases often persist for prolonged periods at low incidence (Klepac *et al.*, 2013), with at least as much effort required to achieve elimination as needed to bring disease under control (Freuling *et al.*, 2013). The epidemiological impact of practicalities that may interrupt the schedule of control programmes or cause operational delays in implementation, are also not well understood. Realistic estimates of eliminate time horizons and improved understanding of the impact of logistical constraints on progress to elimination should inform better policy and practice.

Vaccination works to interrupt the transmission of infection as contacts with vaccinated individuals, which do not result in infections, occur more frequently. Indirect protection of non-vaccinated individuals from infectious disease can occur when a sufficient proportion of the population is vaccinated, P_{crit} , (Fine *et al.*, 2011). The resulting ‘herd immunity’ is spatially and temporally dynamic as a result of demographic processes. This is especially true for wildlife populations which are often characterized by faster population turnover compared to humans and where seasonal birth pulses are frequently observed (Peel *et al.*, 2014). Influxes of new susceptible individuals may support ongoing transmission by reducing levels of herd immunity (Peel *et al.*, 2014). It is therefore important to understand how demographic processes may affect vaccination strategies for wildlife.

Once a disease has been eliminated from a given region, the movement of infected individuals between regions and the transmissibility of the pathogen determine the probability of re-emergence, or ‘rescue effects’ (Klepac *et al.*, 2013). By seeding new epidemics and preventing localised extinctions, rescue effects prolong disease persistence (Brown & Kodric-Brown, 1977; Earn *et al.*, 1998; Hanski, 1998; Keeling, 2000). In the absence of vaccination, the proportion of susceptible individuals in the population may increase, leaving a region vulnerable to potentially large outbreaks if infection is reintroduced. Accounting for the connectivity of populations in the planning of vaccination strategies is central to maintaining freedom from

disease.

Oral rabies vaccination (ORV) of foxes has, in just over three decades, eliminated fox rabies from 9 countries in Western and Central Europe (Cliquet *et al.*, 2014; Freuling *et al.*, 2013; Müller & Freuling, 2012). However, fox rabies remains in large parts of Eastern Europe and Russia. Since the late 1980s the European Union (EU) has co-financed ORV efforts to eliminate disease in EU member and border states and aims to maintain freedom from disease via a protective vaccination belt (cordon sanitaire). Determining the best vaccination strategies for different epidemiological situations has immediate application to the rabies situation in Europe, including the design of cordons sanitaires to maintain rabies freedom, expanding ORV efforts to bordering endemic states, and strategies to rapidly eliminate emerging disease in high-risk countries such as Greece and Turkey.

Using detailed records documenting the long-term ORV programme in Eastern Germany and fox rabies incidence, I developed an epidemiological model that captures the main features of rabies spread, uncertainties in detection and environmental fluctuations, and ORV impacts (Baker *et al.* Chapter 1). Here, I extend the model, quantifying uncertainty in the outcomes, to determine the best vaccination strategy, in terms of scale and duration of ORV efforts, under different epidemiological scenarios. I focus on three common scenarios found in Europe and elsewhere: **endemic** circulation of rabies; **high-risk** situations where rabies has been partly eliminated from an area but remains in more than half of the regions; and an **endgame** scenario when only a single endemic foci remains. I evaluate the effectiveness of different vaccination strategies in terms of reductions in cases and increases in probability of elimination. I also identify crucial and sensitive points in a vaccination strategy where logistic constraints can setback time to elimination. Based on my findings, I generate recommendations on the time horizon and the placement and timing of vaccination campaigns required to achieve and maintain freedom from fox rabies.

3.3 Methods

I simulated rabies cases from a hierarchical Bayesian state-space model fit to monthly time series of fox rabies cases for 5 federal states (area = 16,172-29,479 km²), hereafter referred to as regions, in Eastern Germany from 1982-2013, for three epidemiological scenarios (Figure 3.1):

1. Endemic: Rabies circulates endemically in all five regions.
2. High-risk: Two regions are rabies free, but neighbour three endemic regions.
3. Endgame: Rabies eliminated from four regions but present in one region.

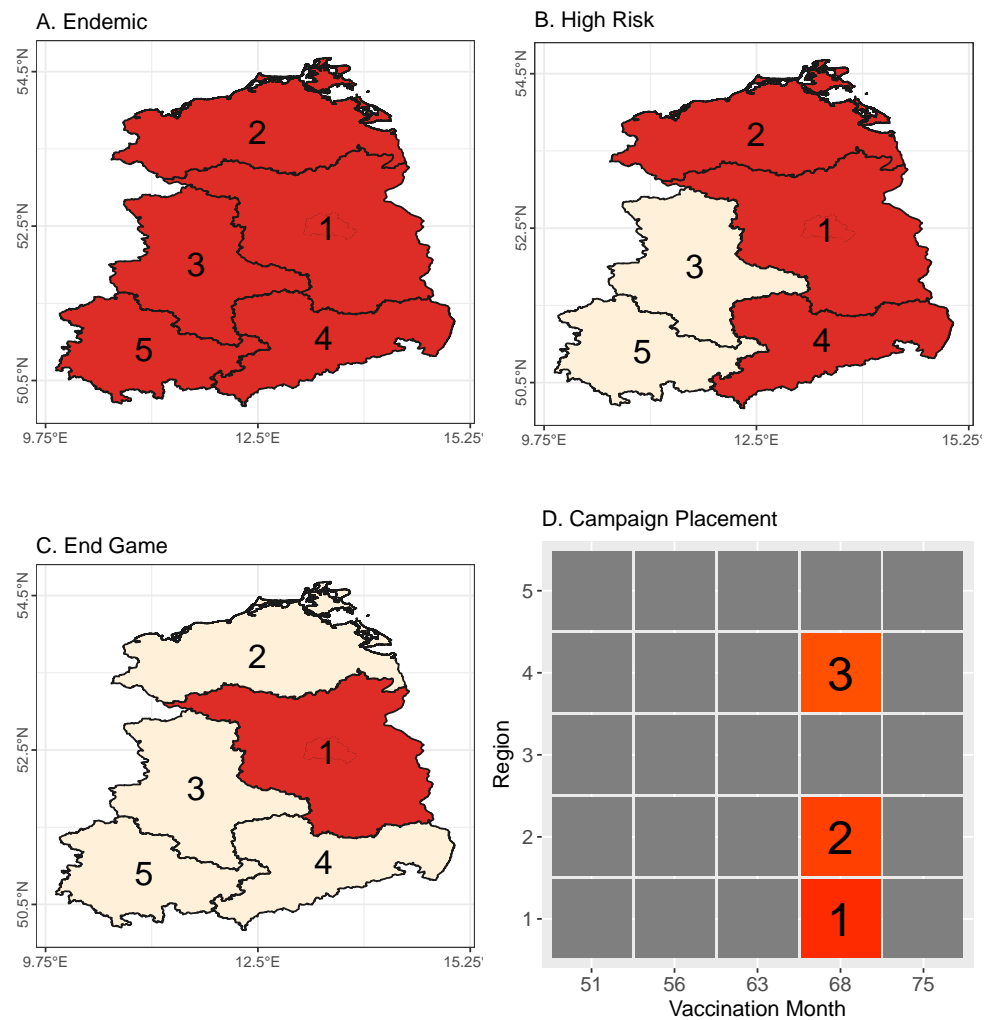


Figure 3.1: Map showing epidemiological scenarios investigated in Eastern Germany where red = Rabies, white = Rabies free. A. Endemic: All regions have rabies, B. High-risk: Rabies is partly eliminated but remains in more than half of the regions. C. Endgame: Rabies has been eliminated in all regions but one. D. Illustration of the algorithm used to decide the order of campaign placement. Campaigns are sequentially placed based on the position (month and region) that resulted in the greatest increase in the probability of eliminating rabies across all 5 regions. The numbers 1-3 in the grid cells represent when (month) and where (region) the first 3 campaigns were placed. The grey boxes represent possible campaign slots where campaigns can be allocated for the 4, 5, ... 25 campaigns.

Specifically, I sought to determine: where vaccination campaigns should be strategically placed to increase the probability of elimination (Figure 3.1D); the time to control and to eliminate rabies; the impact of incomplete vaccination under the endemic scenario and how incursions affect vaccination strategies in rabies-free and rabies-endemic regions. Here, I use the term vaccination campaign to refer to a single vaccination event (i.e. vaccination in one region) and the term vaccination campaign set to refer to a vaccination conducted in all regions within a short period of time (1 month).

In the next sections, I provide a brief description of the hierarchical Bayesian state-space model full details of which are provided in Chapter 1, followed by details of my simulation.

3.3.1 Hierarchical Bayesian state-space model

In Chapter 1, I developed a hierarchical model to explain local transmission (within-region) and spatial coupling (between region) dynamics of rabies and to evaluate the impact of ORV on monthly rabies incidence for 5 regions in Eastern Germany from 1982-2013. The model comprised both a biological and an observation process. The biological process consisted of a discrete-time stochastic metapopulation model with three states: Susceptible ($S_{r,t}$), Infected ($I_{r,t}$), and Vaccinated ($V_{r,t}$), developed to track foxes and rabies cases in different regions through time. Susceptible individuals were modeled as a function of new births and surviving individuals and those removed due to vaccination or infection. Stochasticity in the form of an environmental noise term was included to account for annual variability in fecundity (Lindström, 1988). I modeled infections generated from within the region and incursions (migrating infected foxes) from outside. Incursions were expressed as a function of incidence in neighbouring regions, the probability of infected animals leaving those regions, and the length of the border shared between focal and neighboring regions. Heterogeneous mixing at the population level was incorporated via a transmission function that asymptotes as numbers of infected individuals increase. Vaccination campaigns were incorporated in the month when they took place. Because both susceptible and vaccinated individuals consume baits, I accounted for bait depletion by previously vaccinated foxes in my estimates of the rate of bait uptake.

I estimated parameters for migration of rabid foxes between regions ρ_{max} , rabies transmission h , the annual probability of observing rabies cases θ_y , and fluctuations in fecundity due to environmental noise τ (Figure 3.2). I was not able to estimate a parameter for vaccination coverage or efficacy as it was confounded with the transmission parameter h . Therefore the rate of bait uptake, ν , was drawn from a Beta distribution with mean 0.4 and a variance: 0.001 based on estimates from field studies (Robardet *et al.*, 2016). For the simulation, I assumed a conservative bait uptake rate of 0.30 based on estimates from field studies (Robardet *et al.*, 2016).

3.3.2 Rabies Scenario Simulation

For all three scenarios I seeded each region with 30 infected cases. I ran simulations for 4.25 years (50 months) prior to introducing vaccination campaigns to allow the system to settle towards an endemic equilibrium. In the high-risk scenario (2), cases were removed from regions 3 and 4 at month 50 to create two rabies-free regions. In the endgame scenario (3),

cases were removed from all regions at month 50 except for region 1. I used the time series from the initial simulations of the three scenarios in the absence of vaccination as a baseline from which to assess increases in the probability of elimination for different vaccination effort.

I restricted my analysis to feasible vaccination strategies within operational and financial constraints; with a maximum of two campaigns per year, in the Spring (March) and Autumn (October). To determine the order in which campaigns should be placed to maximize the probability of elimination, vaccination campaigns were sequentially placed in the 5 regions from a schedule of predetermined dates corresponding to each March and October over 2.5 years (referred to as Spring 1: month 51, Autumn 1: month 58, Spring 2: month 63, Autumn 2: month 70, Spring 3: month 75) (Figure 3.1D). The location and date of each campaign was determined based on the placement (i.e. in one of the 25 grid cells, 3.1D) that most increased the probability of elimination by the end of the simulation (month 201). The process was repeated to determine the location and date of the next most important campaign, until rabies was eliminated from all 5 regions in all simulations (Figure 3.1D). Campaigns placed first were defined as ‘highest priority’ for managers, as they had the greatest impact on the probability of elimination. The best vaccination strategy was determined based on the timing and spatial arrangement of vaccination campaigns that eliminated rabies by month 201 (12.5 years after the start of vaccination) with least effort (number of campaigns) for each scenario.

I looked at time to control (months) and time to elimination (months) using metrics based on levels of incidence and the probability of elimination. I defined time to control as the month when monthly incidence across all regions was 10% of what would result in the absence of vaccination. I defined time to elimination as the month when the probability of elimination in all regions was >99.9%.

For the endemic scenario, I explored how unexpected logistical issues, due to budget or operational constraints, affect the time to elimination. Assuming the full vaccination programme, that is 5 complete campaign sets (25 campaigns) that would ideally be carried out in practice, I explored the impact of missing one campaign set, two consecutive campaign sets, or two non-consecutive campaign sets. The relative effect of each logistical constraint was estimated by measuring the delay in time to elimination and the number of additional campaign sets required to achieve elimination. To account for uncertainty in the parameter fits from my hierarchical Bayesian state-space model, I took 200 random draws from the joint posterior distributions of the parameters estimated (Figure 3.2). I ran ten simulation for each draw to give a total of 2000 iterations of the rabies time series for each vaccination campaign placement trialed. In order to obtain a set of reproducible simulations to compare different vaccination configurations and scenarios I set the seed for each draw from the joint posterior distribution of the time series, with the ten random seeds yielding 2000 iterations (10 seeds x 200 random draws from the joint posterior distribution).

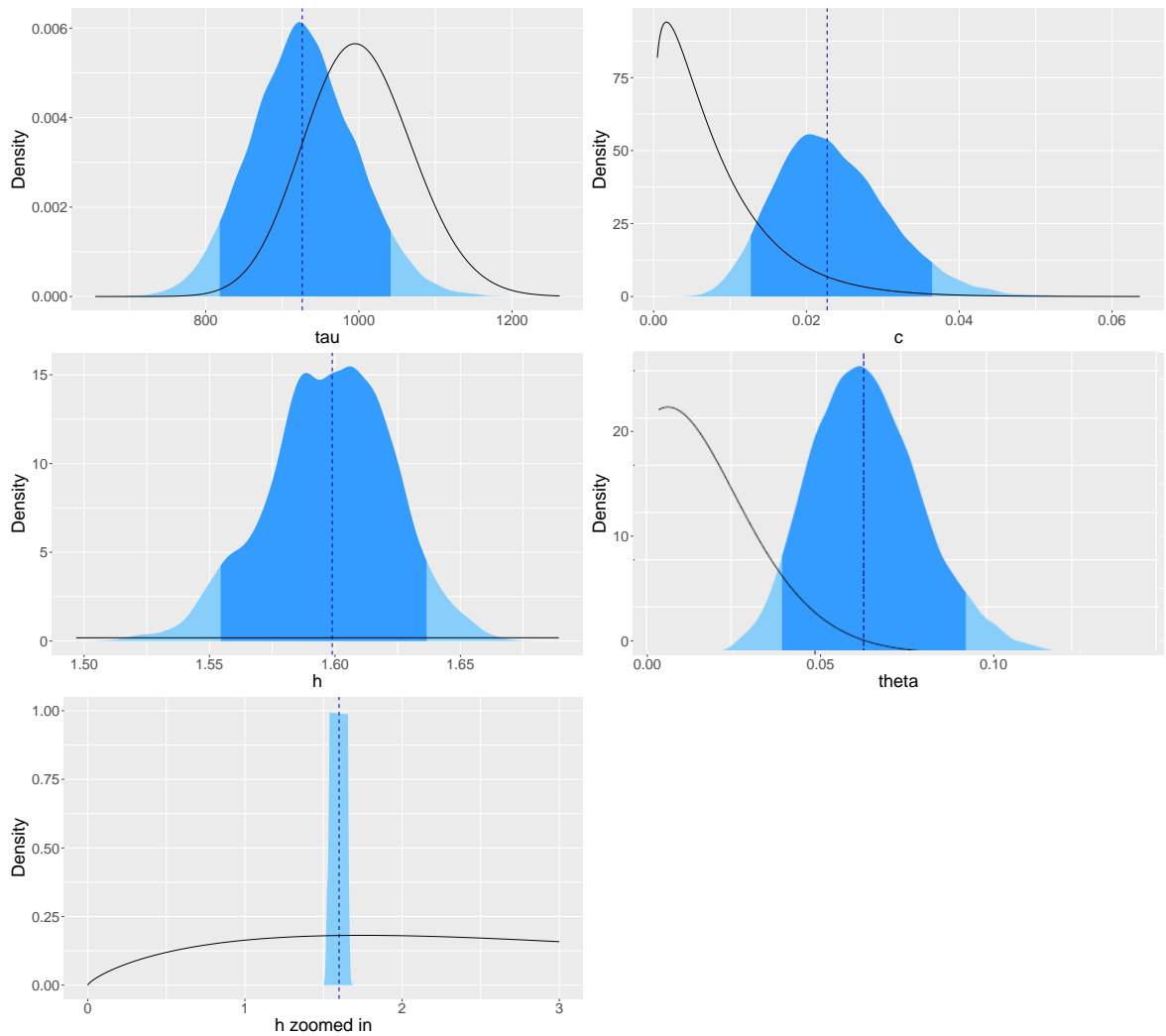


Figure 3.2: The posterior distribution and priors for the parameters estimated in the hierarchical Bayesian state-space model. The posterior distribution is shaded in blue, the black line represents the prior distribution. In the simulation I took random draws from the posterior distribution of parameters estimated for rabies transmission h , migration of rabid foxes between regions ρ_{max} , fluctuations in fecundity due to environmental noise τ , and the annual probability of observing rabies cases θ . The posterior and prior for the transmission parameter h is shown again in the bottom left panel of the plot to better show the prior chosen. Random draws were taken from the posterior distribution of parameters estimated and used to simulate the different rabies scenarios.

3.4 Results

3.4.1 Vaccination placement

The optimal vaccination strategy for a particular area will vary based on the epidemiological situation encountered. I sought to determine where vaccination campaigns should be strategically placed to increase the probability of elimination for three epidemiological scenarios:

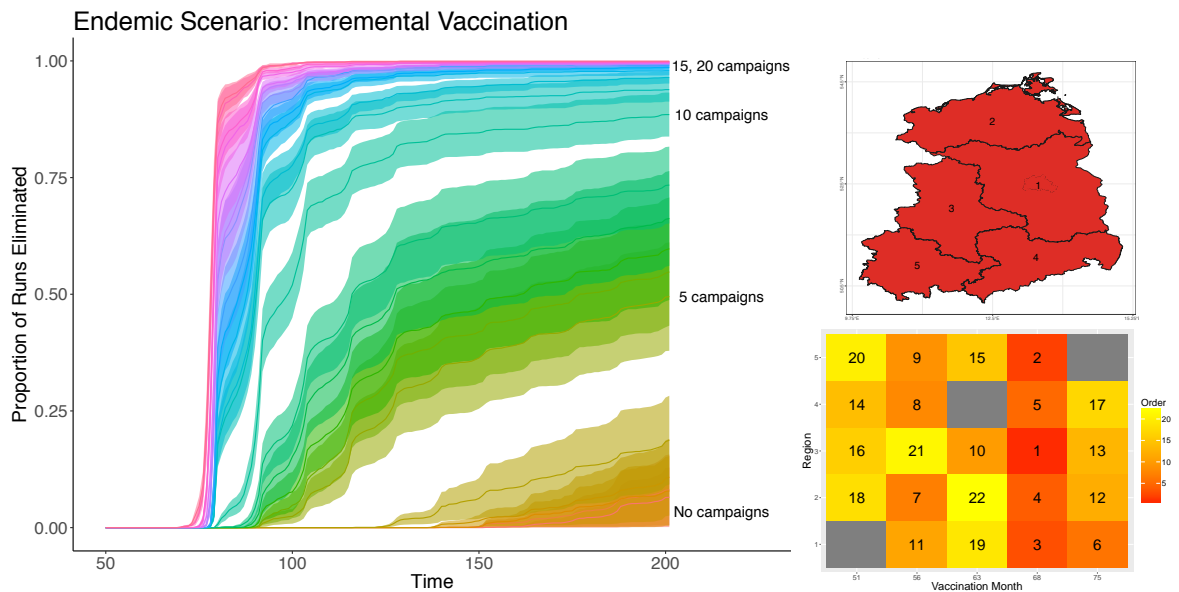


Figure 3.3: Proportion of runs where rabies was eliminated from all 5 regions in response to incremental vaccination (mean and shaded 95% CI). In the endemic scenario, 22 campaigns were required to eliminate rabies from all regions. Labels mark the proportion of runs eliminated in response to no vaccination and 5, 10, 15 and 20 campaigns. Map showing the endemic scenario where all regions have rabies. Order of vaccination in the endemic scenario was determined based on the campaign placement that increased the proportion of runs eliminated.

endemic, high-risk, and endgame. In the endemic and high-risk scenarios, 22 and 20 campaigns respectively were required to achieve elimination in all regions (Figures 3.3, 3.5), whereas in the endgame scenario, only 9 vaccination campaigns were required to eliminate the disease (Figure 3.6). I found that Autumn vaccination campaigns had the biggest impact on the probability of elimination across all scenarios (Figure 3.3, 3.5, 3.6). Autumn campaigns (October) occur after entry of juvenile foxes into the population (July) when the susceptible population is at its largest following the birth pulse (Figure 3.4). In the endemic scenario, Autumn campaigns accounted for 8 of the first 9 campaigns conducted, and these 8 campaigns eliminated infection in $\sim 70\%$ of runs (Figure 3.3). In the high-risk scenario, the first 7 campaigns were Autumn campaigns, and these eliminated infection in $>80\%$ of runs (Figure 3.5). In the endgame scenario, 4 out of the first 5 campaigns placed were Autumn campaigns, and these eliminated infection in $\sim 90\%$ of runs eliminated (Figure 3.6).

In the endemic scenario, effort was evenly spread across the 5 regions, with 5, 10, 15, and 20 campaigns marking when each region had received their 1st, 2nd, 3rd, and 4th campaigns respectively (Figure 3.3). Each region was vaccinated at least 4 times with only the Autumn vaccination dates requiring a full campaign set (vaccination in all 5 regions) (Figure 3.3). However, no strong pattern emerged in terms of the largest or most connected regions (those sharing the largest proportion of their border with other regions) being prioritized first for vaccination (Figure 3.3).

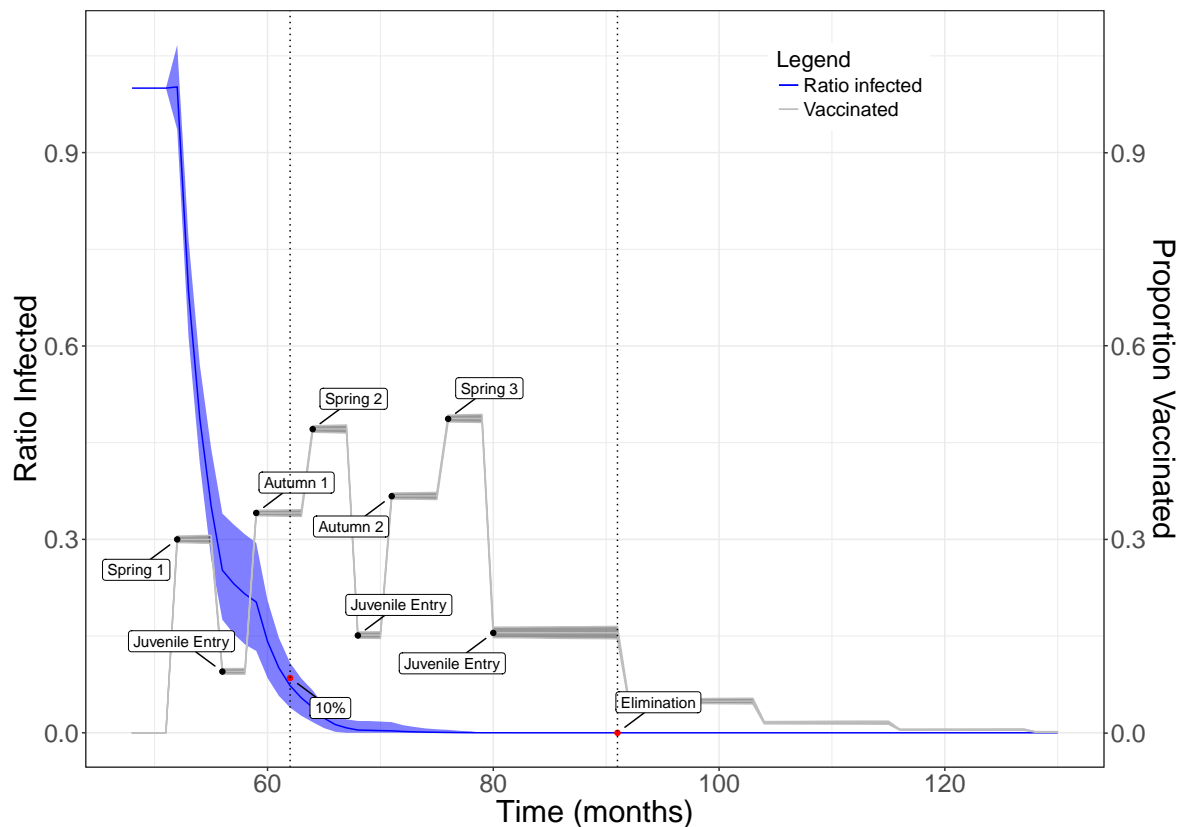


Figure 3.4: Ratio of the proportion of infected individuals in the population with vaccination and without vaccination (blue) and the proportion of the population vaccinated (grey). Vertical lines indicate the month where the ratio of infected individuals dropped to 10% and elimination (> 99.9% of runs eliminated).

In the high-risk and endgame scenarios, early implementation of vaccination campaigns in endemic regions had the greatest impact on probability of elimination (Figures 3.5 and 3.6). More vaccination campaigns were required in the endemic regions and the most connected neighbouring regions (those bordering several other regions, and sharing a large proportion of their border with other regions) to eliminate rabies in all regions in these scenarios (Figure 3.5 and 3.6). In the high-risk scenario, 4-5 campaigns were required in the endemic regions and a minimum of 3 campaigns were required in the neighbouring rabies-free regions in order to eliminate rabies in all regions (Figure 3.5). Similar to the endemic scenario, full Autumn campaign sets across all regions were required in order to eliminate rabies from all regions. Overall, earlier vaccination was favoured in the high-risk scenario, with 3 out of the 5 unused campaign slots occurring in the last vaccination month (Figure 3.5). In the endgame scenario, the endemic region was vaccinated 4 times and regions neighbouring the endemic region were vaccinated a total of 5 times: 3 campaigns in region 2, which is the largest neighbouring region in terms of both size and shared border, and a single campaign in both region 3 and region 4. Vaccinating early in rabies-free regions that bordered endemic regions was not always the best strategy. Delayed vaccination sometimes had a greater impact on the probability of

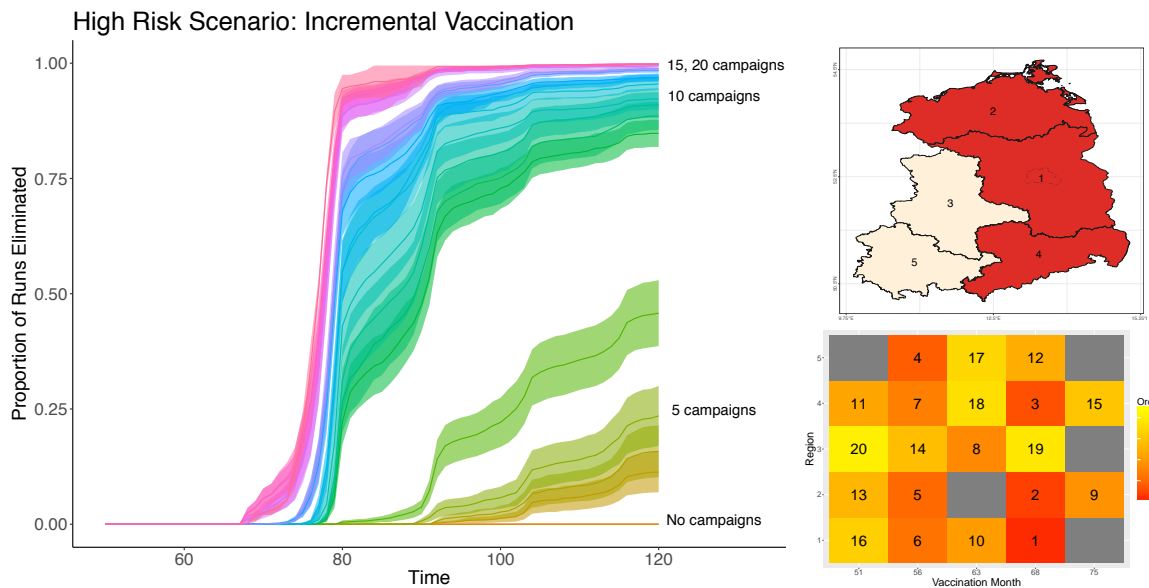


Figure 3.5: Proportion of runs where rabies was eliminated from all 5 regions over time in response to incremental vaccination (mean and shaded 95% CI). The high-risk scenario required 20 campaigns to eliminate rabies from all regions. Labels mark the proportion of runs eliminated in response to no vaccination and 5, 10, 15, and 20 campaigns. Map showing the high-risk scenario where some regions are free (white) but neighbour infected regions (red). Heatmap shows the order of vaccination in the high-risk scenario determined based on the campaign placement that increased the proportion of runs eliminated. Vaccination of the endemic regions was prioritised first, with vaccination after the birth pulse in month 56 and 68 having the greatest reductions in the proportion of runs eliminated. A minimum of 3-4 campaigns was required in neighbouring, previously rabies free regions.

elimination in all regions (e.g. in region 2 and 4, Figure 3.6) and meant that fewer overall campaigns were required.

3.4.2 Time to control vs. time to elimination

To gain a greater understanding of the time required to eliminate a pathogen and the impact of logistical constraints on these timelines, I estimated the time required to control and eliminate rabies and the impact of missed campaign sets in the endemic scenario. I found that more than twice as much effort was required to eliminate the disease than was required to control rabies in the endemic scenario (Figure 3.4). Employing full vaccination (5 campaign sets) in the endemic scenario, it took one year and 2 vaccination campaign sets to reduce monthly rabies incidence to 10% of endemic levels in the absence of vaccination (Figure 3.4). An additional 3 campaign sets over 2.5 years were required to eliminate rabies from across all 5 regions, that is rabies was eliminated 3.5 years after the introduction of ORV with a total of 5 campaign sets (Figure 3.4). I estimated that the Autumn campaigns increased the proportion of the population protected to about 34 and 37% (Sets 2 and 4), with Spring

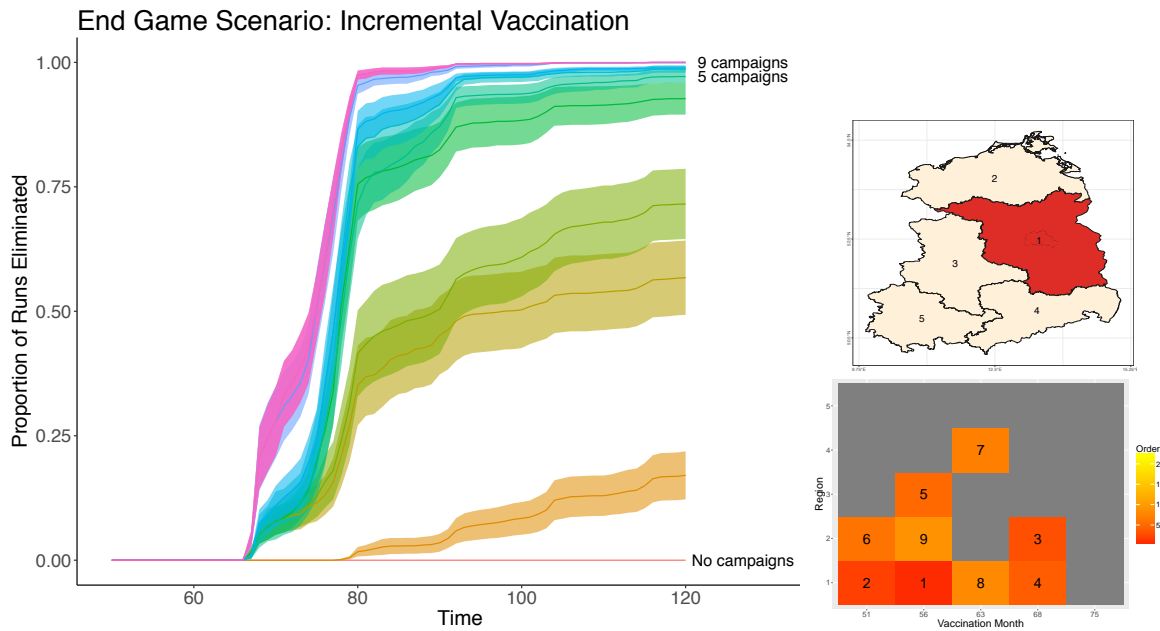


Figure 3.6: Proportion of runs where rabies was eliminated from all 5 regions over time in response to incremental vaccination (mean and shaded 95% CI). In the endgame scenario, 9 campaigns were required to eliminate rabies from all regions. Labels mark the proportion of runs eliminated in response to no vaccination and 5 and 9 campaigns. Heatmap shows the order of vaccination in the endgame scenario, determined based on the campaign placement that increased the proportion of runs eliminated. Vaccination of the last remaining endemic region was prioritised first. Three campaigns were required in region 2, which is the largest neighbouring region in terms of both size and shared border. One campaign was required in the two other neighbouring regions (region 3 and 4).

campaigns increasing the proportion of the population protected by a further 12-13%, with peak coverage reaching 47 and 49% in Sets 3 and 5 (Figure 3.4). Following entry of juvenile foxes into the population three months after the birth pulse, I estimate that the proportion of the population protected declines by about 20% following a single Spring campaign (Set 1). The following two years, entry of juvenile foxes following the Autumn and Spring campaigns (Set 2 and 3, and Set 4 and 5), the proportion of the population protected declines by about 32-33%. The proportion of the population protected remains constant between birth pulses as both susceptible and vaccinated individuals experience the same levels of natural mortality (Figure 3.4).

To understand how logistical constraints may affect time to elimination, I explored the impact of different logistical scenarios: missing campaign sets (1 set, 2 consecutive sets, 2 non-consecutive sets) on elimination timelines with and without additional campaign sets (Figure 3.7 and 3.8). In only two scenarios, where either the 1st or 3rd campaign set was missed, was elimination achieved in the absence of additional campaign sets (Figure 3.8: Panel 1). Missing a single campaign set delayed elimination by on average 6 months, but by up to 12 months, as long as one additional campaign set was also undertaken. Missing a Spring

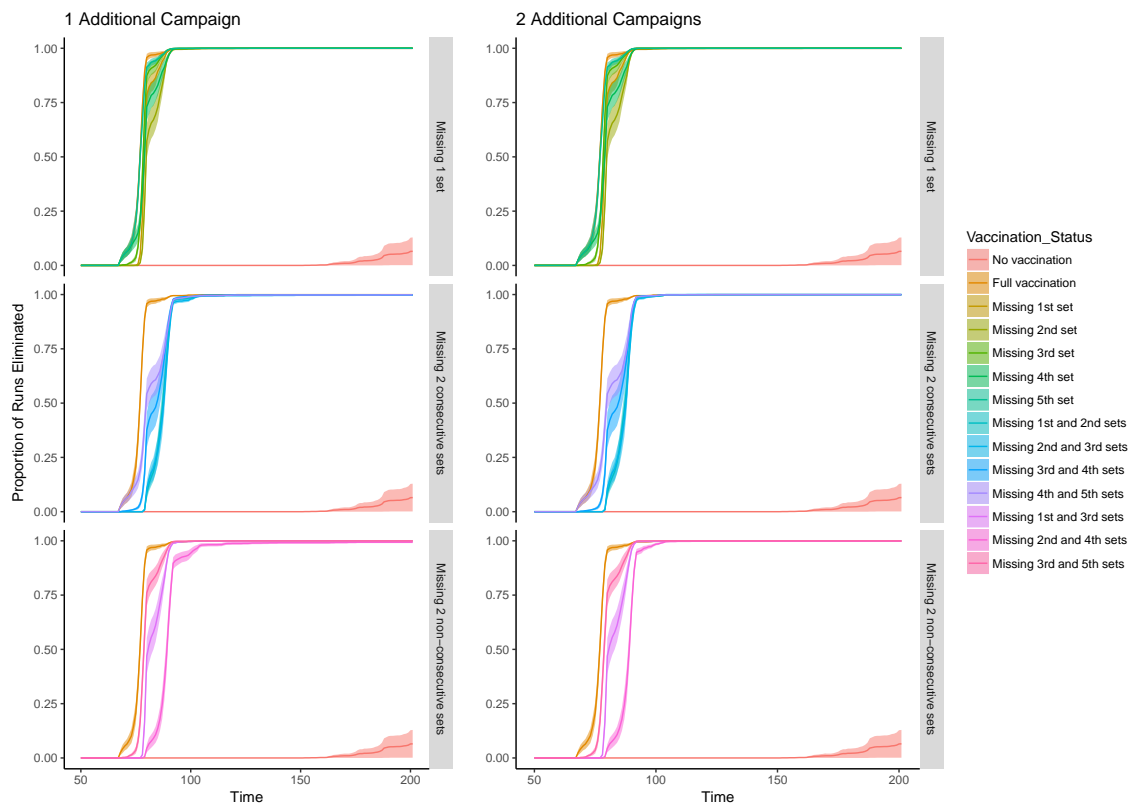


Figure 3.7: Proportion of runs where rabies was eliminated from all 5 endemic regions over time under different logistical scenarios (mean and shaded 95% CI). Facets show the impact of missing 1 set of vaccination campaigns, missing 2 consecutive campaigns, and missing 2 non-consecutive campaigns and the response of adding one or two additional campaigns. Lines are coloured according to which set of campaigns were missed as shown in the legend. Sets are labeled in order of vaccination date: 1st set (month 51), 2nd set (month 58), 3rd set (month 63), 4th set (month 70), 5th set (month 75) and combinations thereof.

campaign set (Set 1 or 3) resulted in shorter delays of 1-3 months compared with 11-12 months when missing an Autumn campaign set (Set 2 and 4) (Figure 3.8: Panel 2). With the addition of two campaigns sets (Figure 3.8: Panel 3), rabies elimination was achieved across all logistical scenarios apart from when both Autumn campaign sets were missed (2 and 4). When two campaign sets were missed, the delay to elimination ranged from about 1 to 2 years, with 2 additional campaign sets required to ensure elimination. The longest delays (~1.5-2 years) occurred mainly in logistical scenarios where two consecutive campaign sets (e.g. the 2nd and 3rd or the 3rd and 4th sets) were missed (Figure 3.8: Panel 3).

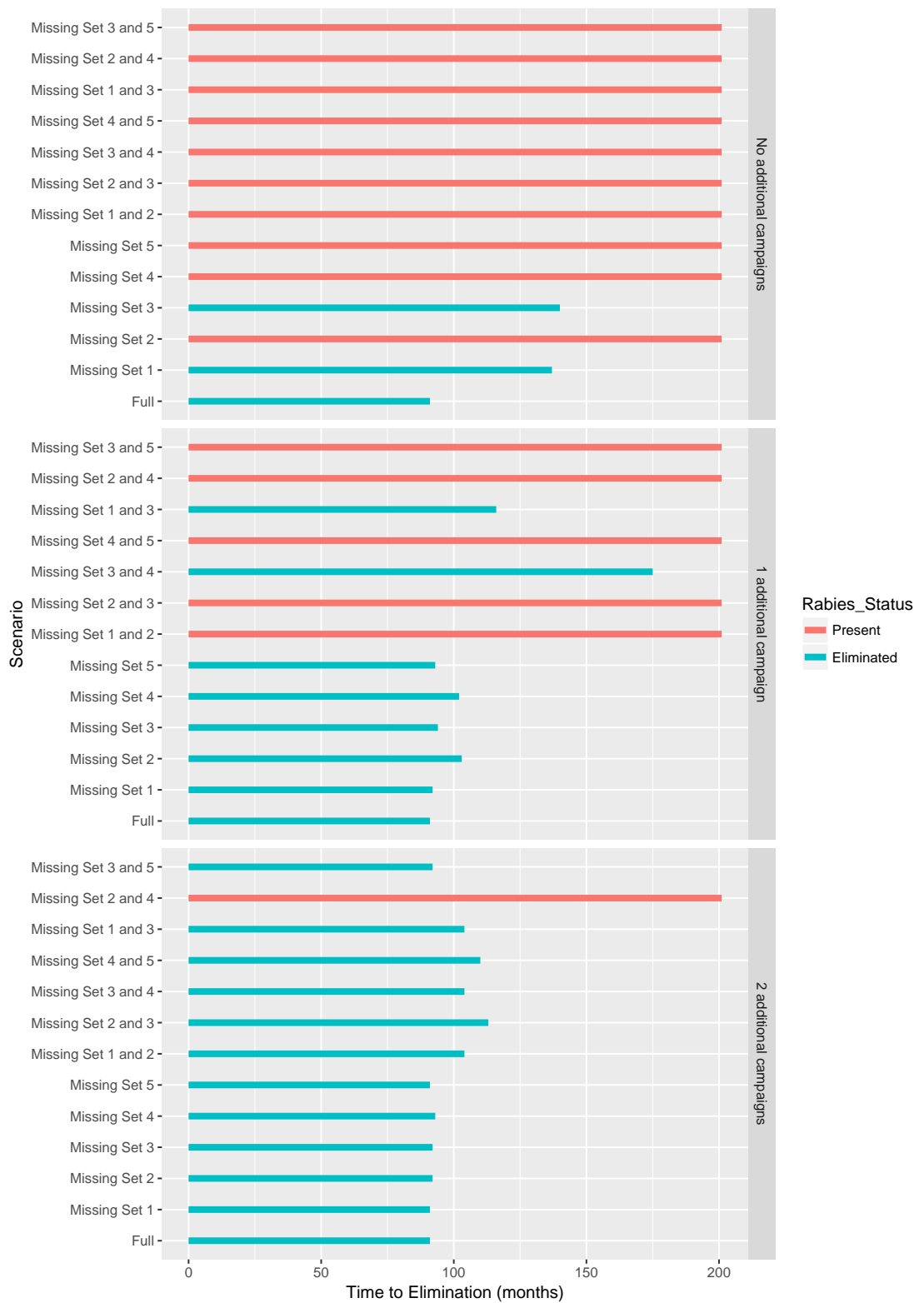


Figure 3.8: Time to elimination in response to missed campaign sets with and without additional campaign sets. Panels 1-3 show the time to elimination with no additional campaign sets, 1 additional campaign set, and 2 additional campaign sets respectively.

3.5 Discussion

My findings indicate that consecutive campaigns sets and coordinated vaccination across all regions are required to rapidly control and eliminate rabies. This appears to be due to the need to maintain sufficient herd immunity in the face of large birth pulses; Autumn vaccination campaigns had the greatest impact on increasing the probability of elimination and reducing time to elimination across a range of epidemiological scenarios. I hypothesise that this is because vaccinations in Autumn, reach a larger proportion of the population, as they occur after the entry of susceptible juvenile foxes into the population three months after the birth pulse, than vaccinations carried out in Spring; incomplete vaccination (missing campaign sets) compromises time to elimination with the same or more effort required to achieve elimination and meet similar timelines; missing one campaign set can be remedied with an additional campaign set and only leads to delays in time to elimination of one month to a year; in contrast, missing two consecutive campaign sets or two Autumn campaign sets caused the greatest delays in time to elimination (1-2 years), in some cases requiring a further campaign set beyond those compensating for the missing campaign sets. Together these findings have important practical implications for designing elimination programmes and informing decision-making including contingency plans.

3.5.1 Vaccination Placement

Autumn vaccination campaigns had the biggest impact on the probability of elimination across all scenarios. Autumn campaigns occur after entry of juvenile foxes into the population, three months after the birth pulse, at which point the fox population approximately doubles (Iossa *et al.*, 2008). This large influx of susceptible individuals into the population leads to a sharp drop in herd immunity. It is unsurprising then that campaigns occurring soon after entry of juvenile foxes into the population were most critical to achieving elimination, as the most foxes can be vaccinated at this time. The importance of vaccination campaigns following the birth pulse is potentially applicable to vaccination of other wildlife with seasonal birth pulses (Peel *et al.*, 2014). The timing and causes of seasonality can substantially impact herd immunity and should be considered in determining how and when control measures should be applied.

Several studies have found that connectivity plays a key role in disease persistence (Bolker & Grenfell, 1996; Keeling & Rohani, 2002) and that the size of populations also determines time to control (Keeling & Grenfell, 1997). However, I found no strong pattern in either the largest or the most connected regions being prioritized first. I hypothesise that the relative gains in across region probability of elimination may be a combination of the size and connectivity (in terms of shared borders) of the region as well as the past history of where has already

been vaccinated. This hypothesis could be tested by exploring the impact of varying the size and connectivity of regions to determine their influence on vaccination.

3.5.2 Time to control vs. time to elimination

Realistic predictions of the time to eliminate a pathogen and greater understanding of how logistical constraints set this back can help to manage expectations regarding the impacts of control measures. Previous work has shown that in practice the final stage of elimination is often the most challenging, with the same if not more effort required to eliminate the remaining 10% of cases as to eliminate the first 90% of cases (Freuling *et al.*, 2013). My simulations are consistent with these empirical observations and show that while rabies can be rapidly controlled through vaccination, more than twice as much effort is required to eliminate the disease entirely. Incomplete vaccination seriously compromised time to elimination with the same or more effort (campaign sets) required to achieve elimination. In general, missing one campaign set delayed time to elimination by on average 6 months with delays of up to 1 year. However, delays of one to two years in time to elimination occurred when two consecutive or two campaign sets following the birth pulse were missed, even if missed campaign sets were followed by the same amount of additional vaccination effort.

Consecutive campaign sets are crucial in building and maintaining high levels of herd immunity. In the simulation, herd immunity rapidly declines following influx of new susceptible foxes into the population after entry of juvenile foxes into the population. Consecutive campaigns were necessary to achieve high levels of herd immunity and had important consequences when missed. Insufficient vaccination coverage has been predicted to prolong rabies epidemics in raccoons by increasing the total number of cases, presenting a threat to neighbouring rabies-free areas (Rees *et al.*, 2013). Consecutive campaign sets are important for disease elimination and logistical scenarios in which consecutive campaign sets are missed should be considered in contingency planning.

3.5.3 Incursions

Rabies-free regions that are contiguous with endemic areas are vulnerable to reintroduction. My results show that large and well-connected regions (i.e. those with the longest borders with endemic regions) are often at highest risk from reintroductions, because they can support larger susceptible populations and have a greater probability of incursions along their shared borders. In the high-risk and endgame scenarios early vaccination of endemic regions was prioritized to reduce and prevent rescue effects. Directing surveillance efforts to areas bordering endemic regions is recommended for early detection and control of incursions (Castillo-Neyra *et al.*, 2017; Mulatti *et al.*, 2012). Low probabilities of disease detection may

mean persistent foci may be missed entirely, which could result in a delayed response to incursions or premature discontinuation of vaccination efforts that could result in resurgence (Castillo-Neyra *et al.*, 2017; Mulatti *et al.*, 2012; Townsend *et al.*, 2013b).

3.5.4 Future directions

Patterns of disease spread are influenced by variation in host densities, transmission processes and incubation periods (Lloyd, 2001), vaccination coverages (Selhorst *et al.*, 2005; Townsend *et al.*, 2013b), and landscapes (Rees *et al.*, 2013; Selhorst *et al.*, 2006). Although undoubtedly important, there is often only limited data on these heterogeneities, especially for wildlife diseases. The model makes several simplifying assumptions, for example using a monthly time-step to capture the generation interval, but in practice some longer generation intervals will occur (Toma & Andral, 1977). Since the model was fitted to large-scale (regional) data, I expect that the effects of landscape and population heterogeneities will have been captured in so far as they influence large-scale dynamics. Studies have found that natural barriers impede rabies spread (Real *et al.*, 2005; Rees *et al.*, 2013; Russell *et al.*, 2005; Smith *et al.*, 2002). But, I do not expect habitat heterogeneity to greatly influence rabies in Eastern Germany, as this area is fairly homogeneous with an absence of natural barriers (e.g. large rivers, mountains, lakes). However, incursions from neighbouring regions, incomplete vaccination campaigns and rare events not captured in our model, e.g. long incubators, could lead to shorter modelled estimates of time to elimination than observed in practice (Freuling *et al.*, 2013). I do not consider the location of remaining foci within a region in my model, so all neighbouring regions are considered under threat even at low levels of incidence. Low probabilities of detection mean that remaining foci are often missed, leading to delayed responses to incursions or premature discontinuation of vaccination that could result in resurgence (Castillo-Neyra *et al.*, 2017; Mulatti *et al.*, 2012; Townsend *et al.*, 2013a). This approach is suited to such situations where there is a lack of spatially resolved surveillance data and a conservative vaccination strategy is warranted. However, to guide control programmes in a specific location, geographically tailored simulations would therefore be required, and finer scale approaches may be necessary for examining spatially strategic responses to incursions, such as those modelled by Thulke *et al.* (2008). Extensions to this approach incorporating how surveillance effort and quality influence disease detection, and exploring the impact of heterogeneities in the size and connectivity of regions, could further improve vaccination planning. One of the drawbacks of determining the optimal vaccination strategy using a sequential approach is that this will naturally miss some optimal scenarios. However, to look at all possible vaccination combinations would have meant testing an impractical number of scenarios ($25! = 15511210043330985984000000$ scenarios).

In practice, vaccination strategies are rarely conducted with equal efficacy across the population. In my simulation, I took a conservative approach, by assuming a low vaccination uptake, however, an area of future research would be to incorporate scenarios with more realistic heterogeneity in coverage and the probability of uptake across vaccination campaigns and within regions. Individual based models have been used to demonstrate how spatial heterogeneity in the landscape interacts with the effectiveness of vaccination (Rees *et al.*, 2013). Vaccine uptake can be difficult to quantify over large and diverse regions. However, local knowledge and field studies may be used to inform estimates of uptake rates over time and across space.

3.5.5 Conclusion

Dynamic demographic processes govern levels of vaccine-induced immunity across populations and stochastic infection processes underlie patterns of infection in space/time. My findings have important practical implications that may be useful to guide policies for rabies containment and elimination in Europe and elsewhere. Overall I recommend i) prioritising ORV campaign sets following the birth pulse when resources are limited (in Autumn in Western Europe), ii) implementing consecutive vaccination campaign sets to build up and sustain high levels of herd immunity, iii) ensuring that sufficient resources are in place to eliminate rabies which requires considerable time and monetary investment beyond that required for control.

By capturing disease dynamics and quantifying uncertainty in outcomes, modelling strategies like this one can help managers plan effective vaccination strategies tailored to their local epidemiological situation and generate realistic timelines for disease elimination. They can also be used to manage expectations and justify continued control. By presenting different rabies scenarios and exploring the impact of logistical constraints, I provide insights for managers to plan vaccination strategies including short and long-term budgeting, as well as to understand the impact of missed campaigns. Further analyses incorporating how surveillance effort and quality influence disease detection, heterogeneities in vaccination uptake, and size and connectivity of regions, can be used to shed further light on these questions and improve the planning of vaccination.

CHAPTER 4

Resolving the spatial scale of rabies transmission

Resolving the spatial scale of rabies transmission

4.1 Abstract

Models capable of capturing local infection dynamics in wildlife populations have great potential to improve the planning of disease control programmes. However, developing models that can capture spatiotemporal infectious processes in wildlife populations remains a challenge, both due to a lack of spatially resolved data and statistical tools capable of dealing with such data.

Recent advances in statistical computing allow for the development and application of sophisticated modelling techniques to capture the localised spatiotemporal dynamics of diseases in wildlife populations and to understand the effects of data aggregation on estimates of key transmission parameters. Using detailed spatial and temporal data on the occurrence of fox rabies cases, I developed a space-time model in INLA capable of capturing fox rabies dynamics over the last 3 decades in Eastern Germany. I used the output from this model to explore the effect of scale on the estimates of transmission terms by aggregating incidence data at different spatial resolutions.

I find that (i) rabies cases are clustered within 5km, with spatial autocorrelation decaying over an approximately 20 km radius (ii) a heterogeneous mixing term is required even when data is aggregated at fine spatial scales (2x2 km grid) (iii) local disease dynamics are approximated by lower transmission and more population mixing as incidence data are aggregated at increasingly coarser scales. Together these findings have important implications for the understanding of transmission processes.

4.2 Introduction

Developing an understanding of spatial and temporal infection dynamics at a local level has great potential to improve the planning of control programmes. However, while there is a

considerable body of theory studying the wave-like spread of infection into new populations (Diekmann, 1978; Grenfell *et al.*, 2001; Murray & Seward, 1992; Smith *et al.*, 2002) and the role of seasonal forcing in disease dynamics (Bolker & Grenfell, 1995; Grenfell *et al.*, 2002), less is known about the endemic spatiotemporal dynamics of wildlife disease. Stochastic infection processes and the spatial distribution of infected individuals, host populations, and control interventions underlie patterns of infection in space and time. However, developing models that can capture and explain spatiotemporal infectious processes at a local level remains a challenge, due to a lack of high-resolution spatial and temporal data and computationally efficient statistical approaches for model fitting.

Most diseases circulate primarily through local interactions (Anderson *et al.*, 1992; Keeling & Rohani, 2008). However, data is often aggregated at the scale of administrative units rather than epidemiologically relevant ones, obscuring local transmission dynamics. Furthermore, many wildlife diseases lack the necessary combination of host and pathogen data required to understand how infection moves. There is therefore a need for approaches that can capture local heterogeneities in transmission even when dealing with surveillance data that is aggregated at larger spatial scales. Approximations have been used to try to capture the heterogeneities in transmission resulting from localised interactions between infected and susceptible individuals (Glass *et al.* (2003), Chapter 2). However, it is unclear how well they capture localized interactions for disease transmission in spatially-structured wildlife populations.

Variability in epidemiological data arises from both infectious disease dynamics, including stochastic spatial transmission processes, and the observation errors in detecting cases. The Bayesian approach allows us to incorporate many of the uncertainties inherent in epidemiological data and model latent, unobserved processes hidden from direct observation. Until recently, high computational costs have limited the simultaneous analysis of spatial and temporal patterns in disease fit to data. Rue *et al.* (2009) have developed an efficient, and flexible computational algorithm for model fitting that uses Laplace approximations rather than simulations (e.g. MCMC). Their method, called the integrated nested Laplace approximation (INLA), is designed to fit latent Gaussian models in a Bayesian context, in which spatial and temporal autocorrelation in the latent field assume a shared spatial structure and are reflected by Gauss Markov random fields (GMRF) (Rue & Held, 2005). This powerful approach makes the fitting of complex models feasible by speeding up computation and providing a flexible framework for fitting different types of spatial data (e.g. point process, areal data). Within the INLA framework, the stochastic partial differential equations (SPDE) approach constructs flexible fields that are able to model datasets with complex spatial structure (Krainski, 2018; Lindgren *et al.*, 2011). Krainski (2018) has extended the SPDE model to consider non-separable space-time SPDE model that are closely-linked to heat equations in physics. The non-separable space-time SPDE model simultaneously captures spatial and temporal autocorrelation in the latent field. The temporal extensions offered by the non-separable space-time SPDE model mean that spatially-explicit dynamical problems can

now be approached with numerical efficiency. This approach may be able to capture the spatiotemporal nature of disease transmission and therefore has considerable application for understanding epidemiological processes in disease ecology, particularly for wildlife diseases such as rabies that spread through direct contact.

Rabies is a deadly and terrifying disease that exacts a heavy toll on human lives and national economies, with over 50,000 human deaths each year and many millions more requiring expensive life-saving post-exposure vaccines (Hampson *et al.*, 2015). Elimination of rabies is feasible through mass vaccination; oral rabies vaccination (ORV) campaigns have eliminated fox rabies from Western Europe. However, scientific guidance could improve elimination efforts elsewhere and is still needed for contingency planning to maintain rabies freedom and for emergency response to incursions (when infections are introduced from endemic areas into disease free areas). The long-term, large-scale nature of the oral rabies vaccination programme in Europe together with spatially resolved data on rabies cases present a unique opportunity to study wildlife disease dynamics using sophisticated spatial modeling techniques.

Here, I examine local rabies dynamics and the effect of scale of aggregation of surveillance on estimate of transmission using a latent Gaussian model fit to GPS locations of observed rabies cases from five federal states in Eastern Germany pre-vaccination from 1982-1992. The model is fit using R-INLA Rue *et al.* (2009) and spatial and temporal autocorrelation in rabies cases is modelled using a non-separable SPDE model. I first model the infected individuals, estimating the spatial correlation between rabies cases. In the absence of detailed information on fox population density, I then simulate the host population stochastically, incorporating demographic processes and environmental spatiotemporal variability. I then combine the infected and susceptible density fields generated from the first two steps in a generalized linear model (GLM), where I model the number of infected individuals as a function of past infected individuals and the susceptible population to estimate key parameters relating to transmission. I investigate how the scaling of local processes is approximated as the resolution of incidence data becomes coarser by aggregating the infected and susceptible individuals at different spatial resolutions and estimating the transmission parameters from the GLM fit to these data. Insights from this work can be used to inform our understanding of the effect of spatial aggregation on estimating key transmission parameters and represents a first step in capturing local spatiotemporal infection dynamics in a wildlife disease.

4.3 Methods

4.3.1 Data Collection

Georeferenced laboratory-confirmed rabies cases in foxes were compiled from regular reports by the national veterinary authorities for 5 federal states in East Germany from 1982-2006 on a monthly basis. Shape files for each ORV campaign in the area were also compiled (Freuling *et al.*, 2013).

4.3.2 Space-time SPDE Fox Rabies Model

I performed three steps in analyzing the data: 1. Creating the infected density surface, 2. Creating the susceptible density surface, 3. Constructing a GLM using the infected and susceptible density surfaces generated in the first two steps to estimate key transmission parameters. The infected and susceptible density surfaces were created by modelling the infected individuals and susceptible individuals respectively using a latent Gaussian model where spatial and temporal autocorrelation in the latent (unobserved) field were modelled using a non-separable space-time SPDE model (Krauski, 2018). The computational aspects of the model fitting were carried out in R-INLA using the INLA approach (Rue *et al.*, 2009). Lastly, I fit several GLMs to future infectious cases using the susceptible and infected density fields generated from the first two steps to estimate key terms for rabies transmission. I investigated how the scaling of local processes is approximated as the resolution of incidence data becomes coarser by aggregating the infected and susceptible individuals at different spatial resolutions and estimating the transmission parameters from the GLMs fit to these data.

1. Creating the infected density surface, 2. Creating the susceptible density surface, and 3. Constructing a GLM from the infected and susceptible density surfaces.

4.3.3 Creating the infected density surface

I modeled the infected individuals from the space-time location of reported rabies cases, \hat{I} , using a log-Gaussian Cox space-time point process (Simpson *et al.*, 2016) in which the intensity function (i.e. the intensity of infected individuals), $\lambda(s, t)$, varies continuously over time and space. The likelihood of the log-Gaussian Cox space-time point process can be specified as

$$\pi(\hat{I}|\lambda) = \prod_i \lambda(s_i, t_i) \exp(|\Omega||L| - \int_{\Omega,L} \lambda(s, t) \partial s \partial t) \quad (4.1)$$

where Ω is the spatial domain, L is the time domain, (s_i, t_i) is the set of space-time coordinates for the events i , which in this case correspond to the reported locations and times when infection occurred.

The number of infected individuals in an area r over a time window l can be estimated by integrating the intensity function over this domain as

$$I_{r,l} = \int_{r,l} \lambda(s, t) \partial s \partial t . \quad (4.2)$$

It also follows that the number of observed cases in a predefined area r (i.e. the grid cells used for the GLMs) over the time period l is Poisson distributed with mean $I_{r,l}$. I model the intensity function as

$$\log(\lambda(s, t)) = \log(\theta) + \beta_0 + d(s, t) \quad (4.3)$$

where $d(s, t)$ is a latent field that captures the spatial and temporal relationships in the occurrence of infected individuals and follows a non-separable space-time random process, θ is the observation probability, and β_0 is the mean density of infected individuals per km² over time and across space. The intensity field was specified considering the non-separable SPDE model detailed in B.1 and B.2 in Appendix B. From these equations it is possible to estimate the spatial and temporal autocorrelation that generate $d_{s,t}$ based on changes in the location of infected individuals across time and space. In this case, I was predominantly interested in the spatial autocorrelation. In order to estimate the spatial marginal correlation from a non-separable model I compute the spatial marginal spectral density by integrating out the temporal frequency. Then I use the Bochner's theorem to compute the spatial marginal correlation, which can be computed with equation 7.23 in Lindgren (2012) rewritten 4.4.

The spectral density $f(\omega)$ for an isotropic random field is given for $\omega = \|\boldsymbol{\omega}\|$. This is then considered for computing the covariance at distance $h = \|\mathbf{h}\|$, $r(h)$, as follows

$$r(\mathbf{h}) = r(h) = (2\pi)^{p/2} \int_0^\infty \frac{J(p-2)/2(\omega h)}{(\omega h)^{(p-2)/2}} \omega^{p-1} f(\omega) d\omega \quad (4.4)$$

where the spatial dimension $p = 2$, $J(\cdot)$ is the modified Bessel function of the second kind, and $f(\cdot)$ is the marginal spatial spectral frequency. This gives me the spatial covariance at distance h at any time point. In practice, I get the posterior marginal distribution for each one of the three parameters of the space-time model after fitting the model for the infected foxes (equations B.1 and B.2 in Appendix B). I can then take the posterior mean of

these parameters and plug-in the formula for the spatial marginal correlation from Lindgren (2012). To account for some uncertainty in the marginal correlation function, I also calculated the spatial marginal correlation using the 95% quantiles of the posterior marginals for each parameter.

To create the triangulated mesh on top of which the SPDE/GMRF representation is built, the spatial domain is first discretized into a triangulated mesh with m nodes. The mesh function in R-INLA creates a constrained refined Delaunay triangulation (CRDT) in a region of interest. Using the CRDT, smaller size triangles can be defined in areas that have data and larger ones in areas with no information. This reduces computation costs and increases the accuracy of the spatial field where there is data. To avoid boundary effects (i.e. higher variance near the boundary), (Lindgren & Rue, 2015), I extended the mesh beyond the area of interest.

4.3.4 Creating the susceptible density surface

The susceptible population was modelled as follows:

$$S_{r,t} = \alpha_t(1 - v_{r,t}) \exp(x_{r,y})X_r \quad (4.5)$$

where the susceptible individuals $S_{r,t}$ in a predefined area r (i.e. the grid cells used for the GLMs) at month t are a function of changes in the population over time resulting from birth and death, α_t , vaccination, where $1 - v_{r,t}$ is the proportion of the population that is not vaccinated, and annual fluctuations, $x_{r,y}$, around the mean susceptible population in each grid cell X_r . An average density of 2.4 foxes per km² was assumed based on estimates from the literature (Ansorge, 1990; Iossa *et al.*, 2008; Lloyd *et al.*, 1976) and used to determine the mean susceptible population, X_r in each predefined area r (grid cell). $x_{r,y}$ is an environmental noise term representing spatial and annual fluctuations in fox fecundity resulting from changes in resource availability. $x_{r,y}$, represents the latent spatial-temporal correlation in susceptible individuals across the landscape, and comes from a space-time SPDE $x_{r,y}$ (Appendix B) and has a mean of 0 and variance of σ^2 . I set σ^2 to allow the birth pulse to fluctuate in a given area by +/- 10%, based on fluctuations in fecundity observed from a long-term study of fox population dynamics citeplindstrom1988reproductive. The spatial autocorrelation was also informed from the literature. Because foxes occupy non-overlapping territories and are generalists, occupying a wide range of habitats (Baker *et al.*, 2004), one can expect fox population density to vary across space based on changes in resource availability/habitat suitability. However, the relationship between specific habitat types and fox density is not well established. I therefore assumed a gradual spatial autocorrelation range decaying out to 20km for this analysis.

Changes in the size of the population α_t are modeled as a product of the birth pulse, α_0 and the survival rate $1 - m$ as follows

$$\alpha_t = \alpha_0(1 - m)^b \quad (4.6)$$

where $\alpha_0 = 3.183977$ and $m = 0.092$, b is the number of months since the birth pulse the last April. After the birth pulse, newborn foxes remain primarily in the den where they are sheltered from infectious interactions. Juvenile foxes enter the susceptible population three months after the birth pulse in July (month 7).

To account for the depletion of baits by already vaccinated conspecifics, the rate of bait uptake ν by susceptible individuals is determined relative to their proportion in the population where $v_{r,t}$ is the proportion of the population vaccinated and comes from

$$\text{where } v_{r,t} = \begin{cases} v_{r,t-1} + \nu(1 - v_{r,t-1}) & \text{if } B_{r,t} = 1 \text{ and } b \neq 7 \\ \frac{v_{r,t-1}}{\alpha_t} & \text{if } B_{r,t} = 0 \text{ and } b = 7 \\ v_{r,t-1} & \text{, otherwise} \end{cases} \quad (4.7)$$

Vaccination is switched on and off by an indicator variable $B_{r,t}$ that is 0 in all months apart from those when a vaccination campaign occurred when it equals 1. I account for reductions in the proportion of vaccinated individuals in the population following the entry of juvenile foxes into the population, by dividing the proportion vaccinated $v_{r,t-1}$ by the birth pulse effect α_t in July ($b = 7$) which corresponds to the factor by which the population is changing (e.g. doubling). When there is no vaccination campaign $B_{r,t} = 0$ and it is not an entry month $b \neq 7$ then the proportion of the population not vaccinated remains the same $1 - v_{r,t-1}$.

4.3.5 Constructing a GLM from the infected and susceptible density surfaces.

In the third step, I used the susceptible and infected density fields from the first step to estimate the transmission term ρ and the mixing term c in Equation 4.8 using a GLM. I used only the data before vaccination (1982-1992) to estimate these parameters as transmission dynamics may vary after the start of vaccination.

$$I_{r,t} = \rho S_{r,t-1} I_{r,t-1}^c \quad (4.8)$$

where ρ is the transmission parameter and c is a coefficient that accounts for heterogeneity in mixing patterns, hereafter referred to as the mixing term. This can be rewritten as a linear model in log scale as:

$$\log(I_{r,t}) = \log(\rho) + \log(S_{r,t-1}) + c \log(I_{r,t-1}) + \epsilon \quad (4.9)$$

where the transmission term $\log(\rho)$ becomes the intercept, $\log(S_{r,t-1})$ is a known offset, and the mixing parameter c is estimated as the coefficient for $\log(I_{r,t-1})$ and ϵ is a noise term. The biological rationale behind the mixing term is that mixing is not expected to be homogeneous, especially in larger areas, as individuals that are further apart from one another are less likely to be in contact with one another. The mixing term c allows us to capture saturation effects that occur at high incidence, when infected individuals cause less infections due to local susceptible depletion — either through disease-induced mortality or contact with already exposed (incubating) individuals.

I hypothesize that the mixing term c is only necessary to approximate the scaling of local interactions when incidence data is aggregated at large spatial scales. To test the hypothesis that c approaches 1 and the transmission term ρ is larger as data is aggregated at increasing smaller spatial scales (where local interactions take place), I aggregated the data for varying grid sizes r (Figure 4.1) and estimated the transmission term ρ and the mixing parameter c .

4.3.6 Exploring the spatial autocorrelation using kernel density smoothing

To compare the model fit, I also estimated the spatial autocorrelation in rabies cases using kernel density smoothing. Due to the high computational cost, I did this only for a small subset of the data in the south-west of Thuringen at a few different time lags. Data was aggregated at 1 km^2 grid sizes. Kernel density smoothing of the rabies cases was conducted using the `spkernel2d` function in the `splanx` package in R, which uses a quartic smoothing kernel (Berman & Diggle, 1989; Rowlingson & Diggle, 1993).

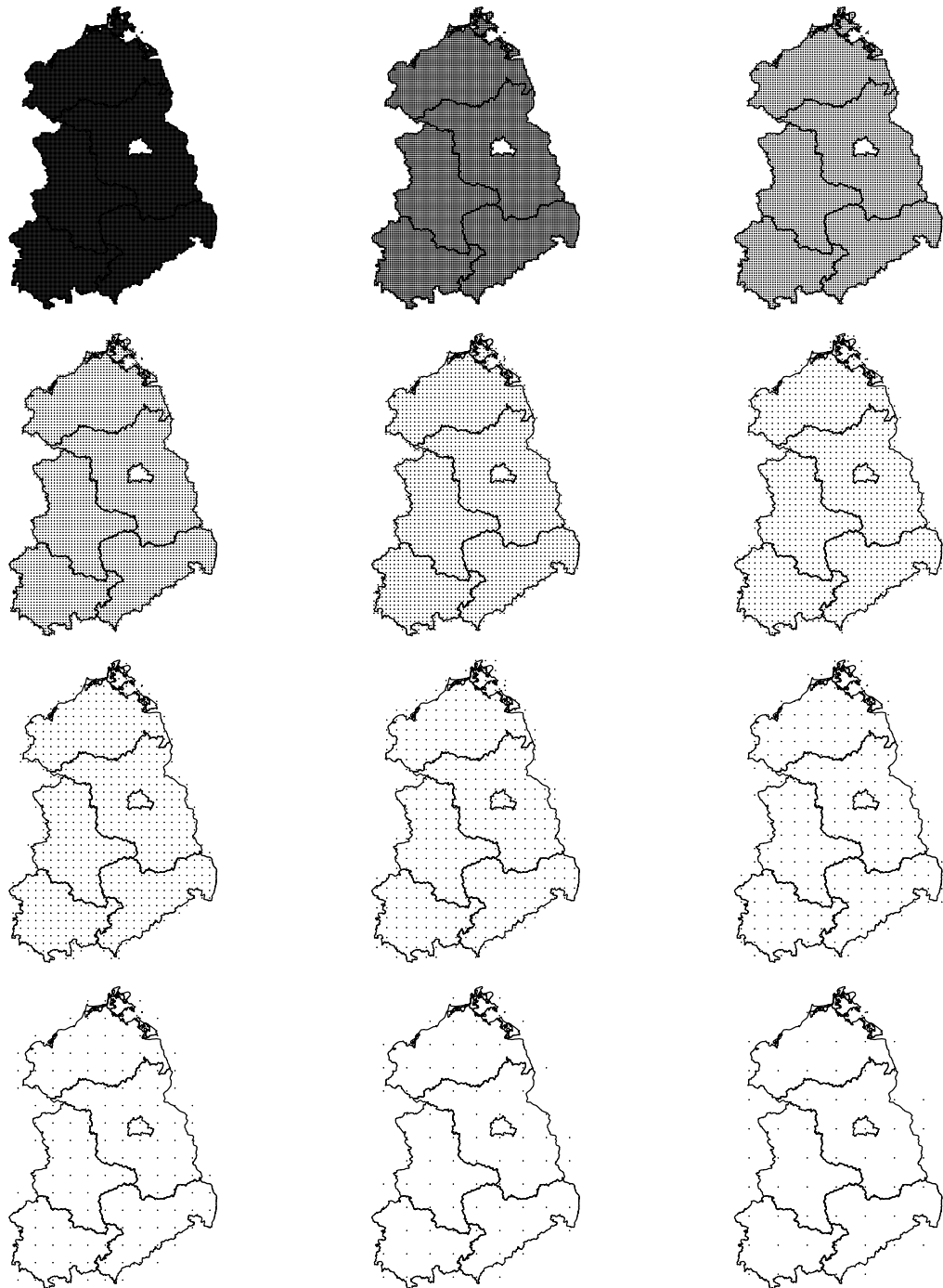


Figure 4.1: Scales explored when estimating the transmission parameters using a generalized linear model. Grid sizes range from $50 \times 50 \text{ km}^2$ to $2 \times 2 \text{ km}^2$.

4.4 Results

Understanding of spatial and temporal infection dynamics at a local level has great potential to improve the planning of control programmes. Using a log-Cox latent Gaussian model fit

to infected cases, I investigated the local rabies transmission dynamics using a non-separable SPDE model to estimate the spatial correlation between cases. The resulting model was able to capture local spatial dynamics of rabies (Figure 4.3) and yielded a close fit to rabies case time series reported at the federal state level when the intensity function was calculated at this level of data aggregation (Figure 4.4). I estimated that rabies cases are typically clustered within 5km of each other, with a spatial autocorrelation of 0.25, that decays gradually out to 20km (Figure 4.5). The spatial autocorrelation estimated using the non-separable SPDE model suggests that rabies cases are clustered more locally (within 20km) compared to the kernel density smoothing estimates calculated from the reported rabies cases (25-50km) (Figure 4.2). The kernel density estimates also show a slow decay, with most cases clustered locally (within 5-10km). However, the extent to which the cases were correlated were variable across time (sometimes decaying to 25km or 50km). Overall the spatial autocorrelation estimates suggested that cases occurring further away were correlated irrespective of the bandwidth used ($h = 1, 3, 5, 10$ km).

Data is often aggregated at the scale of administrative units rather than epidemiologically relevant ones, obscuring local transmission dynamics. To explore the effect of data aggregation on the estimate of transmission parameters, I aggregated the data at different grid sizes, ranging from 2x2 km to 50x50 km, and estimated the transmission rate and heterogeneous mixing terms using a GLM fit to future infectious cases using the susceptible and infected density fields. Overall, the models achieved a good fit to the data, with the adjusted R^2 in all cases being above 83% Figures 4.8 and 4.9. My results reveal that even when data is aggregated at a fine-spatial resolution (2x2 km), approximations of local mixing in the form of a lower transmission rate and greater heterogeneous mixing ($c < 1$) are needed to recreate observed rabies dynamics (Figure 4.6). To estimate the transmission parameter ρ when c is 1 (i.e. homogenous mixing) I extrapolated from the GLM estimates of ρ using a second order polynomial to get the line of best fit (Figure 4.6). The mean estimate for ρ was 0.15, however, there is a lot of uncertainty in the prediction, as shown by the wide 95% credible intervals (dotted blue line). Comparisons to contact tracing studies for fox rabies and exploring the data at a finer spatial-scales is needed to further assess this prediction. Similarly, the prediction may be sensitive to the choice for the functional form of the line of best fit.

To investigate the effect of data aggregation on our estimates of the key transmission parameters, I aggregated the data at different grid sizes, ranging from 2x2 km² to 50x50 km², and estimated the transmission rate and heterogeneous mixing terms using a GLM (Model fits in Figures 4.8 and 4.9. My results reveal that even when data is aggregated at a fine-spatial resolution (2x2 km²), approximations of local mixing in the form of a lower transmission rate and greater heterogeneous mixing ($c < 1$) are needed to recreate observed rabies dynamics. The transmission rate gets progressively smaller and mixing becomes more heterogeneous at larger spatial scales (Figures 4.6 and 4.7), with estimates of c declining accordingly. A

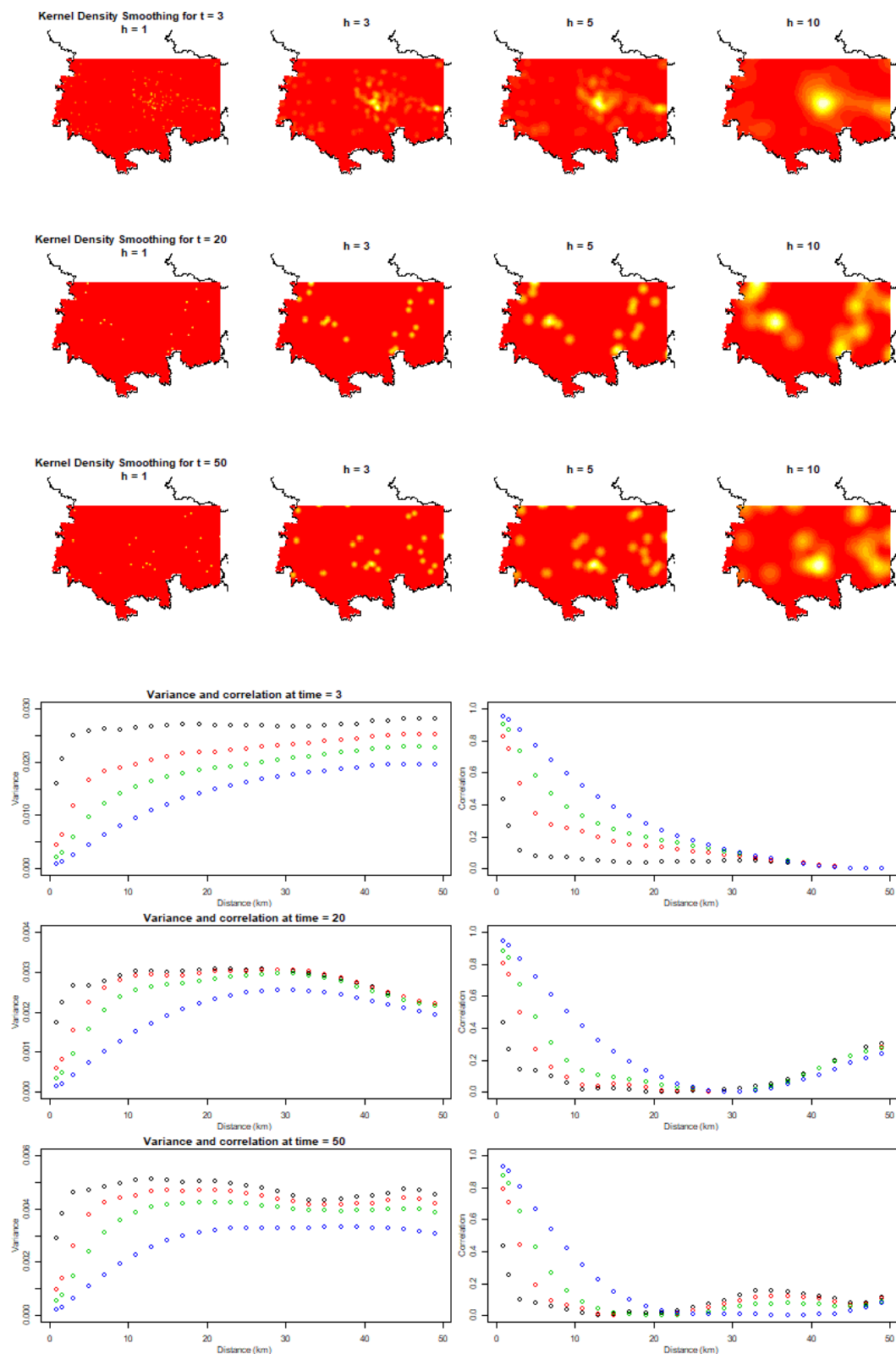


Figure 4.2: Kernel density estimation of observed rabies cases in Thuringen at months 3, 20 and 50. The top panel shows the resulting smoothed kernel density surfaces for different bandwidths ($h = 1, 3, 5$, and 10 km) where red = no rabies cases, yellow = rabies cases. The bottom panel shows the variogram and correlation estimated in cases with distance. Colours represent the different bandwidths used: $h = 1, 3, 5, 10$ (black, red, green, blue).

lower transmission rate ρ and lower mixing term c both reduce the new cases per infected individual.

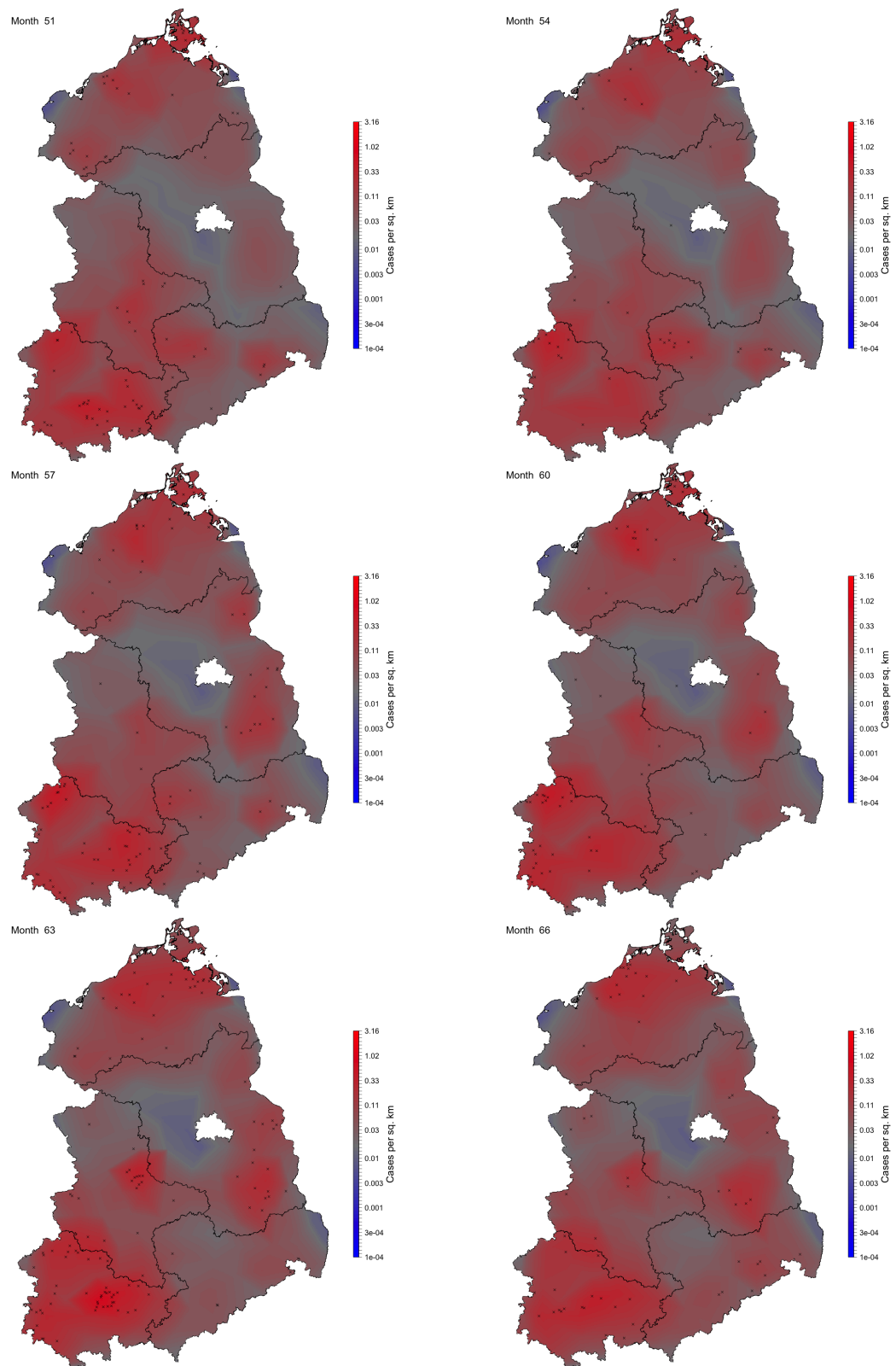


Figure 4.3: Model fit of the true infected individuals over space and time shown at 3 month intervals from 1987-1989. Colours reflect cases per sq km. Red represents high rabies incidence, gray represents low incidence, and blue represents little to no rabies incidence. In this plot you can see the different rabies foci, varying intensity in rabies cases, and the movement of rabies through time.

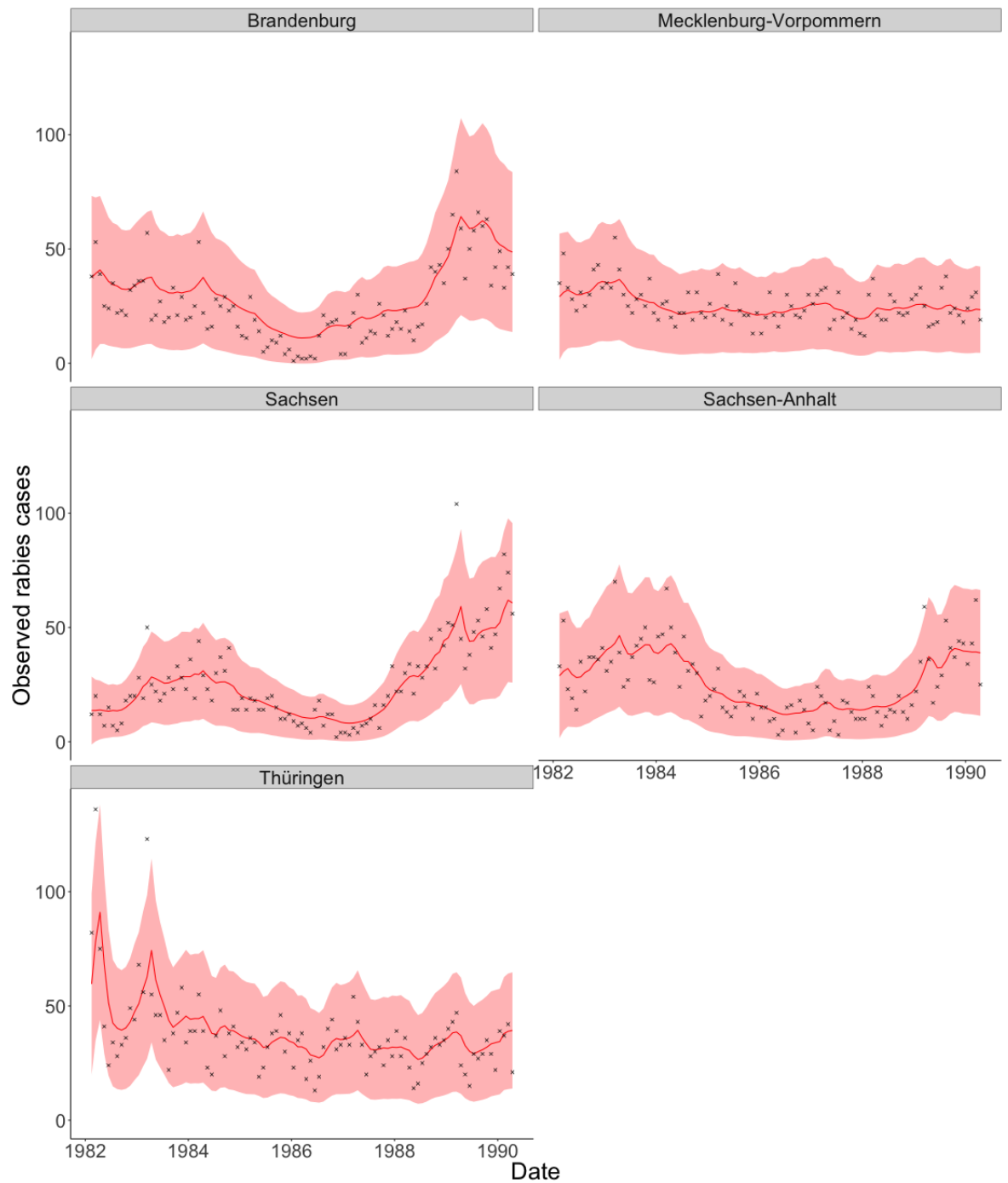


Figure 4.4: Estimated observed rabies cases from the non-separable space-time SPDE model fit to every 3rd month for each federal state level in East Germany. The red line is the mean fit to rabies case data, the shaded red region represents the 95% confidence intervals, and the black x's represent the observed cases.

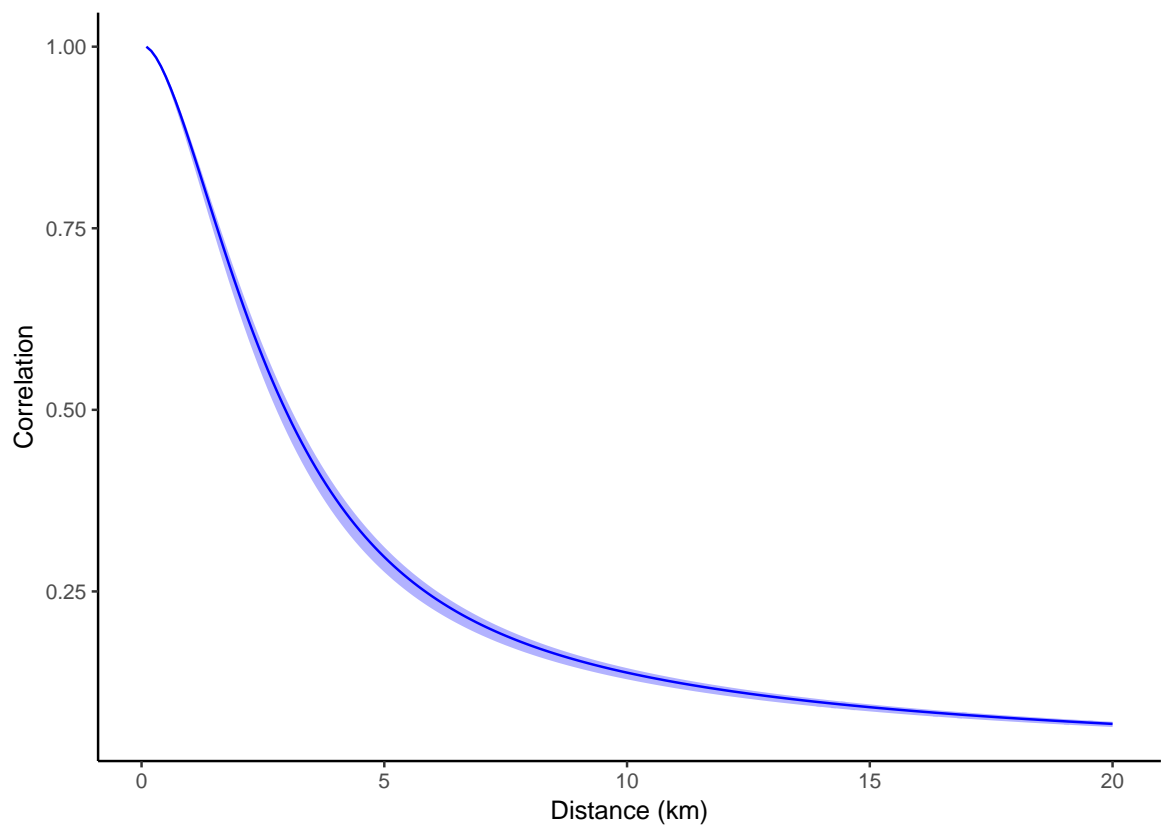


Figure 4.5: Marginal spatial autocorrelation estimate from the non-separable space-time random process $d(s, t)$ in Equation 4.3 with mean (blue line) and 95% credible intervals (shaded).

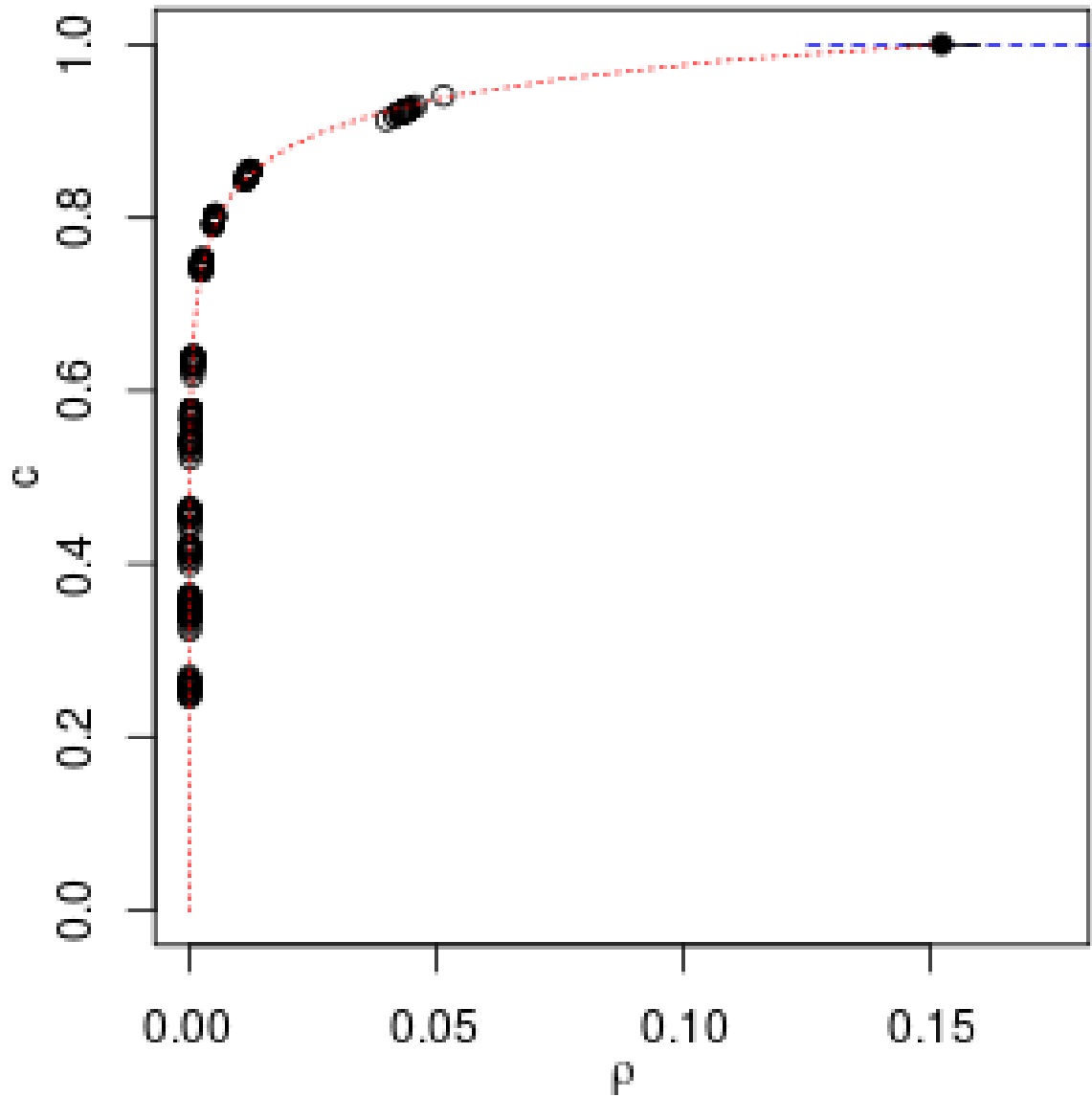


Figure 4.6: Estimates of c , the heterogeneity parameter, and ρ , the transmission parameter. The multiple black circles are the parameter estimates for the different grid sizes for different realisations of the Susceptible population simulation. The red dotted line is the line of best fit used to predict ρ when c is 1. The blue dotted line shows the uncertainty (95% credible intervals) around the prediction for ρ .

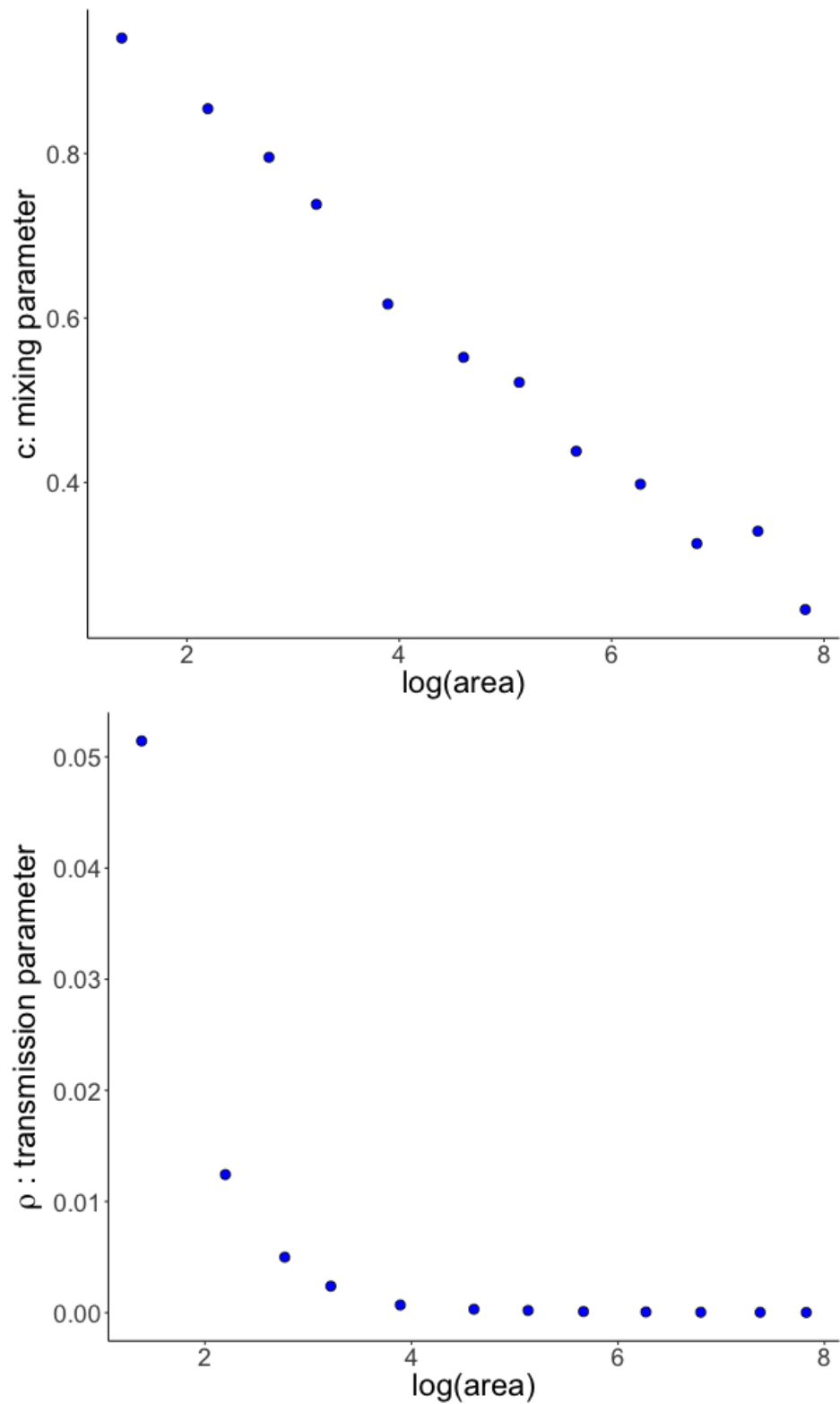


Figure 4.7: Estimates of c , the heterogeneous mixing parameter (top panel), and ρ , the transmission rate (bottom panel) plotted against the log of the aggregated grid cell size (range: log of 2 km^2 to 50 km^2).

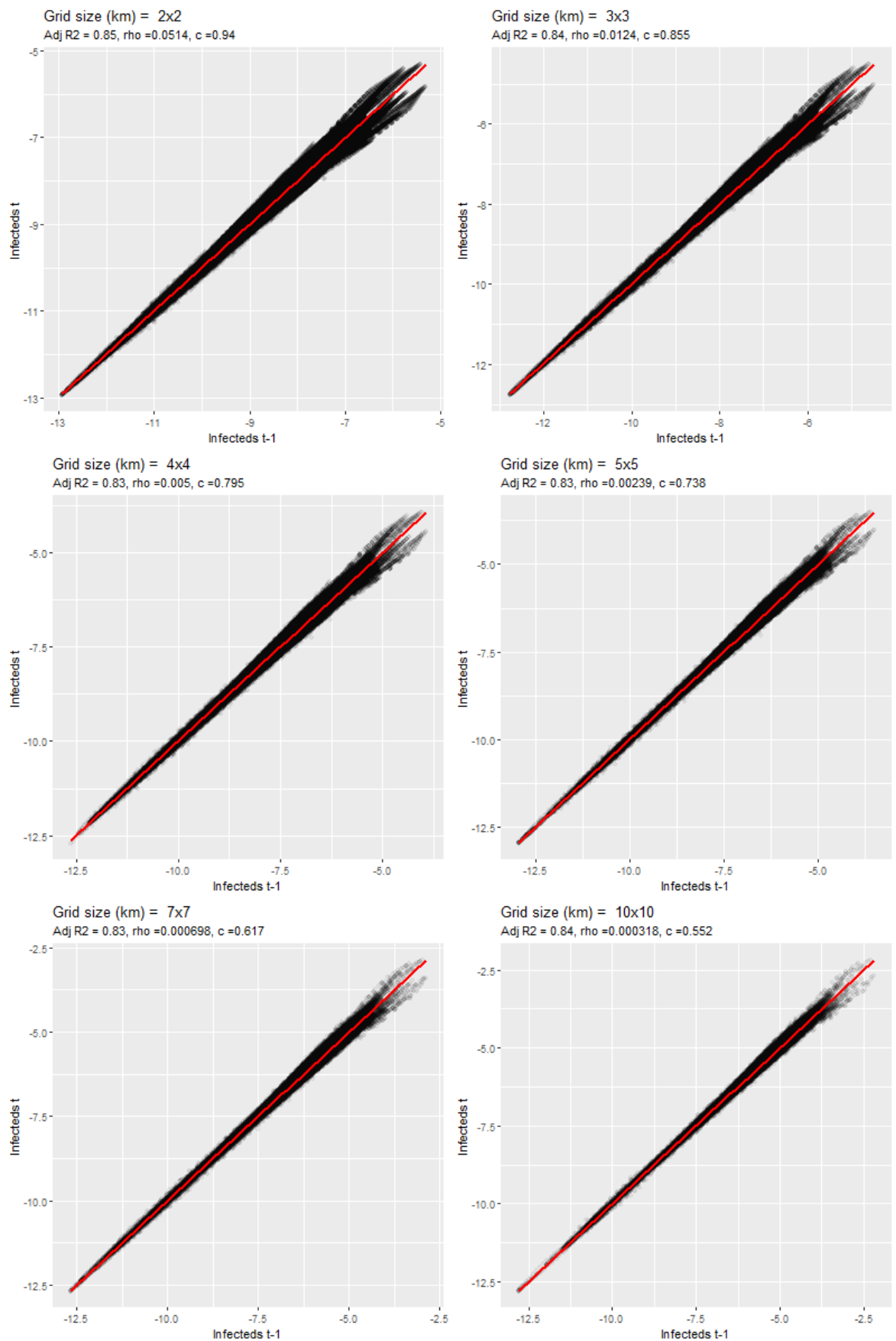


Figure 4.8: GLM model fit of infected cases at time t for the smallest 6 grid sizes ($2 \times 2 \text{ km}^2$ - $10 \times 10 \text{ km}^2$) as a function of past infected cases at time $t-1$.

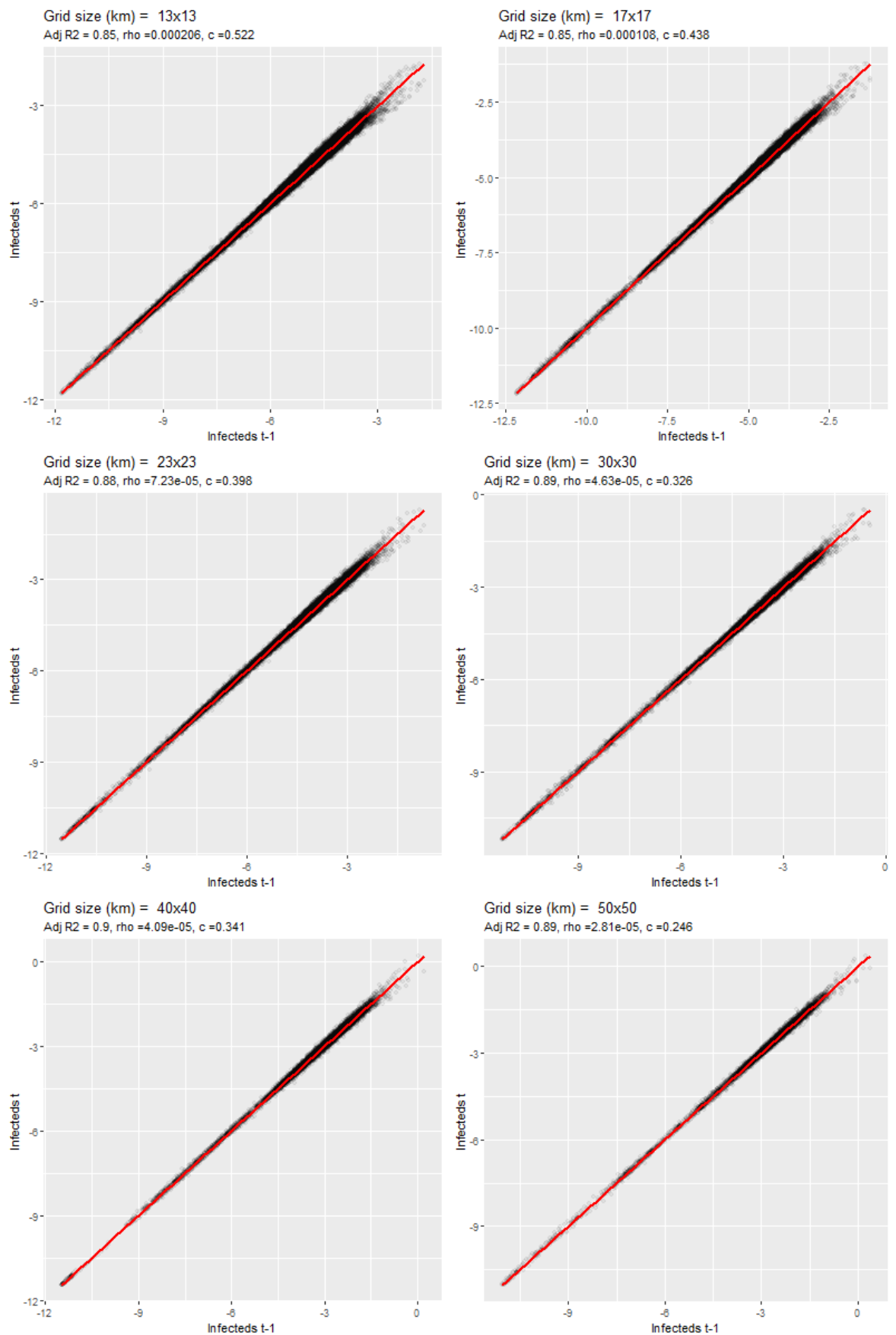


Figure 4.9: GLM model fit of infected cases at time t for the larger 6 grid sizes ($13 \times 13 \text{ km}^2$ - $50 \times 50 \text{ km}^2$) as a function of past infected cases at time $t-1$.

4.5 Discussion

High-resolution spatiotemporal models capable of capturing local infection dynamics in wildlife populations can generate fundamental insights into transmission processes. Here, I present a computationally efficient approach for modelling spatial and temporal rabies dynamics fit to partially-observed case data. Using this model, I estimated the spatial correlation between cases and explored the effect of scale on estimates of transmission terms. Specifically I found that (i) rabies cases are clustered within 5km with spatial dependency gradually reducing out to 20km; (ii) estimates of transmission terms vary depending on the scale at which the data is aggregated; (iii) local disease dynamics are approximated by lower transmission and more heterogeneous mixing as surveillance data are aggregated at coarser scales.

Recent rabies outbreaks around the world highlight the need for accurate predictions of disease spread and spatial planning at a local scale (Castillo-Neyra *et al.*, 2017; Mulatti *et al.*, 2012; Townsend *et al.*, 2013b). Estimates of spatial models of infection can help us to understand the spatial scale of transmission and inform control strategies by identifying areas of high prevalence where there is a greater risk of infection. Using this information, intervention strategies can be matched to the anticipated distribution of cases. The aerial distribution of baits containing vaccine is highly accurate even for complex spatial distributions (Breitenmoser & Müller, 1997). It is therefore feasible to tailor vaccination planning to local patterns in disease incidence.

Previous studies have used the home range of foxes to inform estimates of disease spread (Thulke *et al.*, 2008). However, studies of rabid animals suggest that behavioural changes during the infectious stage mean that the distance an infected animal moves is highly variable and could differ from home ranges of healthy animals (Andral *et al.*, 1982; Hampson *et al.*, 2007). Furthermore, between-individual variation in transmission may arise from differences in behaviour, immune status, and environmental and stochastic factors among others, which play an important role in determining spatial and temporal disease dynamics (Lloyd-Smith *et al.*, 2005b). By fitting the model to data, one can infer heterogeneities in transmission directly (Lloyd-Smith *et al.*, 2005b). My estimates show that spatial dependency in rabies is on the order of 5 km but reaches 10-20 kms. This is similar to patterns reflected in the rabies cases data which is encouraging. However, the kernel density smoothing approach only serves as a descriptive inspection of the data and does not include the observation process. By modeling the latent field using a non-separable SPDE model, we are able to explicitly model the spatial and temporal relationships in the data and learn about the dynamics of rabies transmission. These estimates may have important implications for the design of spatial control strategies and could shed light on whether resources should be concentrated where the case was detected or in a protective ring around the detected case as a means to build up immunity (Rees *et al.*, 2011; Thulke *et al.*, 2008).

Many wildlife diseases are spread through direct transmission, yet surveillance data is often aggregated at the level of administrative units which can vary in size from towns to provinces to states. Aggregation of incidence data can obscure local dynamics of transmission and makes it difficult to interpret transmission parameters. Understanding how the scaling of local processes is approximated as the resolution of incidence data becomes more coarse can therefore add to our fundamental understanding of disease dynamics by increasing interpretability of transmission parameters by estimating population mixing. I was able to explore when it becomes necessary to approximate local mixing by aggregating the data at different spatial resolutions and whether these approximations are an accurate scaling of local processes. Very rapidly approximations in the form of a lower transmission term and higher heterogeneous mixing are necessary to capture the scaling up of individual interactions to regional dynamics. Population mixing is known to be heterogeneous, with individuals that are further apart being less likely to interact ((Glass *et al.*, 2003), Chapter1). The mixing term c allows me to capture saturation effects that occur at high incidence, when infected individuals produce less infections due to local susceptible depletion — either through disease-induced mortality or contact with already exposed (incubating) individuals. These two effects are approximated by a lower transmission rate and reduced population mixing as the scale at which the data is aggregated increases. Predictions of the transmission, ρ , when c is 1, suggest that transmission when there is homogeneous mixing can be quite high (0.15) (Figure 4.6), however, there is a lot of uncertainty in this estimate and further explorations of the data and comparisons to contact tracing studies are needed to assess the prediction which could also be sensitive to the line of best fit model choice. Spatial approximations at the administrative level probably work better for human diseases where social structures act to increase mixing (e.g. schools) or for wildlife populations that are heavily structured (e.g. herds). The mixing term, I infer at coarser scales is therefore likely to be quite different from other cases and should be considered when carrying out similar analyses for other populations.

Many wildlife diseases lack the necessary combination of host and pathogen data required to understand spatial dependency in infection dynamics. Here, I demonstrate how the host population can be simulated in the absence of incidence data by modelling the host population stochastically incorporating demographic processes and environmental spatiotemporal variability using the SPDE approach. Further extensions to this work would include relating the susceptible population to habitat data that could be used to provide more refined estimates of environmental variability. Sensitivity analyses would also reveal how sensitive these estimates are to assumptions about the spatial variation in population density.

There are several advantages and limitations to the approach I have used in this chapter to analyse the data. One advantage of the INLA framework and non-separable SPDE approach is that you can estimate easily latent (unobserved) processes like the spatial and temporal dynamics of infection. The non-separable SPDE approach assumes that the spatial and temporal dynamics of infection are not independent of one another, which is realistic for fox

rabies, where the disease is spread by the movement of infected foxes through time and space. Another useful feature of the INLA framework is its additive structure. An effect can be easily removed or added which means that you can add other latent parts to the model and new hyperparameters and the modelling framework and computations staying the same. However, one disadvantage of this structure is that you cannot link the components within an SIR model (e.g. that the infected individuals are removed from the susceptible population). Although it is not epidemiologically accurate, in the case of rabies where the disease only affects a very small percentage of the population (less than 1% of the population per month, Katie Hampson pers. comm), I can assume that this removal of infected individuals is negligible. Similarly, with the SPDE approach I am constructing a smoothed intensity surface of infected individuals, meaning that even in regions with no rabies the model assumes there is a small intensity of infected individuals because it is computationally more tractable. To work around this, in future versions of the model where I wish to explore vaccination strategies, I can set a threshold for the intensity for when I can include that there are zero cases in an area (i.e. that rabies has been eliminated locally).

Targeted spatial vaccination planning has great potential to inform elimination strategies, reduce costs, and guide expectations regarding the impacts of control measures. The model is able to capture the local dynamics underlying spatial patterns in incidence. There is the potential to extend this work to inform how newly introduced epidemics spread and can be controlled by testing different vaccination configurations. This work has immediate application to the design of cordon sanitaires in Europe and to strategies aiming to rapidly eliminate re-emergence in high-risk countries such as Greece and Turkey. It may also be applicable to answering analogous questions for the elimination of dog-mediated rabies and for other vaccine-preventable diseases in spatially structured populations. The analytical and statistical framework developed here has the potential to generate fundamental and applied insights into the elimination of infectious disease and the modelling of wildlife disease data.

CHAPTER 5

Discussion

Discussion

To improve our understanding of wildlife rabies, a disease that has major implications for public health, wildlife conservation and economics, I developed and applied state-of-art statistical approaches to analyse extensive spatial and long-term surveillance data documenting the unique history of fox rabies elimination. The work in this thesis contributes to our fundamental understanding of how infectious diseases persist and how control programmes can be optimized to eliminate infection. Lessons learnt from the successful elimination of fox rabies in Western Europe through oral rabies vaccination (ORV) can be directly applied to increase the probability of success and reduce the time and money spent on these programmes. Furthermore, the methodological approaches developed demonstrate how strategic guidance and biological understanding can be achieved from sparse and partially observed data for wildlife diseases.

5.1 How do infectious diseases persist?

The study of fox rabies in Europe sheds light on the fundamental question of how acute infectious diseases persist and may be controlled through vaccination. My analyses reveal that incursions (migrating infected individuals), demographic processes (e.g. birth and death), local transmission, and heterogeneous mixing all play a key role in rabies dynamics.

Once a disease has been eliminated locally, the migration of infected individuals (incursions) can lead to re-emergence, termed ‘rescue effects’ Klepac *et al.* (2013). By seeding new epidemics and preventing localised extinctions, rescue effects prolong disease persistence (Brown & Kodric-Brown, 1977; Earn *et al.*, 2000, 1998; Hanski, 1998; Keeling, 2000). Incorporating incursions into the Bayesian state-space hierarchical metapopulation model allowed for disease re-emergence in neighbouring regions. In chapter 3, results from my model simulations reveal that large and well-connected regions are often at highest risk from reintroductions, likely due to larger susceptible populations and a greater probability of incursions across extensive shared borders. Directing surveillance efforts to areas bordering endemic regions is important for early detection and control of incursions. The Bayesian state-space modelling approach provides a useful framework for quantifying the role of incursions between regions and exploring configurations of vaccination campaigns and their deployment.

The demographic processes of birth and death played an important role in sustaining infection within the fox population. Foxes exhibit a marked birth pulse in April when the population more than doubles (Anderson *et al.*, 1981; Iossa *et al.*, 2008). The resulting influx of unprotected newborn foxes and the relatively short life-span of foxes (~ 4 years, Iossa *et al.* (2008)) leads to a rapid turnover of the population such that high levels of herd immunity achieved during ORV campaigns are short-lived. In chapter 3, I found that missing Autumn vaccination campaigns following the birth pulse lead to the greatest setbacks in terms of time to elimination. Missing Autumn campaigns should be avoided where possible to avoid setbacks and the need for additional campaigns. The timing of campaigns in relation to demographic processes should be considered more generally in the planning of vaccination for other populations with seasonal birth pulses and/or rapid population turnover (Peel *et al.*, 2014).

Population connectivity and local transmission play a key role in wildlife disease dynamics. Infected individuals are more likely to spread disease to their neighbours. In a fatal disease, like rabies, where disease is spread through direct contact and there is a lack of disease induced immunity, this results in redundant exposures of already latent (incubating) animals and local susceptible depletion as individuals bitten within an area die. As incidence increases, transmission per infected individual decreases as the host population is depleted and contacts occur with already exposed individuals. In chapter 2 and 4, I found that incorporating heterogeneous mixing when modelling transmission at the regional level was important to capturing local patterns of infection. In chapter 2, I used a transmission form that incorporated heterogeneous mixing, whereby the rate of transmission depended on the size of the region. In this functional form, the transmission per infected individual decreased as the number of infected individuals increased, and was used to account for local susceptible depletion and contacts occurring with already exposed individuals. In chapter 4, analysis of georeferenced fox rabies cases allowed me to explore these processes at the local spatial scale at which they were occurring. My analyses of the monthly spatiotemporal correlation between rabies cases revealed that fox rabies cases are clustered within 5km decaying to 20 km. Further details of the methodical approaches used are provided in section 5.3.2.

5.2 How can control strategies be optimized to eliminate infection?

Vaccination interrupts the chain of transmission as contacts occur increasingly between infected and vaccinated individuals that do not lead to infection. However, there is little scientific guidance as to how long control programmes must operate to eliminate infection. A challenge faced by disease control programme managers is estimating timelines for control and elimination and their resulting programmatic and budget implications. Theoretical estimates

of the time required to eliminate a pathogen are typically shorter than what is observed in practice (Wearing *et al.*, 2005). Models typically do not capture all elements of stochasticity and heterogeneity of any kind usually prolongs circulation (and thus persistence) of disease. Moreover, most theoretical models assume closed systems without incursions, however we know for most diseases that incursions are frequent, and for rabies, my study system, they are increasingly recognized to be important for persistence (Bourhy *et al.*, 2016; Zinsstag *et al.*, 2017). Finally, most theoretical models assume idealized implementation of control strategies, for instance, high and even vaccine coverage, but in practice implementation is never perfect and therefore we may overestimate the potential the potential impact of interventions.

Infectious diseases often persist for prolonged periods at low incidence (Klepac *et al.*, 2013; Tischendorf *et al.*, 1998), with at least as much effort required to achieve elimination as needed to bring disease under control (Freuling *et al.*, 2013). At the same time, campaigns are often missed or delayed due to logistical and financial constraints. The epidemiological impact of these practicalities are not well understood. Realistic estimates of elimination time horizons and improved understanding of the impact of logistical constraints on progress to elimination should inform better policy and practice. Dynamic demographic processes govern levels of vaccine-induced immunity across populations. In wildlife species with a marked seasonal birth pulse like foxes (Peel *et al.*, 2014), vaccination campaigns following the birth pulse, when the largest number of animals can be vaccinated, play an important role in maintaining high levels of herd immunity. Seasonal dynamics are common in a range of diseases and hosts. Seasonal birth pulses are not limited to animal populations (Martinez-Bakker *et al.*, 2014). Martinez-Bakker *et al.* (2014) observed variation in seasonal birth pulses in human populations across latitudinal gradients and found variations in the timing of birth pulses had a significant impact on childhood disease dynamics. Seasonal changes may also influence the spatial distribution of hosts. Seasonal spatial clustering of host populations has been linked with outbreaks of measles in humans (Bharti *et al.*, 2011), Ebola in Central African gorillas (Caillaud *et al.*, 2006), and mycoplasmal conjunctivitis in birds (Dhondt *et al.*, 2005). In chapter 3, I found that consecutive campaign sets (campaigns occurring in all regions in the same month) and campaign sets following the birth pulse were the most important in maintaining herd immunity and increasing the probability of elimination. In the absence of vaccination, the birth pulse can swiftly reduce herd immunity as unprotected newborn foxes enter the population. Sustained effort in all regions was necessary to eliminate the disease from all regions. Incomplete vaccination extended time to elimination. The same if not more effort was required to eliminate the disease after a campaign set was missed. Together, these findings have important implications for the planning of ongoing control programmes of fox rabies in Europe and may also apply to other diseases with seasonal dynamics; namely, managers should strive not to miss campaigns, especially those following the birth pulse, and should secure funding and plan for additional campaigns in case campaigns are missed for logistical reasons.

In chapter 4, I estimated the spatial correlation of rabies cases using a space-time stochastic partial differential equation (SPDE) model. Rabies cases were clustered within 5 km of each other, with correlation declining out to 20km. By capturing the local dynamics underlying spatial patterns in incidence, the space-time model I developed can be used to generate fundamental insights into local persistence and inform how newly introduced epidemics spread. These insights could be particularly valuable for outbreak responses to incursions and be used to inform the spatial extent of vaccinations. Field studies show that the aerial distribution of baits containing vaccine is highly accurate even for complex spatial distributions (Breitenmoser & Müller, 1997). It is therefore possible to explore different spatial configurations that are not limited to administrative regions and use these findings to inform spatially targeted vaccination programmes in Europe and elsewhere.

5.3 What advances have been made in the modelling of wildlife diseases?

Epidemiological data are inherently complex due to variability arising from both the infectious disease dynamics, including stochastic spatial transmission processes, and the observation errors in detecting cases. Here I describe several reasons why the study of wildlife disease is challenging, while noting that many of the same challenges exist for infectious diseases circulating in human populations. First, there tends to be less information available for wildlife. Observing transmission directly is rarely possible. In most cases, the state variable (disease incidence) is only known through indirect measures, with the probability of observing the disease varying over time. Because surveillance only captures a small proportion of circulating infections, failed invasions or low level persistence may be missed entirely. In addition, surveillance data is often aggregated, making the study of local transmission processes challenging. Wildlife populations are not usually monitored, therefore key information regarding their size and spatial distribution are unknown. Wildlife vaccination programmes are similarly difficult to implement and monitor. Herd immunity in wildlife is more short-lived compared to humans due to a higher population turnover. Wildlife movement also differs compared to humans in terms of social groups, territory boundaries, limited dispersal etc. (Altizer *et al.*, 2003).

The sources of observation and process error mentioned above can be classified into uncertainty due to incomplete/missing data and challenges in capturing local transmission processes at coarse spatial resolution. I present several approaches applied during this thesis for dealing with these challenges.

5.3.1 Dealing with incomplete and missing data

The Bayesian framework provides a flexible approach for dealing with missing data and applying statistical inference to mechanistic models. In the absence of data about a particular quantity or process, a missing parameter or state can be estimated from a *prior* probability distribution that reflect one's beliefs about the missing quantity before some evidence (usually the data being modelled) is taken into account. The use of informed priors, based on past studies and the literature, directs the model fitting to biologically plausible parameter space. An advantage of the Bayesian approach is that it allows different data sources and data types to be included when constructing priors. It is also possible to estimate latent processes. Latent processes are variables or states (when part or all of the population time series are unknown) that are not directly observed but are inferred through statistical models from observed processes. In this thesis I used two Bayesian approaches: State-space models and latent Gaussian models.

State-space models are time series models that are able to accommodate uncertainty in epidemiological data through linked biological and observation process models. In the hierarchical Bayesian state-space modelling approach in chapter 2, I used studies from the literature on rabies and foxes to inform key parameters including: birth rate, survival rate, carrying capacity of the susceptible population, environmental noise (representing environmental fluctuations in the birth rate), the transmission rate, and variations in the observation rate. One of the difficulties I encountered in modelling these data was that certain parameters were confounded, including population size, transmission rate, and observation probability. These parameters were difficult to disentangle from one another because the same disease dynamics could be explained by a larger population and smaller transmission rate, or a lower observation rate and higher transmission rate. Simulating data with set parameter values and then assessing whether these parameters could be retrieved by the model was useful for determining what was confounded and what could be estimated using the hierarchical Bayesian state-space model in chapter 2. The addition of other data was also useful in disentangling the parameter estimates. In chapter 2, I was able to estimate the risk of transmission and observation probability by using cross-sectional hunting data to inform the estimates of the risk of transmission. This highlights how diverse sources of data can help fill gaps in an analysis and allow parameters to be estimated that would otherwise be confounded.

The integrated nested Laplace approximation (INLA) approach developed by Rue *et al.* (2009) allows for the modelling of hidden (latent) processes to the spatial domain. By fitting latent Gaussian models in a Bayesian context in which spatial and temporal autocorrelation in the latent field assume a shared spatial structure and are reflected by Gauss Markov random fields (GMRF) (Rue & Held, 2005), hidden spatial and temporal processes can be estimated. These may include effects of unobserved environmental processes (collectively termed environmental noise) or hidden states (e.g. the susceptible population). In the absence

of detailed information on the fox population, I simulated the host population stochastically incorporating key demographic processes and environmental spatiotemporal variability using estimates from the literature (chapter 4). Bayesian methods can be used to increase our understanding of epidemiological processes by providing a flexible and practical approach to fitting data that allows the user to make the best use of the data available.

5.3.2 Dealing with aggregated data

Many diseases spread through local contact, however incidence data is often collected at coarser scales. Researchers therefore model disease at the population level, necessitating the use of approximations to account for the scaling up of local processes. In chapter 2, I found that accounting for heterogeneous mixing and local susceptible depletion was crucial to capturing fox rabies dynamics. I was unable to fit the model assuming homogeneous mixing as the model was not able to generate even a poor fit to data. In chapter 2, I used a decay function to approximate the scaling of local interactions (heterogeneous mixing) within a region. The biological rationale behind this function was to capture local susceptible depletion and redundant infection of incubating individuals. I think this was an appropriate solution for data aggregated at this level, however in chapter 4 I was able to explore in greater detail the effect of scale on the estimate of parameters related to transmission and population mixing using a regression model applied to incidence data aggregated at different spatial resolutions. At very fine spatial scales ($2 \times 2 \text{ km}^2$) the mixing term approaches but never reaches 1. This suggests that even at small spatial scales a model with homogenous mixing does not capture susceptible depletion or redundant infections. Overall, these findings show that reducing the scale over which rabies incidence is modelled means that the transmission term equates more to the actual number of contacts an infected individual makes, whereas at larger scales both mixing and transmission need to be approximated. This takes the form of an increasingly reduced transmission rate and level of population mixing, supporting my hypothesis that local transmission dynamics underly patterns in infection observed at regional scales.

5.3.3 Modelling the spatiotemporal dynamics of disease

Encounter rates between hosts and their pathogens are influenced by the density and connectivity of other populations, and these processes can fluctuate through time (Bolker & Grenfell, 1995; Keeling *et al.*, 2001; Levin & Durrett, 1996; Rohani *et al.*, 1999). There are several ways in which space can be represented ranging from a continuous landscape to a network (Keeling & Eames, 2005) or as a metapopulation (Hanski & Ovaskainen, 2000). There are also a variety of ways to quantify the spatial components of transmission, including multiple classes of host (Diekmann *et al.*, 1990), spatial structure at the household and farm level (Ball *et al.*, 1997; Fulford *et al.*, 2002; Keeling, 1999; Prentice *et al.*, 2017) and mechanistic

movement between groups (Cross *et al.*, 2005; Hess, 1996; Keeling & Rohani, 2002; Thrall *et al.*, 2000). Here I briefly discuss the modelling approaches used to study rabies in the past. I then present the approaches used in this thesis.

Rabies is well studied in the field of disease ecology and has yielded important insights into our understanding of spatial infectious disease processes. Early approaches to understanding fox rabies used reaction-diffusion models of coupled partial differential equations to simulate rabies spread, that included terms for heterogeneity in the density of foxes (Murray & Seward, 1992). Since then, spatially explicit individual-based models (IBM) have been used to evaluate vaccination strategies for elimination (Eisinger & Thulke, 2008; Thulke *et al.*, 1999) and emergency vaccination (Eisinger *et al.*, 2005; Thulke *et al.*, 2008). Similar questions have been approached in the study of raccoon rabies. Smith *et al.* (2002) developed a stochastic spatial model of rabies spread through 169 townships in Connecticut. They found that large rivers act as semipermeable barriers and together with long-distance dispersal account for the observed irregular pattern of disease spread across the state (Smith *et al.*, 2002). Russell *et al.* (2005) extended the model in Smith *et al.* (2002) to forecast the spatial spread of rabies in Ohio and were able to identify regions for vaccine delivery and expanded surveillance effort. Movement and mating patterns revealed by genetic data have been applied to understand raccoon rabies infectious disease dynamics in the presence of landscape heterogeneities and quantify the permeability of barriers such as rivers (Rees *et al.*, 2008, 2009). While these theoretical models have led to important insights into rabies dynamics, particularly on rates of rabies spread into new populations, statistical inference approaches hold several advantages. Theoretical models can tell us what the logical and quantitative consequences are of a set of mechanistic assumptions and parameter values. In contrast, statistical inference approaches can tell us which models and parameters most agree with the data within a predefined space of models and parameters. Fitting models directly to data allows one to test hypotheses which are provided in the form of priors.

I used two modelling approaches to understand the spatiotemporal spread of rabies: metapopulation models using state-space modelling, and space-time models fit using R-INLA. Metapopulation models explicitly model the spatial structure of processes by representing space as a network of multiple subpopulations or patches with different rates of movement (or coupling) between them (Bolker & Grenfell, 1996). This framework is convenient for understanding the spatial coupling between regions and is useful for the planning of vaccination campaigns conducted at a regional level. The state-space modelling approach allowed me to build a detailed ecological (mechanistic) model of rabies dynamics with data. The underlying model included a demographic model of the fox population and an epidemiological model of rabies transmission. In this model local transmission was approximated by incorporating local saturation and heterogeneous mixing into the transmission equation.

The second approach used was a space-time SPDE model fit using R-INLA developed by

(Krainski, 2018). Krainski (2018) extended the SPDE model developed by Lindgren *et al.* (2011) to simultaneously capture spatial and temporal autocorrelation rather than fitting these processes separately. The temporal extensions offered by this non-separable model mean that spatially-explicit dynamical problems can now be approached with numerical efficiency and provide the opportunity to generate new insights into these processes through fitting these models to data. Using this approach I was able to capture the spatiotemporal nature of rabies transmission opening up exciting avenues for understanding epidemiological processes in disease ecology, particularly for wildlife diseases such as rabies that spread through direct contact. Estimates of spatial dependence can allow us to understand the spatial scale of transmission and inform control strategies by identifying areas of high prevalence where there is a greater risk of infection. The tradeoff with this approach is that it did not allow for the susceptible and infected models to be directly and explicitly coupled. This means that infected individuals were not removed from the susceptible population. Similarly, the effects of density dependence on the susceptible population were not included due to similar constraints. These two processes are undoubtedly important to the transmission of fox rabies but play a minor role compared to the strong seasonal forcing of the birth pulse.

5.4 Future Work

Lessons learnt from the successful elimination of fox rabies in Europe can be used to increase our understanding of disease persistence and inform control programmes inside and outside of Europe including for domestic dog rabies which continues to be a major public health burden in low- and middle-income countries but is now targeted for elimination. Further work could focus on exploring how the approaches developed in this thesis can be applied to other areas and diseases.

The hierarchical Bayesian state-space model presented in chapter 2 provides a useful approach for modelling disease data at a regional scale. In chapter 3, I demonstrated how this model can be applied to design the timing and placement of vaccination campaigns to improve prospects of elimination. This model is easily scalable and may be applicable to other areas throughout Europe and diverse rabies situations. Further work is required to explore what size of regions this model is appropriate for and how well it performs in other areas. Similarly, there is scope to include landscape heterogeneities, which can restrict/direct disease spread, into this approach. A first test would be to incorporate landscape heterogeneities into the connectivity matrix used to determine infected fox immigration rates between regions.

The space-time SPDE model in chapter 4 is able to capture key aspects of rabies dynamics and provides the basis for extending this model to generate realistic spatiotemporal predictions. The development of this approach opens up an exciting opportunity to develop strategic guidance for disease control programmes at a local scale. As a first step, this would

include exploring and predicting the success of different vaccination strategies in Europe. The approach is also highly flexible and can be expanded to fit more complex observation processes and to explore the effects of habitat and landscape features on disease spread and persistence by incorporating important covariate information. This would allow us to explore the impact of different physical barriers such as lakes, rivers, elevation, and habitat on connectivity.

5.5 Conclusion

Data-driven modelling has been used to guide policy, design vaccination strategies (e.g. FMD (Keeling *et al.*, 2003), measles (Grais *et al.*, 2008; Grassly *et al.*, 2006), and predict the impacts of control programmes (Hampson *et al.*, 2009; Metcalf *et al.*, 2012; Smith *et al.*, 2009) for a range of infections. My work adds to this body of knowledge by presenting approaches that can be used to explore vaccination strategies, time to elimination, and capture regional and local transmission dynamics. Specifically, in this PhD, I have added to our understanding of how acute infectious diseases persist. I have also generated methods to guide vaccination policies for disease elimination. The insights and approaches developed in this thesis have immediate application to the design of cordon sanitaires in Europe and to strategies aiming to rapidly eliminate re-emergence in high-risk countries such as Greece and Turkey. Through my research I have been able to explore tradeoffs in the scale and duration of ORV efforts and generate recommendations on the time horizon and investment required to achieve and maintain freedom from disease. The space-time model developed in chapter 4 can be extended to examine practical questions such as the best width of cordon sanitaires and placement of vaccination campaigns with respect to landscape features. The approaches used in this thesis also have wider implications and can be used to model and explore the dynamics of a range of diseases. In particular, the additive structure of the INLA framework means that heterogeneities (e.g. degree of seasonality in transmission, host demography, spatial connectivity) can be easily added as covariates or spatial and temporal effects.

The analytical and statistical framework developed in this thesis is also applicable to answering analogous questions for the elimination of dog-mediated rabies and for other vaccine-preventable diseases. Large reductions in the incidence of rabies have been achieved through mass dog vaccination, with disease eliminated in several countries, and regional elimination now targeted (Vigilato *et al.*, 2013). Moreover the World Health Organisation (WHO), Food and Agricultural Organisation (FAO) and the OIE (World Organization for Animal Health) have recently committed to the global elimination of canine rabies as a goal. The insights from this PhD are therefore widely applicable to the study of acute infectious diseases and the planning of vaccination strategies to eliminate disease.

APPENDIX A

Chapter 2: Carrying Capacity Derivation and Trace, Posterior, and Autocorrelation Plots

Chapter 2: Carrying Capacity Derivation and Trace, Posterior, and Autocorrelation Plots

A.1 Carrying Capacity Derivation

Starting with the following population model,

$$N_{t+1} = N_t \left(s + \frac{by}{y_r + N_t} \right) \quad (\text{A.1})$$

where N_{t+1} is the population at time $t + 1$ and is a function of the survival probability s , the maximum birth rate b , the reproductive population N_t , at time t which includes both susceptible S and vaccinated V individuals. The scalar y_r controls the strength of density dependence in the respective regions r .

Setting this to equilibrium at carrying capacity (i.e. $N_t = N_{t+1} = K$),

$$s + \frac{by}{y_r + K} = 1 \quad (\text{A.2})$$

Rearranging gives

$$y_r = \frac{K(1 - s)}{s + b - 1} \quad (\text{A.3})$$

The realised per capita annual birth rate for each region r with density dependence y_r takes the form:

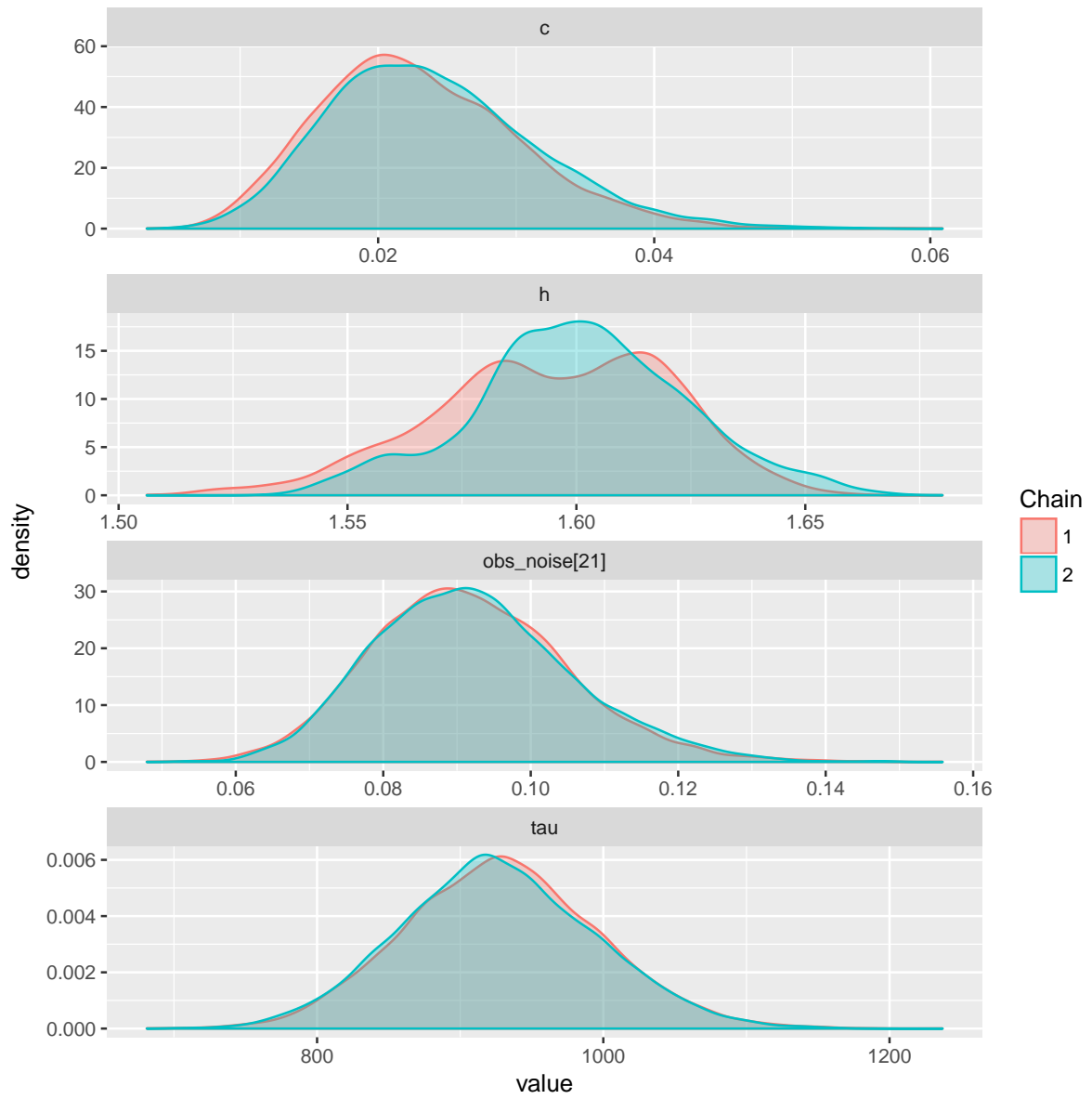
$$\alpha_{r,t} = \frac{by_r}{y_r + S_{r,t} + V_{r,t}} \quad (\text{A.4})$$

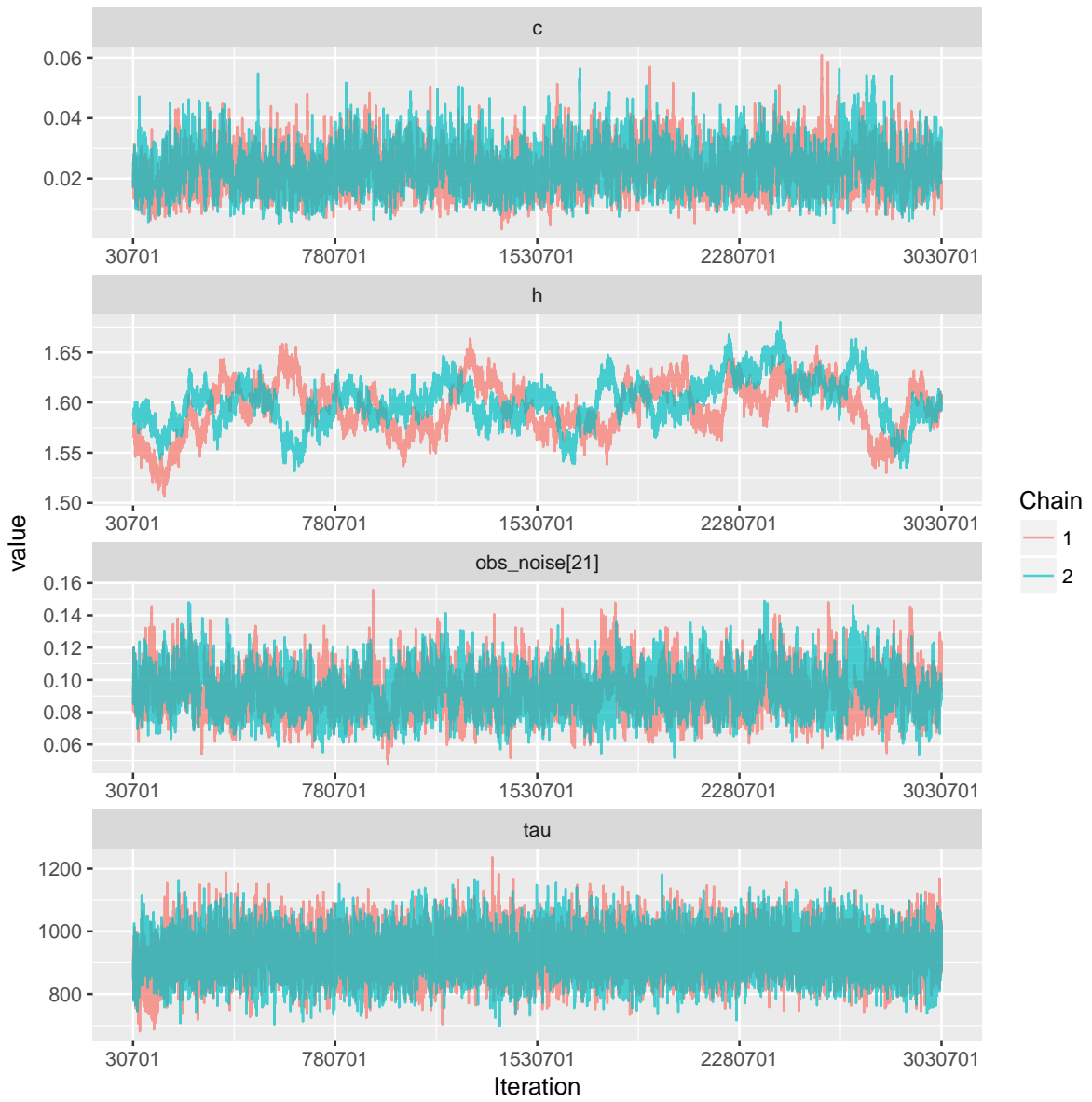
Here, the inclusion of S and V leads to density dependence, while y_r controls the strength of density dependence in the respective regions r .

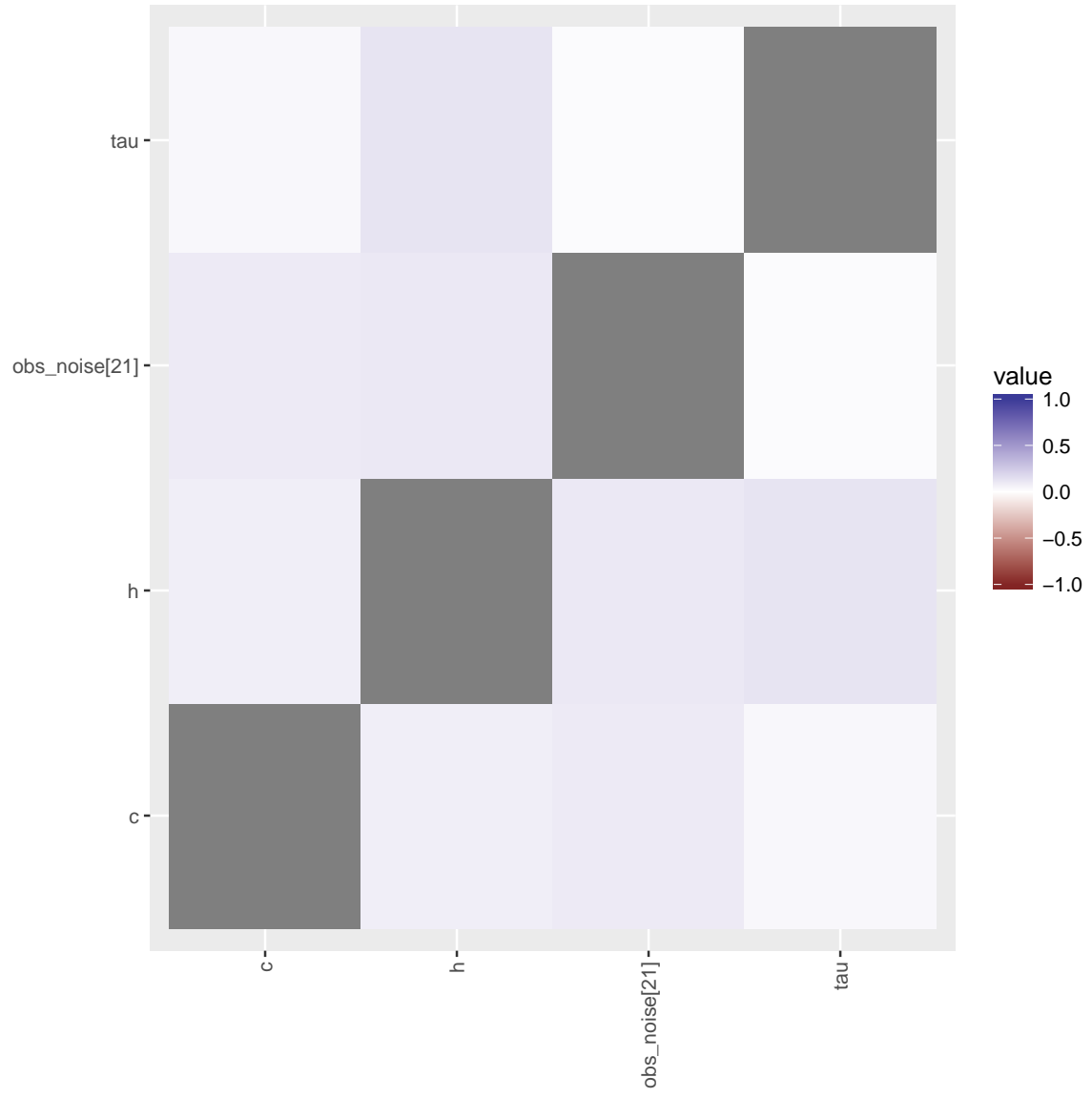
A.2 Posteriors, Trace Plots, and Correlation of fitted parameters

Posteriors, trace plots, and correlation of the fitted parameters for rabies transmission h , migration of rabid foxes between regions ρ_{max} , fluctuations in fecundity due to environmental noise τ , and the annual probability of observing rabies cases θ .

All models were fitted using the software JAGS (Plummer, 2002) which uses Gibbs sampling to generate posterior distributions of the parameters given the likelihood, prior distributions and the data itself. I ran the models for 3,000,000 iterations, with a burn-in of 30,000 and a thin interval of 300 giving 10,000 samples. I inspected the model for convergence and effective sample size. To account for the fact that rabies had been circulating in Germany since the late 1940s, I started the model 10 years (120 time steps) prior to when the time series began to allow the system to settle at an endemic equilibrium. Fitting of the model required considerable computational time and a compromise in what parameters were estimated in order for the model to converge.







APPENDIX B

Introduction to the intrinsically stationary
iterated heat equation in Chapter 4

Introduction to the intrinsically stationary iterated heat equation in Chapter 4

The non-separable space-time stochastic partial differential equation (SPDE) approach we are using is based on an iterated intrinsically stationary heat equation with a stationary spatially correlated driving noise (Krainski, 2018). It can be written as

$$\tau(\rho \frac{\partial}{\partial t} - \Delta)^{\alpha_t} u(\mathbf{s}, t) = \mathcal{E}(\mathbf{s}, t) \tag{B.1}$$

$$(1 - \gamma_\varepsilon \Delta)^{\alpha_\varepsilon/2} \mathcal{E}(\mathbf{s}, \delta t) = \mathcal{W}_\varepsilon(\mathbf{s}, \delta t) \tag{B.2}$$

where \mathcal{W}_ε is a space-time white noise process, $\mathcal{E}(\mathbf{s}, t)$ is a spatially correlated stationary process with white noise properties in time, α_t and α_ε are smoothness parameters which will usually be fixed when estimating the other model parameters, τ , ρ and γ_ε which are real positives related to the overall precision, temporal dependency and spatial dependency, respectively. The full derivations of these equations are provided in (Krainski, 2018).

Parameter	Description	Equation	Prior	References
W_{ε}	space-time white noise process	Eq B.1		
$\mathcal{E}(\mathbf{s}, t)$	spatially correlated stationary process with white noise properties in time	Eq B.2		
τ	overall precision	Eq B.1		
ρ	temporal dependency	Eq B.1		
γ_{ε}	spatial dependency	Eq B.2		
$\hat{I}_{r,t}$	observed infected individuals	Eq 4.1		
θ	observation probability	Eq 4.3		
β_0	log of the mean infected individuals	Eq 4.3		
$I_{r,t}$	true infected individuals	Eq 4.8	space-time SPDE: Eqs B.1 and B.2	
$S_{r,t}$	Susceptible individuals	Eqs 4.5 & 4.8		
$X_{r,t}$	mean susceptible population			
$x_{r,t}$	environmental noise		space-time SPDE: Eqs B.1 and B.2, mean 0 and variance σ^2	Lindström (1988)
ρ	transmission rate	Eq 4.8		
c	mixing term	Eq 4.8		
α	Birth pulse	Eq 4.6	3.29	Iossa <i>et al.</i> (2008); Thulke <i>et al.</i> (1999)
$(1 - m)$	Survival rate	Eq 4.6	0.908	Iossa <i>et al.</i> (2008); Thulke <i>et al.</i> (1999)
ν	bait uptake rate	Eq 4.7	0.3	Robardet <i>et al.</i> (2016)

BIBLIOGRAPHY

Bibliography

- ALTIZER, S., NUNN, C. L., THRALL, P. H., GITTLEMAN, J. L., ANTONOVICS, J., CUNNINGHAM, A. A., DOBSON, A. P., EZENWA, V., JONES, K. E., PEDERSEN, A. B. *et al.* (2003). Social organization and parasite risk in mammals: integrating theory and empirical studies. *Annual Review of Ecology, Evolution, and Systematics*, **34**(1); pages 517–547.
- ANDERSON, R., JACKSON, H., MAY, R., & SMITH, A. (1981). Population dynamics of fox rabies in Europe. *Nature*, **289**; page 765.
- ANDERSON, R. M. (1991). Mathematical models of transmission and control. *Oxford textbook of public health*, **2**; pages 225–252.
- ANDERSON, R. M., MAY, R. M., & ANDERSON, B. (1992). *Infectious diseases of humans: dynamics and control*, volume 28. Wiley Online Library.
- ANDRAL, L., ARTOIS, M., AUBERT, M., & BLANCOU, J. (1982). Radio-tracking of rabid foxes. *Comparative immunology, microbiology and infectious diseases*, **5**(1-3); pages 285–291.
- ANSORGE, H. (1990). Daten zur fortpflanzungsbiologie und zur reproduktionsstrategie des rotfuchses, *vulpes vulpes*, in der oberlausitz. *Säugetierkd. Inf.*, **3**(14); pages 185–199.
- ANTOLIN, M. F. (2008). Unpacking β : within-host dynamics and the evolutionary ecology of pathogen transmission. *Annual Review of Ecology, Evolution, and Systematics*, **39**; pages 415–437.
- BAKER, P. J., HARRIS, S., ROBERTSON, C. P., SAUNDERS, G., & WHITE, P. C. (2004). Is it possible to monitor mammal population changes from counts of road traffic casualties? An analysis using Bristol's red foxes *Vulpes vulpes* as an example. *Mammal Review*, **34**(1-2); pages 115–130.
- BALL, F., BRITTON, T., HOUSE, T., ISHAM, V., MOLLISON, D., PELLIS, L., & TOMBA, G. S. (2015). Seven challenges for metapopulation models of epidemics, including households models. *Epidemics*, **10**; pages 63–67.
- BALL, F., MOLLISON, D., & SCALIA-TOMBA, G. (1997). Epidemics with two levels of mixing. *The Annals of Applied Probability*, pages 46–89.
- BARLOW, N. (1991). Control of endemic bovine Tb in New Zealand possum populations: results from a simple model. *Journal of applied ecology*, pages 794–809.
- BARLOW, N. (1996). The ecology of wildlife disease control: simple models revisited. *Journal of Applied Ecology*, pages 303–314.

- BARTLETT, M. (1956). Deterministic and stochastic models for recurrent epidemics. In *Proceedings of the third Berkeley symposium on mathematical statistics and probability*, volume 4, page 109.
- BARTLETT, M. S. (1957). Measles periodicity and community size. *Journal of the Royal Statistical Society. Series A (General)*, pages 48–70.
- BECKER, D. J., STREICKER, D. G., & ALTIZER, S. (2015). Linking anthropogenic resources to wildlife–pathogen dynamics: a review and meta-analysis. *Ecology letters*, **18**(5); pages 483–495.
- BEGON, M., BENNETT, M., BOWERS, R. G., FRENCH, N. P., HAZEL, S., & TURNER, J. (2002). A clarification of transmission terms in host-microparasite models: numbers, densities and areas. *Epidemiology & Infection*, **129**(1); pages 147–153.
- BERMAN, M. & DIGGLE, P. (1989). Estimating weighted integrals of the second-order intensity of a spatial point process. *Journal of the Royal Statistical Society. Series B (Methodological)*, pages 81–92.
- BEYER, H. L., HAMPSON, K., LEMBO, T., CLEAVELAND, S., KAARE, M., & HAYDON, D. T. (2012). The implications of metapopulation dynamics on the design of vaccination campaigns. *Vaccine*, **30**(6); pages 1014–1022.
- BHARTI, N., TATEM, A. J., FERRARI, M. J., GRAIS, R. F., DJIBO, A., & GRENFELL, B. T. (2011). Explaining seasonal fluctuations of measles in niger using nighttime lights imagery. *Science*, **334**(6061); pages 1424–1427.
- BJØRNSTAD, O. N., FINKENSTÄDT, B. F., & GRENFELL, B. T. (2002). Dynamics of measles epidemics: estimating scaling of transmission rates using a time series SIR model. *Ecological Monographs*, **72**(2); pages 169–184.
- BOLKER, B. & GRENFELL, B. (1995). Space, persistence and dynamics of measles epidemics. *Philosophical Transactions of the Royal Society of London B: Biological Sciences*, **348**(1325); pages 309–320.
- BOLKER, B. & GRENFELL, B. (1996). Impact of vaccination on the spatial correlation and persistence of measles dynamics. *Proceedings of the National Academy of Sciences*, **93**(22); pages 12,648–12,653.
- BOURHY, H., NAKOUNÉ, E., HALL, M., NOUVELLET, P., LEPELLETIER, A., TALBI, C., WATIER, L., HOLMES, E. C., CAUCHEMEZ, S., LEMEY, P. *et al.* (2016). Revealing the micro-scale signature of endemic zoonotic disease transmission in an African urban setting. *PLoS pathogens*, **12**(4); page e1005,525.
- BREITENMOSER, U. & MÜLLER, U. (1997). How to do the wrong thing with the highest possible precision—a reflection on the use of GPS in rabies vaccination campaigns. *Rabies Bulletin Europe*, **21**(4); pages 11–3.
- BROCHIER, B., THOMAS, I., BAUDUIN, B., LEVEAU, T., PASTORET, P.-P., LANGUET, B., CHAPPUIS, G., DESMETTRE, P., BLANCOU, J., & ARTOIS, M. (1990). Use of a vaccinia-rabies recombinant virus for the oral vaccination of foxes against rabies. *Vaccine*, **8**(2); pages 101–104.
- BROWN, J. H. & KODRIC-BROWN, A. (1977). Turnover rates in insular biogeography: effect of immigration on extinction. *Ecology*, **58**(2); pages 445–449.

- CAILLAUD, D., LEVRÉRO, F., CRISTESCU, R., GATTI, S., DEWAS, M., DOUADI, M., GAUTIER-HION, A., RAYMOND, M., & MÉNARD, N. (2006). Gorilla susceptibility to ebola virus: the cost of sociality. *Current Biology*, **16**(13); pages R489–R491.
- CASTILLO-NEYRA, R., BROWN, J., BORRINI, K., AREVALO, C., LEVY, M. Z., BUTTENHEIM, A., HUNTER, G. C., BECERRA, V., BEHRMAN, J., & PAZ-SOLDAN, V. A. (2017). Barriers to dog rabies vaccination during an urban rabies outbreak: Qualitative findings from Arequipa, Peru. *PLoS neglected tropical diseases*, **11**(3); page e0005460.
- CLIQUET, F., PICARD-MEYER, E., & ROBARDET, E. (2014). Rabies in Europe: what are the risks?
- CROSS, P. C., JOHNSON, P. L., LLOYD-SMITH, J. O., & GETZ, W. M. (2007). Utility of r_0 as a predictor of disease invasion in structured populations. *Journal of the Royal Society Interface*, **4**(13); pages 315–324.
- CROSS, P. C., LLOYD-SMITH, J. O., JOHNSON, P. L., & GETZ, W. M. (2005). Duelling timescales of host movement and disease recovery determine invasion of disease in structured populations. *Ecology Letters*, **8**(6); pages 587–595.
- CZADO, C., GNEITING, T., & HELD, L. (2009). Predictive model assessment for count data. *Biometrics*, **65**(4); pages 1254–1261.
- DEL RIO VILAS, V. J., FREIRE DE CARVALHO, M. J., VIGILATO, M. A., ROCHA, F., VOKATY, A., POMPEI, J. A., MOLINA FLORES, B., FENELON, N., & COSIVI, O. (2017). Tribulations of the last mile: sides from a regional program. *Frontiers in Veterinary Science*, **4**; page 4.
- DEMETRIOU, P. & MOYNAGH, J. (2011). The European Union strategy for external cooperation with neighbouring countries on rabies control. *Rabies Bulletin Europe*, **35**(1); pages 5–7.
- DEVIATKIN, A. A., LUKASHEV, A. N., POLESHCHUK, E. M., DEDKOV, V. G., TKACHEV, S. E., SIDOROV, G. N., KARGANOVA, G. G., GALKINA, I. V., SHCHELKANOV, M. Y., & SHIPULIN, G. A. (2017). The phylodynamics of the rabies virus in the Russian Federation. *PloS one*, **12**(2); page e0171855.
- DHONDT, A. A., ALTIZER, S., COOCH, E. G., DAVIS, A. K., DOBSON, A., DRISCOLL, M. J., HARTUP, B. K., HAWLEY, D. M., HOCHACHKA, W. M., HOSSEINI, P. R. *et al.* (2005). Dynamics of a novel pathogen in an avian host: mycoplasmal conjunctivitis in house finches. *Acta tropica*, **94**(1); pages 77–93.
- DIEKMANN, O. (1978). Thresholds and travelling waves for the geographical spread of infection. *Journal of Mathematical Biology*, **6**(2); page 109.
- DIEKMANN, O. & HEESTERBEEK, J. A. P. (2000). *Mathematical epidemiology of infectious diseases: model building, analysis and interpretation*, volume 5. John Wiley & Sons.
- DIEKMANN, O., HEESTERBEEK, J. A. P., & METZ, J. A. (1990). On the definition and the computation of the basic reproduction ratio r_0 in models for infectious diseases in heterogeneous populations. *Journal of mathematical biology*, **28**(4); pages 365–382.
- EARN, D. J., LEVIN, S. A., & ROHANI, P. (2000). Coherence and conservation. *Science*, **290**(5495); pages 1360–1364.

- EARN, D. J., ROHANI, P., & GRENFELL, B. T. (1998). Persistence, chaos and synchrony in ecology and epidemiology. *Proceedings of the Royal Society of London B: Biological Sciences*, **265**(1390); pages 7–10.
- EISINGER, D. & THULKE, H.-H. (2008). Spatial pattern formation facilitates eradication of infectious diseases. *Journal of Applied Ecology*, **45**(2); pages 415–423.
- EISINGER, D., THULKE, H.-H., SELHORST, T., & MÜLLER, T. (2005). Emergency vaccination of rabies under limited resources—combating or containing? *BMC Infectious Diseases*, **5**(1); page 10.
- FINE, P., EAMES, K., & HEYMANN, D. L. (2011). “herd immunity”: a rough guide. *Clinical infectious diseases*, **52**(7); pages 911–916.
- FREULING, C. M., HAMPSON, K., SELHORST, T., SCHRÖDER, R., MESLIN, F. X., METTENLEITER, T. C., & MÜLLER, T. (2013). The elimination of fox rabies from Europe: determinants of success and lessons for the future. *Philosophical Transactions of the Royal Society B: Biological Sciences*, **368**(1623).
- FULFORD, G., ROBERTS, M., & HEESTERBEEK, J. (2002). The metapopulation dynamics of an infectious disease: a case study of tuberculosis in possums. *Theoretical population biology*, **61**(1); pages 15–29.
- GANI, R. & LEACH, S. (2004). Epidemiologic determinants for modeling pneumonic plague outbreaks. *Emerging infectious diseases*, **10**(4); page 608.
- GLASS, K., XIA, Y., & GRENFELL, B. (2003). Interpreting time-series analyses for continuous-time biological models — measles as a case study. *Journal of Theoretical Biology*, **223**(1); pages 19–25.
- GRAIS, R., CONLAN, A., FERRARI, M., DJIBO, A., LE MENACH, A., BJØRNSTAD, O., & GRENFELL, B. (2008). Time is of the essence: exploring a measles outbreak response vaccination in niamey, niger. *Journal of the Royal Society Interface*, **5**(18); page 67.
- GRASSLY, N. C., FRASER, C., WENGER, J., DESHPANDE, J. M., SUTTER, R. W., HEYMANN, D. L., & AYLWARD, R. B. (2006). New strategies for the elimination of polio from india. *Science*, **314**(5802); pages 1150–1153.
- GRENFELL, B., BJØRNSTAD, O., & KAPPEY, J. (2001). Travelling waves and spatial hierarchies in measles epidemics. *Nature*, **414**(6865); page 716.
- GRENFELL, B. & HARWOOD, J. (1997). (meta)population dynamics of infectious diseases. *Trends in Ecology & Evolution*, **12**(10); pages 395 – 399. ISSN 0169-5347.
- GRENFELL, B. T., BJØRNSTAD, O. N., & FINKENSTÄDT, B. F. (2002). Dynamics of measles epidemics: scaling noise, determinism, and predictability with the TSIR model. *Ecological Monographs*, **72**(2); pages 185–202.
- GRENFELL, B. T. & DOBSON, A. P. (1995). *Ecology of infectious diseases in natural populations*, volume 7. Cambridge University Press.
- HAGENAARS, T., DONNELLY, C., & FERGUSON, N. (2004). Spatial heterogeneity and the persistence of infectious diseases. *Journal of theoretical biology*, **229**(3); pages 349–359.

- HAMPSON, K., COUDEVILLE, L., LEMBO, T., SAMBO, M., KIEFFER, A., ATTLAN, M., BARRAT, J., BLANTON, J. D., BRIGGS, D. J., CLEAVELAND, S. *et al.* (2015). Estimating the global burden of endemic canine rabies. *PLoS Negl Trop Dis*.
- HAMPSON, K., DUSHOFF, J., BINGHAM, J., BRÜCKNER, G., ALI, Y., & DOBSON, A. (2007). Synchronous cycles of domestic dog rabies in sub-Saharan Africa and the impact of control efforts. *Proceedings of the National Academy of Sciences*, **104**(18); pages 7717–7722.
- HAMPSON, K., DUSHOFF, J., CLEAVELAND, S., HAYDON, D. T., KAARE, M., PACKER, C., & DOBSON, A. (2009). Transmission dynamics and prospects for the elimination of canine rabies. *PLoS Biology*.
- HANSKI, I. (1998). Metapopulation dynamics. *Nature*, **396**(6706); page 41.
- HANSKI, I. & OVASKAINEN, O. (2000). The metapopulation capacity of a fragmented landscape. *Nature*, **404**(6779); page 755.
- HARRIS, S. & SMITH, G. (1987). Demography of two urban fox (*Vulpes vulpes*) populations. *Journal of Applied Ecology*, pages 75–86.
- HAY, S. I., GUERRA, C. A., GETHING, P. W., PATIL, A. P., TATEM, A. J., NOOR, A. M., KABARIA, C. W., MANH, B. H., ELYAZAR, I. R., BROOKER, S. *et al.* (2009). A world malaria map: *Plasmodium falciparum* endemicity in 2007. *PLoS medicine*, **6**(3); page 286.
- HESS, G. (1996). Disease in metapopulation models: implications for conservation. *Ecology*, **77**(5); pages 1617–1632.
- HOSSEINI, P. R., DHONDT, A. A., & DOBSON, A. (2004). Seasonality and wildlife disease: how seasonal birth, aggregation and variation in immunity affect the dynamics of *Mycoplasma gallisepticum* in house finches. *Proceedings of the Royal Society of London B: Biological Sciences*, **271**(1557); pages 2569–2577.
- IOSSA, G., SOULSBURY, C. D., BAKER, P. J., & HARRIS, S. (2008). Body mass, territory size, and life-history tactics in a socially monogamous canid, the red fox *Vulpes vulpes*. *Journal Information*, **89**(6).
- KEELING, M., WOOLHOUSE, M., MAY, R., DAVIES, G., & GRENFELL, B. (2003). Modelling vaccination strategies against foot-and-mouth disease. *Nature*, **421**(6919); page 136.
- KEELING, M. J. (1999). The effects of local spatial structure on epidemiological invasions. *Proceedings of the Royal Society of London B: Biological Sciences*, **266**(1421); pages 859–867.
- KEELING, M. J. (2000). Metapopulation moments: coupling, stochasticity and persistence. *Journal of Animal Ecology*, **69**(5); pages 725–736.
- KEELING, M. J. & EAMES, K. T. (2005). Networks and epidemic models. *Journal of the Royal Society Interface*, **2**(4); page 295.
- KEELING, M. J. & GRENFELL, B. (1997). Disease extinction and community size: modeling the persistence of measles. *Science*, **275**(5296); pages 65–67.
- KEELING, M. J. & ROHANI, P. (2002). Estimating spatial coupling in epidemiological systems: a mechanistic approach. *Ecology Letters*, **5**(1); pages 20–29. ISSN 1461-0248.

- KEELING, M. J. & ROHANI, P. (2008). *Modeling infectious diseases in humans and animals*. Princeton University Press.
- KEELING, M. J., WOOLHOUSE, M. E., SHAW, D. J., MATTHEWS, L., CHASE-TOPPING, M., HAYDON, D. T., CORNELL, S. J., KAPPEY, J., WILESMITH, J., & GRENFELL, B. T. (2001). Dynamics of the 2001 UK foot and mouth epidemic: stochastic dispersal in a heterogeneous landscape. *Science*, **294**(5543); pages 813–817.
- KERMACK, W. O. & MCKENDRICK, A. G. (1927). A contribution to the mathematical theory of epidemics. In *Proceedings of the Royal Society of London A: mathematical, physical and engineering sciences*, volume 115, pages 700–721. The Royal Society.
- KLEPAC, P., METCALF, C. J. E., MCLEAN, A. R., & HAMPSON, K. (2013). Towards the endgame and beyond: complexities and challenges for the elimination of infectious diseases. *Philosophical Transactions of the Royal Society of London B: Biological Sciences*, **368**(1623).
- KOELLE, K. & PASCUAL, M. (2004). Disentangling extrinsic from intrinsic factors in disease dynamics: a nonlinear time series approach with an application to cholera. *The American Naturalist*, **163**(6); pages 901–913.
- KRAINSKI, E. (2018). *Statistical analysis of space-time Data: new models and applications*. Ph.D. thesis.
- KUZMIN, I. V., BOTVINKIN, A. D., MCELHINNEY, L. M., SMITH, J. S., ORCIARI, L. A., HUGHES, G. J., FOOKS, A. R., & RUPPRECHT, C. E. (2004). Molecular epidemiology of terrestrial rabies in the former Soviet Union. *Journal of wildlife diseases*, **40**(4); pages 617–631.
- LEMBO, T., HAMPSON, K., KAARE, M. T., ERNEST, E., KNOBEL, D., KAZWALA, R. R., HAYDON, D. T., & CLEAVELAND, S. (2010). The feasibility of canine rabies elimination in Africa: dispelling doubts with data. *PLoS neglected tropical diseases*, **4**(2); page e626.
- LEVIN, S. A. & DURRETT, R. (1996). From individuals to epidemics. *Philosophical Transactions of the Royal Society of London B: Biological Sciences*, **351**(1347); pages 1615–1621.
- LINDGREN, F. & RUE, H. (2015). Bayesian spatial modelling with R-INLA. *Journal of Statistical Software*, **63**(19).
- LINDGREN, F., RUE, H., & LINDSTRÖM, J. (2011). An explicit link between Gaussian fields and Gaussian Markov random fields: the SPDE approach (with discussion). *JR 671 Stat Soc, Series B*, **73**; pages 423–498.
- LINDGREN, G. (2012). *Stationary stochastic processes: theory and applications*. CRC Press.
- LINDSTRÖM, E. (1988). Reproductive effort in the red fox, *Vulpes vulpes*, and future supply of a fluctuating prey. *Oikos*, **52**(1); pages 115–119. ISSN 00301299, 16000706.
- LINDSTRÖM, E. (1989). Food limitation and social regulation in a red fox population. *Ecography*, **12**(1); pages 70–79.
- LIU, W.-M. (1987). *Dynamics of epidemiological models—recurrent outbreaks in autonomous systems*. Ph.D. thesis, Cornell University.

- LIU, W.-M. & LEVIN, S. A. (1989). Influenza and some related mathematical models. *Applied Mathematical Ecology*, **18**; page 235.
- LIU, W.-M., LEVIN, S. A., & IWASA, Y. (1986). Influence of nonlinear incidence rates upon the behavior of SIRS epidemiological models. *Journal of mathematical biology*, **23**(2); pages 187–204.
- LLOYD, A. L. (2001). Destabilization of epidemic models with the inclusion of realistic distributions of infectious periods. *Proceedings of the Royal Society of London B: Biological Sciences*, **268**(1470); pages 985–993.
- LLOYD, H. G., JENSEN, B., HAAFTEN, J., NIEWOLD, F., WANDELER, A., BÖGEL, K., & ARATA, A. (1976). Annual turnover of fox populations in Europe. *Zentralblatt für Veterinärmedizin Reihe B*, **23**(7); pages 580–589.
- LLOYD-SMITH, J. O., CROSS, P. C., BRIGGS, C. J., DAUGHERTY, M., GETZ, W. M., LATTO, J., SANCHEZ, M. S., SMITH, A. B., & SWEI, A. (2005a). Should we expect population thresholds for wildlife disease? *Trends in Ecology & Evolution*, **20**(9); pages 511–519.
- LLOYD-SMITH, J. O., SCHREIBER, S. J., KOPP, P. E., & GETZ, W. M. (2005b). Superspreading and the effect of individual variation on disease emergence. *Nature*, **438**(7066); page 355.
- MANCY, R. (2015). *Modelling persistence in spatially-explicit ecological and epidemiological systems*. Ph.D. thesis, University of Glasgow.
- MARTINEZ-BAKKER, M., BAKKER, K. M., KING, A. A., & ROHANI, P. (2014). Human birth seasonality: latitudinal gradient and interplay with childhood disease dynamics. *Proceedings of the Royal Society B: Biological Sciences*, **281**(1783).
- MATTHEWS, L., HAYDON, D., SHAW, D., CHASE-TOPPING, M., KEELING, M., & WOOLHOUSE, M. (2003). Neighbourhood control policies and the spread of infectious diseases. *Proceedings of the Royal Society of London B: Biological Sciences*, **270**(1525); pages 1659–1666.
- MCCALLUM, H., BARLOW, N., & HONE, J. (2001). How should pathogen transmission be modelled? *Trends in ecology & evolution*, **16**(6); pages 295–300.
- MCCALLUM, H. & DOBSON, A. (2002). Disease, habitat fragmentation and conservation. *Proceedings of the Royal Society of London B: Biological Sciences*, **269**(1504); pages 2041–2049.
- MCCALLUM, H., FENTON, A., HUDSON, P. J., LEE, B., LEVICK, B., NORMAN, R., PERKINS, S. E., VINEY, M., WILSON, A. J., & LELLO, J. (2017). Breaking beta: deconstructing the parasite transmission function. *Phil. Trans. R. Soc. B*, **372**(1719); page 20160,084.
- METCALF, C., LESSLER, J., KLEPAC, P., CUTTS, F., & GRENFELL, B. (2012). Impact of birth rate, seasonality and transmission rate on minimum levels of coverage needed for rubella vaccination. *Epidemiology & Infection*, **140**(12); pages 2290–2301.
- METCALF, C. J. E., HAMPSON, K., TATEM, A. J., GRENFELL, B. T., & BJØRNSTAD, O. N. (2013). Persistence in epidemic metapopulations: quantifying the rescue effects for measles, mumps, rubella and whooping cough. *PLoS One*.
- MULATTI, P., MÜLLER, T., BONFANTI, L., & MARANGON, S. (2012). Emergency oral rabies vaccination of foxes in Italy in 2009–2010: identification of residual rabies foci at higher altitudes in the Alps. *Epidemiology & Infection*, **140**(4); pages 591–598.

- MÜLLER, T., BÄTZA, H.-J., FREULING, C., KLIEMT, A., KLIEMT, J., HEUSER, R., SCHLÜTER, H., SELHORST, T., VOS, A., & METTENLEITER, T. C. (2012). Elimination of terrestrial rabies in Germany using oral vaccination of foxes. *Berl Munch Tierarztl Wochenschr*, **125**(5-6); pages 178–90.
- MÜLLER, T. & FREULING, C. (2012). Rabies elimination in Europe—a success story. OIE Global conference on rabies control: Towards sustainable prevention at the source, 7–9 sept 2011, Incheon-Seoul, Korea.
- MÜLLER, T. F., SCHRÖDER, R., WYSOCKI, P., METTENLEITER, T. C., & FREULING, C. M. (2015). Spatio-temporal use of oral rabies vaccines in fox rabies elimination programmes in Europe. *PLoS Negl Trop Dis*, **9**(8).
- MURRAY, J. & SEWARD, W. (1992). On the spatial spread of rabies among foxes with immunity. *Journal of theoretical biology*, **156**(3); pages 327–348.
- ONSTAD, D. W. & KORNKVEN, E. A. (1992). Persistence and endemicity of pathogens in plant populations over time and space. *Phytopathology*, **82**(5); pages 561–566.
- PASTOR-SATORRAS, R. & VESPIGNANI, A. (2001). Epidemic dynamics and endemic states in complex networks. *Phys. Rev. E*, **63**; page 066,117.
- PASTORET, P., BROCHIER, B., LANGUET, B., THOMAS, I., PAQUOT, A., BAUDUIN, B., KIENY, M., LECOCQ, J., DE, J. B., & COSTY, F. (1988). First field trial of fox vaccination against rabies using a vaccinia-rabies recombinant virus. *The veterinary record*, **123**(19); pages 481–483.
- PEEL, A. J., PULLIAM, J., LUIS, A., PLOWRIGHT, R., O’SHEA, T., HAYMAN, D., WOOD, J., WEBB, C., & RESTIF, O. (2014). The effect of seasonal birth pulses on pathogen persistence in wild mammal populations. *Proceedings of the Royal Society of London B: Biological Sciences*, **281**(1786); page 20132,962.
- PILS, C. M. & MARTIN, M. A. (1978). *Population dynamics, predator-prey relationships and management of the red fox in Wisconsin*. 105. Department of Natural Resources.
- PLUMMER, M. (2002). A program for analysis of Bayesian graphical models using Gibbs sampling. *Technische Universität Wien, Vienna, Austria*.
- PRENTICE, J. C., MARION, G., HUTCHINGS, M. R., MCNEILLY, T. N., & MATTHEWS, L. (2017). Complex responses to movement-based disease control: when livestock trading helps. *Journal of The Royal Society Interface*, **14**(126); page 20160,531.
- PULLIAM, J. R., DUSHOFF, J. G., LEVIN, S. A., & DOBSON, A. P. (2007). Epidemic enhancement in partially immune populations. *PLoS One*, **2**(1); page e165.
- RAMSEY, D., SPENCER, N., CALEY, P., EFFORD, M., HANSEN, K., LAM, M., & COOPER, D. (2002). The effects of reducing population density on contact rates between brushtail possums: implications for transmission of bovine tuberculosis. *Journal of Applied Ecology*, **39**(5); pages 806–818.
- REAL, L. A., HENDERSON, J. C., BIEK, R., SNAMAN, J., JACK, T. L., CHILDS, J. E., STAHL, E., WALLER, L., TINLINE, R., & NADIN-DAVIS, S. (2005). Unifying the spatial population dynamics

- and molecular evolution of epidemic rabies virus. *Proceedings of the National Academy of Sciences*, **102**(34); pages 12,107–12,111.
- REES, E. E., POND, B. A., CULLINGHAM, C. I., TINLINE, R., BALL, D., KYLE, C. J., & WHITE, B. N. (2008). Assessing a landscape barrier using genetic simulation modelling: implications for raccoon rabies management. *Preventive Veterinary Medicine*, **86**(1-2); pages 107–123.
- REES, E. E., POND, B. A., CULLINGHAM, C. I., TINLINE, R. R., BALL, D., KYLE, C. J., & WHITE, B. N. (2009). Landscape modelling spatial bottlenecks: implications for raccoon rabies disease spread. *Biology Letters*, **5**(3); pages 387–390.
- REES, E. E., POND, B. A., TINLINE, R. R., & BÉLANGER, D. (2011). Understanding effects of barriers on the spread and control of rabies. *Adv Virus Res*, **79**; pages 421–47.
- REES, E. E., POND, B. A., TINLINE, R. R., & BÉLANGER, D. (2013). Modelling the effect of landscape heterogeneity on the efficacy of vaccination for wildlife infectious disease control. *Journal of Applied Ecology*, **50**(4); pages 881–891.
- ROBARDET, E., PICARD-MEYER, E., DOBROŠTANA, M., JACEVICIENE, I., MÄHAR, K., MUIŽNIECE, Z., PRIDOTKAS, G., MASIULIS, M., NIIN, E., OLŠEVSKIS, E. *et al.* (2016). Rabies in the Baltic states: decoding a process of control and elimination. *PLoS neglected tropical diseases*, **10**(2); page e0004,432.
- ROHANI, P., EARN, D. J., & GRENFELL, B. T. (1999). Opposite patterns of synchrony in sympatric disease metapopulations. *Science*, **286**(5441); pages 968–971.
- ROWLINGSON, B. S. & DIGGLE, P. J. (1993). Splanx: spatial point pattern analysis code in s-plus. *Computers and Geosciences*, **19**; pages 627–627.
- ROY, M. & PASCUAL, M. (2006). On representing network heterogeneities in the incidence rate of simple epidemic models. *ecological complexity*, **3**(1); pages 80–90.
- RUE, H. & HELD, L. (2005). *Gaussian Markov random fields: theory and applications*. CRC Press.
- RUE, H., MARTINO, S., & CHOPIN, N. (2009). Approximate Bayesian inference for latent Gaussian models by using integrated nested laplace approximations. *Journal of the Royal Statistical Society: Series B (Statistical Methodology)*, **71**(2); pages 319–392.
- RUPPRECHT, C., BARRETT, J., BRIGGS, D., CLIQUET, F., FOOKS, A., LUMBERTDACHA, B., MESLIN, F., MÜLER, T., NEL, L., SCHNEIDER, C. *et al.* (2008). Can rabies be eradicated? *Developments in biologicals*, **131**; pages 95–121.
- RUSSELL, C. A., SMITH, D. L., CHILDS, J. E., & REAL, L. A. (2005). Predictive spatial dynamics and strategic planning for raccoon rabies emergence in Ohio. *PLoS biology*, **3**(3); page e88.
- SAUNDERS, G., MCILROY, J., KAY, B., GIFFORD, E., BERGHOUT, M., & VAN DE VEN, R. (2002). Demography of foxes in central-western New South Wales, Australia. *Mammalia*, **66**(2); pages 247–258.
- SCHIPPER, J., CHANSON, J. S., CHIOZZA, F., COX, N. A., HOFFMANN, M., KATARIYA, V., LAMOREUX, J., RODRIGUES, A. S., STUART, S. N., TEMPLE, H. J. *et al.* (2008). The status of the world's land and marine mammals: diversity, threat, and knowledge. *Science*, **322**(5899); pages 225–230.

- SELHORST, T., MÜLLER, T., & BÄTZA, H. (2006). Epidemiological analysis of setbacks in oral vaccination in the final stage of fox rabies elimination in densely populated areas in germany. *Developments in biologicals*, **125**; pages 127–132.
- SELHORST, T., MÜLLER, T., SCHWERMER, H., ZILLER, M., SCHLÜTER, H., BREITENMOSER, U., MÜLLER, U., BROCHIER, B., PASTORET, P.-P., & MUTINELLI, F. (2005). Use of an area index to retrospectively analyze the elimination of fox rabies in european countries. *Environmental management*, **35**(3); pages 292–302.
- SIBLY, R. M., HONE, J., & CLUTTON-BROCK, T. H. (2003). *Wildlife population growth rates*. Cambridge University Press.
- SIMPSON, D., ILLIAN, J. B., LINDGREN, F., SØRBYE, S. H., & RUE, H. (2016). Going off grid: Computationally efficient inference for log-Gaussian Cox processes. *Biometrika*, **103**(1); pages 49–70.
- SMITH, D. L., HAY, S. I., NOOR, A. M., & SNOW, R. W. (2009). Predicting changing malaria risk after expanded insecticide-treated net coverage in africa. *Trends in parasitology*, **25**(11); pages 511–516.
- SMITH, D. L., LUCEY, B., WALLER, L. A., CHILDS, J. E., & REAL, L. A. (2002). Predicting the spatial dynamics of rabies epidemics on heterogeneous landscapes. *Proceedings of the National Academy of Sciences*, **99**(6); pages 3668–3672.
- SMITH, K. F., DOBSON, A. P., MCKENZIE, F. E., REAL, L. A., SMITH, D. L., & WILSON, M. L. (2005). Ecological theory to enhance infectious disease control and public health policy. *Frontiers in Ecology and the Environment*, **3**(1); pages 29–37.
- SONNENBURG, J., RYSER-DEGIORGIS, M.-P., KUIKEN, T., FERROGLIO, E., ULRICH, R. G., CONRATHS, F. J., GORTÁZAR, C., & STAUBACH, C. (2016). Harmonizing methods for wildlife abundance estimation and pathogen detection in Europe—a questionnaire survey on three selected host-pathogen combinations. *BMC veterinary research*, **13**(1); page 53.
- SWINTON, J., HARWOOD, J., GRENFELL, B., & GILLIGAN, C. (1998). Persistence thresholds for phocine distemper virus infection in harbour seal *Phoca vitulina* metapopulations. *Journal of Animal Ecology*, pages 54–68.
- THRALL, P. H., ANTONOVICS, J., & DOBSON, A. P. (2000). Sexually transmitted diseases in polygynous mating systems: prevalence and impact on reproductive success. *Proceedings of the Royal Society of London B: Biological Sciences*, **267**(1452); pages 1555–1563.
- THULKE, H., EISINGER, D., SELHORST, T., & MULLER, T. (2008). Scenario-analysis evaluating emergency strategies after rabies re-introduction. *Developments in biologicals*, **131**; pages 265–272.
- THULKE, H., GRIMM, V., MÜLLER, M., STAUBACH, C., TISCHENDORF, L., WISSEL, C., & JELTSCH, F. (1999). From pattern to practice: a scaling-down strategy for spatially explicit modelling illustrated by the spread and control of rabies. *Ecological Modelling*, **117**(2); pages 179–202.
- TISCHENDORF, L., THULKE, H.-H., STAUBACH, C., MÜLLER, M., JELTSCH, F., GORETZKI, J., SELHORST, T., MÜLLER, T., SCHLÜTER, H., & WISSEL, C. (1998). Chance and risk of controlling rabies in large-scale and long-term immunized fox populations. *Proceedings of the Royal Society of London B: Biological Sciences*, **265**(1399); pages 839–846.

- TOMA, B. & ANDRAL, L. (1977). Epidemiology of fox rabies. *Advances in Virus Research*, **21**; pages 1–36.
- TOWNSEND, S. E., LEMBO, T., CLEVELAND, S., MESLIN, F. X., MIRANDA, M. E., PUTRA, A. A. G., HAYDON, D. T., & HAMPSON, K. (2013a). Surveillance guidelines for disease elimination: a case study of canine rabies. *Comparative Immunology, Microbiology and Infectious Diseases*, **36**(3); pages 249–261.
- TOWNSEND, S. E., SUMANTRA, I. P., PUDJIATMOKO, B. G., BAGUS, G. N., BRUM, E., CLEVELAND, S., CRAFTER, S., DEWI, A. P., DHARMA, D. M. N., DUSHOFF, J. *et al.* (2013b). Designing programs for eliminating canine rabies from islands: Bali, Indonesia as a case study. *PLoS neglected tropical diseases*, **7**(8); page e2372.
- VIANA, M., MANCY, R., BIEK, R., CLEVELAND, S., CROSS, P. C., LLOYD-SMITH, J. O., & HAYDON, D. T. (2014). Assembling evidence for identifying reservoirs of infection. *Trends in ecology & evolution*, **29**(5); pages 270–279.
- VIGILATO, M. A. N., CLAVIJO, A., KNOBL, T., SILVA, H. M. T., COSIVI, O., SCHNEIDER, M. C., LEANES, L. F., BELOTTO, A. J., & ESPINAL, M. A. (2013). Progress towards eliminating canine rabies: policies and perspectives from Latin America and the Caribbean. *Philosophical Transactions of the Royal Society of London B: Biological Sciences*, **368**(1623); page 20120,143.
- VYNNYCKY, E. & WHITE, R. (2010). *An introduction to infectious disease modelling*. Oxford University Press.
- WEARING, H. J., ROHANI, P., & KEELING, M. J. (2005). Appropriate models for the management of infectious diseases. *PLoS medicine*, **2**(7); page e174.
- WOBESER, G. (2002). Disease management strategies for wildlife. *Revue Scientifique et Technique-Office international des epizooties*, **21**(1); pages 159–178.
- WOOLHOUSE, M. E., HAYDON, D. T., & ANTIA, R. (2005). Emerging pathogens: the epidemiology and evolution of species jumps. *Trends in ecology & evolution*, **20**(5); pages 238–244.
- ZINSSTAG, J., LECHENNE, M., LAAGER, M., MINDEKEM, R., OUSSIGUÉ, A., BIDJEH, K., RIVES, G., TESSIER, J., MADJANINAN, S., OUAGAL, M. *et al.* (2017). Vaccination of dogs in an african city interrupts rabies transmission and reduces human exposure. *Science translational medicine*, **9**(421); page eaaf6984.